The role of lamin B1 in lung cancer development and metastasis

Dissertation

Zur Erlangung des Doktorgrades

Der Naturwissenschaften

Vorgelegt beim Fachbereich Biologie und Chemie

Der Justus-Liebig-Universität Gießen

von

Yanhan Jia

aus Sichuan, China

Angefertigt am Max-Planck-Institut für Herz- und Lungenforschung

Bad Nauheim, 2019

am Medizinische Fakultät Mannheim der Universität Heidelberg

Mannheim, 2019

1. Gutachter:	**Prof. Dr. Reinhard Dammann** Institut für Genetik Fachbereich Biologie und Chemie Justus-Liebig-Universität Giessen
2. Gutachter:	**Prof. Dr. Gergana Dobreva** Medizinische Fakultät Mannheim Universität Heidelberg

Content

Content I
Summary VI
Zusammenfassung VII
1. Introduction 1
1.1 Lung cancer types and markers 1
1.2 Cancer metastasis 2
1.2.1 Metastatic cascade 2
1.2.2 Epithelial–mesenchymal transition 3
1.2.3 Cell signaling pathways that regulate EMT and cancer metastasis 5
1.2.4 Other regulators of EMT and cancer metastasis 9
1.3 Changes in nuclear structure in cancer cells 12
1.3.1 Nuclear shape and size in cancer cells 13
1.3.2 Changes in nuclear matrix in cancer cells 14
1.3.3 Alteration of nucleoli and perinucleolar compartment (PNC) 14
1.3.4 Promyelocytic leukemia (PML) bodies 15
1.3.5 Changes in chromatin organization 16
1.4 Nuclear envelope and nuclear lamins 16
1.4.1 Structure and components of the nuclear envelope 16
1.4.2 Nuclear lamins 18
1.4.3 Function of nuclear lamins 20
1.4.4 Nuclear lamins as cancer biomarkers 23
1.4.5 Nuclear lamins and cell migration 26
1.5 Epigenetic regulation of chromatin in cancer 26
1.5.1 Chromatin remodeling in cancer 27
1.5.2 Posttranslational modifications of histones 28
1.5.3 Role of histone modification in gene expression 29
1.5.4 Role of histone modification in cancer initiation and progression 30
1.5.5 Role of histone modifications in EMT and cancer metastasis 31

1.5.6 The role of Polycomb group complexes and H3K27me3 in cancer initiation and progression 35
1.5.7 The role of Polycomb group complexes and H3K27me3 in EMT and cancer metastasis 37
2. Objectives 39
3. Results 40
3.1 Expression of lamins in lung cancer patients 40
3.1.1 Lamin B1 levels are decreased in lung cancer specimens 40
3.1.2 Lamin A/C levels remain unchanged in NSCLC, but decreases in SCLC specimens 42
3.1.3 Cells in tumor microenvironment highly express lamin B1 43
3.1.4 Lamin B1 expression is decreased in lung cancers cell lines 44
3.2 Lamin B1 depletion promotes EMT, anchorage-independent growth, cell migration and invasion 45
3.2.1 Loss of lamin B1 in mouse lung epithelial cells leads to EMT 45
3.2.2 Lamin B1 depletion promotes cell migration and invasion 47
3.2.3 Lamin B1 depletion enhances cell anchorage-independent growth 48
3.3 Lamin B1 depletion leads to upregulation of migration-related genes .. 49
3.4 Upregulation of the RET plays a key role in mediating the EMT and malignant phenotype upon lamin B1 loss 51
3.4.1 The receptor tyrosine kinase RET is upregulated upon lamin B1 depletion 51
3.4.2 Targeting RET inhibits the migration and invasion of lamin B1-depleted cells 52
3.4.3 RET upregulation promotes lamin B1 depletion mediated EMT 54
3.4.4 P38 MAPK signaling pathway is activated upon RET overexpression in lamin B1-depleted cells 56
3.4.5 RET/p38 axis is responsible for the increased migratory phenotype

upon lamin B1 loss 57
3.4.6 RET upregulation play a key role in promoting migration and metastasis of lamin B1-depleted cells in vivo..... 58
3.5 RET levels negatively correlate with lamin B1 levels in lung cancer patients..... 61
3.5.1 The levels of RET are increased in lung cancer patients 61
3.5.2 RET levels negatively correlate with lamin B1 expression in lung cancer specimens..... 62
3.6 Lamin B1 recruits the EZH1/2 histone methyltransferase to silence RET expression..... 64
3.6.1 RET gene locates in lamina-associated domain with its promoter highly enriched with H3K27me3 64
3.6.2 Lamin B1 depletion leads to repositioning of RET and Gfra1 genes 65
3.6.3 Loss of lamin B1 alters morphology and location of chromosome 6 66
3.6.4 Lamin B1 depletion reduces the enrichment of repressive histone marks at the promoter of both RET and Gfra1..... 67
3.6.5 Loss of lamin B1 activates RET transcription by increasing the binding of transcription factor Ascl1 at Ret promoter 69
3.6.6 Ascl1 does not promote Ret gene positioning..... 70
3.6.7 Lamin B1 binds to EZH1/2 and recruits EZH1/2 to chromatin..... 70
3.6.8 Loss of lamin B1 leads to reduced enrichment of EZH1/2 at Ret promoter and global decrease of H3K27me3 72
3.6.9 Targeting EZH1/2 increases RET expression and phenocopies the enhanced migratory phenotype of lamin B1-depleted cells 73
3.6.10 Depletion or inhibition of EZH1/2 does not affect the positioning of Ret gene..... 75
3.6.11 Low levels of EZH1 are correlated with poorer prognosis of lung

cancer patients 76
3.7 Lamin B1 depletion induces aggressive lung tumor formation 77
3.7.1 Loss of one Lmnb1 allele is sufficient to induce lung tumor formation 77
3.7.2 Most of the lung tumors induced by lamin B1 haploinsufficiency were histologically similar to small cell lung cancer 78
3.7.3 Tumors were also found in the kidney and liver of Lmnb1+/- mice 79
3.7.4 Pulmonary tumors in Lmnb1+/- mice show RET upregulation, RET/p38 activation as well as reduced enrichment of H3K27me3 and EZH1/2 at Ret promoter 80
3.8 Model of the role of lamin B1 as a tumor suppressor in lung cancer development and metastasis 82
4. Discussion 84
4.1 Lamin B1 as a potential marker of lung cancer 84
4.2 The role of lamin B1 in cell proliferation and tumor initiation 85
4.3 The role of lamin B1 in cancer cell migration and metastasis 87
4.4 Loss of lamin B1 upregulates RET thereby triggering EMT and cancer cell migration and metastasis 88
4.5 RET/p38 axis is responsible for lamin B1 depletion-mediated cancer cell migration and metastasis 90
4.6 Loss of lamin B1 leads to specific gene repositioning and chromatin decondensation 91
4.7 Lamin B1 depletion impedes the recruitment of EZH1/2, thus derepressing the transcription of Ret 92
4.8 EZH1/2 mediate the function of lamin B1 in regulating cell migration 93
5. Future perspective 96
6. Materials and Methods 99
6.1 Materials 99
6.1.1 Chemicals and compounds 99

6.1.2 Kits 101
6.1.3 Solutions, reagents and media 102
6.1.4 Antibodies 105
6.1.5 Primers 105
6.1.6 Cell lines and plasmids 107
6.1.7 Mouse lines 107
6.2 Methods 107
6.2.1 Cell culture and generating stable cell lines 107
6.2.2 Immunohistochemistry and immunofluorescence staining 108
6.2.3 Histology 110
6.2.4 Animal experiments 111
6.2.5 Boyden chamber migration and invasion assay 112
6.2.6 Cell proliferation and soft agar colony formation assay 112
6.2.7 RNA Isolation, RT-PCR and Real-Time PCR 113
6.2.8 RNA-Seq data analysis 113
6.2.9 Immunoprecipitation and immunoblotting 114
6.2.10 DNA Fluorescence In Situ Hybridization (FISH) 117
6.2.11 Proximity ligation assay (PLA) 117
6.2.12 Chromatin immunoprecipitation (ChIP) and ChIP sequencing 118
6.2.13 In situ nuclear matrix extraction 119
6.2.14 Statistical analysis 119
7. References 121
8. Acknowledgements 156
9. EIDESSTATTLICHE ERKLÄRUNG 157

Summary

Lung cancer is the leading cause of cancer-related death worldwide, underscoring the importance of understanding the molecular mechanisms responsible of lung cancer initiation, progression and metastasis. One major characteristic and important diagnostic criterion for lung cancer and other neoplasias is the aberrant nuclear structure. The nuclear lamins, which are the structural component of nuclear envelope, has been shown to be critical determinants of nuclear structure, shape and genome integrity.

In the present study, we demonstrate a critical role of lamin B1 loss in facilitating lung cancer development, migration and metastasis. First, we observed significant lower levels of lamin B1 in human lung cancer tissues in comparison with normal lung tissues. Furthermore, lamin B1 haploinsufficiency is sufficient to induce spontaneous pulmonary tumor formation in mice model, suggesting that loss of lamin B1 promotes lung cancer initiation. Moreover, lamin B1 depletion triggers epithelial-mesenchymal transition (EMT) and facilitates cancer cell migration and metastasis via upregulating the receptor tyrosine kinase RET. RET upregulation upon lamin B1 silencing further activates p38 signaling pathway. Targeting both RET and its downstream target p38 repressed lamin B1 depletion mediated cancer cell migration and metastasis. Consistently, lamin B1 and RET expressions show inverse correlation in lung cancer patients.

Mechanistically, we show that loss of lamin B1 results in global decrease in H3K27me3 and reduces the occupancy of H3K27me3 at *Ret* promoter by disrupting the recruitment of methyltransferase EZH1 and EZH2 to the chromatin and *Ret* promoter, thus leading to the transcriptional activation of *Ret* gene. Taken together, our data demonstrate a role of lamin B1 as a tumor suppressor in lung cancer by epigenetically repressing the RET expression, prospecting a novel therapeutic strategy by targeting RET in the treatment of lung cancer patients with lamin B1 loss.

Zusammenfassung

Lungenkrebs ist weltweit die Hauptursache für krebsbedingte Todesfälle. Daher ist es sehr wichtig die Bedeutung des Verständnisses der molekularen Mechanismen, die für den Beginn, die Progression und die Metastasierung von Lungenkrebs verantwortlich sind, zu verstehen. Ein wichtiges charakteristisches und diagnostisches Kriterium für Lungenkrebs und andere Neoplasien ist die abweichende Kernstruktur. Es hat sich gezeigt, dass die nuklearen Lamine, die entscheidenden Determinanten der Kernstruktur, -form und -integrität des Genoms sind.

In der aktuellen Studie zeigen wir, dass die Depletion von Lamin B1 eine entscheidende Rolle bei der Krebsentwicklung, der Migration und der Metastasierung spielt. Erstens beobachteten wir einen signifikant niedrigeren Gehalt an Lamin B1 in menschlichen Lungenkrebsgeweben als das normale Lungengewebe. Darüber hinaus reicht die Lamin-B1-Haploinsuffizienz aus, um die spontane Lungentumorbildung im Mäusemodell zu induzieren, was darauf hindeutet, dass der Verlust von Lamin-B1 den Beginn und die Progression von Lungenkrebs fördert. Des Weiteren löst eine Lamin B1-Depletion den Epithelial-Mesenchymalen-Übergang (EMT) aus und fördert die Migration und Metastasierung von Krebszellen, indem die Rezeptor-Tyrosinkinase-RET hochreguliert wird. Die RET-Hochregulierung bei der Depletion von Lamin B1 aktiviert den p38-Signalweg. Das Targeting sowohl auf RET als auch auf sein nachgeschaltetes Ziel p38 unterdrückte die Lamin B1-Depletion die vermittelte Migration und Metastasierung von Krebszellen. Konsistent zeigen Lamin-B1- und -RET-Expressionen eine inverse Korrelation bei Lungenkrebspatienten.

Mechanistisch zeigen wir, dass der Verlust von Lamin B1 zu einer globalen Abnahme von H3K27me3 führt und die Belegung von H3K27me3 am *Ret*-Promotor verringert, indem die Rekrutierung von Methyltransferase EZH1 und EZH2 für das Chromatin und den *Ret*-Promotor unterbrochen wird, was zur transkriptionellen Aktivierung des *Ret*-Gens führt. Zusammengenommen

zeigen unsere Daten eine Rolle von Lamin B1 als Tumorsuppressor bei Lungenkrebs durch epigenetische Unterdrückung der RET-Expression. Dies könnte neue therapeutische Wege eröffnen, indem RET bei der Behandlung von Lungenkrebspatienten mit Lamin B1-Depletion eingesetzt wird.

1. Introduction

1.1 Lung cancer types and markers

Lung cancer is one of the most frequently diagnosed cancers and results in the largest number of cancer related deaths worldwide (Ferlay et al., 2015; Siegel et al., 2013). Lung cancer is classified into two different groups: Non-small cell lung cancer (NSCLC) and small cell lung cancer (SCLC), based on the morphological features of the cancer cells. NSCLC, which accounts for approximately 85% of all the lung cancer cases, is histologically divided into three different subtypes: adenocarcinoma (AD), squamous cell carcinoma (SCC) and large-cell carcinoma. SCLC, which is considered as a neuroendocrine carcinoma (Park et al., 2011a; Wistuba et al., 2001), represents the remaining 15% of all lung cancer cases (Travis et al., 2013). In contrast to NSCLC, SCLC is characterized by an aggressive clinical course, rapid growth and early metastasis (Karachaliou et al., 2016).

Biological markers are universally used to identify different lung cancer subtypes in order to improve diagnostic efficiency. Napsin A is shown as a specific marker for lung adenocarcinoma (Turner et al., 2012). Napsin A, in combination with the pulmonary marker thyroid transcription factor-1 (TTF1), is used to differentiate primary lung adenocarcinoma from metastatic carcinoma in the lung (Ye et al., 2011). In addition, CK7+/CK20- pattern is also used to characterize lung adenocarcinoma (Khayyata et al., 2009; Kummar et al., 2002; Su et al., 2006). Cytokeratin5/6 (CK5/6) and p63 are specific markers for identifying SCC (Khayyata et al., 2009; Kim et al., 2013). SCLC originates from neuroendocrine cells and overexpresses neuroendocrine markers, including calcitonin gene-related peptide (CGRP) (Sutherland et al., 2011), Synaptophysin (SYP) (Jensen et al., 1990), achaete scute homolog 1 (ASCL1) (Arriola et al., 2008), NCAM (CD56) (Kontogianni et al., 2005), pro-gastrin-releasing peptide (ProGRP) (Molina et al., 2004; Nisman et al., 2009), thus

these markers are helpful in differentiating SCLC from NSCLC together with morphological differences.

1.2 Cancer metastasis

1.2.1 Metastatic cascade

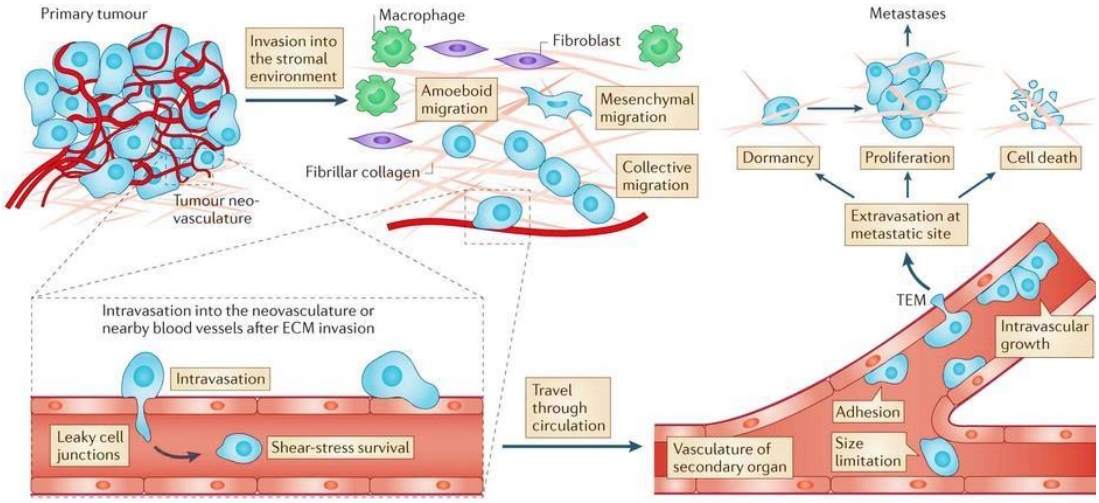

Figure 1. Process of cancer metastasis (Reymond et al., 2013).

The major cancer related mortality is due to the metastasis of primary tumor cells, which is a complex process that remains only partially understood at the biochemical and molecular level. By definition, cancer metastasis is the movement of cancer cells from the site where cancer originate (primary site), to grow in different sites (secondary sites) of the body. Cancer metastasis occurs through a series of sequential steps (Figure 1). First, with the help of tumor-associated macrophages, cancer cells move from the primary tumor site to the vasculature through invading the stroma and adjacent tissues. Then cancer cells transmigrate through endothelial cell junctions into the blood vessels. Once entered the bloodstream, cancer cells are transported through the circulatory system and finally attach to the endothelial wall of a blood vessel at the secondary site. Next, cancer cells transmigrate through the endothelial barrier. Although most of the cancer cells die after extravasation, the surviving

cancer cells start to proliferate immediately or after a period of cellular dormancy, and then form metastases in their new location (Hunter et al., 2008; Mehlen and Puisieux, 2006; Reymond et al., 2013).

Since metastases are responsible for approximately 90% of all human cancer deaths (Mehlen and Puisieux, 2006), dissecting the biological mechanism of metastasis at a molecular level is of great importance to metastasis-directed therapy.

1.2.2 Epithelial–mesenchymal transition

1.2.2.1 Role of epithelial–mesenchymal transition in cancer metastasis

Epithelial–mesenchymal transition (EMT) is a process by which an epithelial cell converts into a cell with mesenchymal phenotype that acquire migratory and invasive capabilities (Kalluri and Weinberg, 2009). Activation of an EMT program is a critical mechanism for acquiring malignant phenotypes by epithelial cancer cells (Kalluri and Weinberg, 2009; Thiery, 2002). More importantly, EMT is widely regarded as the major contributor to cancer metastasis (Heerboth et al., 2015; Kalluri and Weinberg, 2009). Therefore, uncovering the biological mechanism and molecular factors which lead to EMT is of vital importance for establishing therapeutic approaches targeting cancer metastasis.

1.2.2.2 Cellular events and change of molecular markers during EMT

During the process of EMT (Figure 2), the epithelial cells stepwise deconstruct cell–cell junctions (Huang et al., 2012; Lamouille et al., 2014; Yilmaz and Christofori, 2009); lose apical–basal polarity and gain front–rear polarity (Huang et al., 2012; Lamouille et al., 2014); reorganize epithelial cytoskeletal architecture into one that facilitate cell elongation and directional motility (Lamouille et al., 2014; Thiery and Sleeman, 2006; Yilmaz and Christofori, 2009), by which cells acquire invasive and migratory ability. The motility of these cells is enhanced by forming lamellipodia, filopodia and invadopodia (Lamouille

et al., 2014; McNiven, 2013; Ridley, 2011). The whole process of EMT can be characterized by changing of various cell markers, including loss of epithelial markers, such as E-cadherin, ZO-1, cytokeratin and so forth; as well as acquisition of mesenchymal markers, such as N-cadherin, Fibronectin, Vimentin and so on. Among these, loss of E-cadherin is the most intensively investigated one, and is considered as fundamental event for EMT.

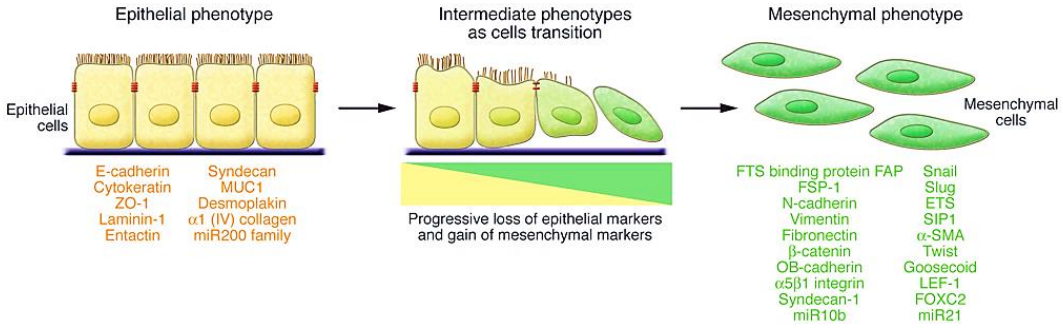

Figure 2. Morphological and phenotypic changes of cells undergo EMT and the representative molecular cell markers used to characterize (Kalluri and Weinberg, 2009).

E-cadherin is a transmembrane protein in charge of cell- cell adherent junction via forming extracellular interaction with another E-cadherin on neighboring cells (Huang et al., 2012; Lamouille et al., 2014). Intracellularly, cytoplasmic part of E-cadherin links to actin cytoskeleton in an α- or ß-catenin dependent manner (Heerboth et al., 2015; Tian et al., 2011). Tight cell-cell junctions assemble cell clusters and tissues together, thus E-cadherin depletion and the subsequent destruction of cell-cell adherent junctions potentiate individual cells to migrate, thereby initiates cancer metastasis. Intensive efforts have been put by scientists to elucidate the mechanisms by which E-cadherin is downregulated during EMT. One of the most well accepted mechanisms is the binding of various EMT transcription factors, such as Snail (Batlle et al., 2000; Cano et al., 2000), Slug (Bolos et al., 2003; Medici et al., 2008), Twist (Dave et al., 2011; Yang et al., 2010), Zeb (Graham et al., 2008; Sanchez-Tillo et al.,

2010), to the E-cadherin promoter, that transcriptionally represses E-cadherin gene. Moreover, these transcription factors also activate several mesenchymal genes (Lamouille et al., 2014). For instance, Twist is shown to induce the transcription of N-cadherin (Alexander et al., 2006). In addition, multiple cell signaling pathways collaborate in stimulating the expression of E-cadherin-repressing transcription factors, thereby promoting EMT through inhibiting transcription of E-cadherin gene (Lamouille et al., 2014).

1.2.3 Cell signaling pathways that regulate EMT and cancer metastasis

1.2.3.1 The role of RET receptor tyrosine kinase in cancer metastasis

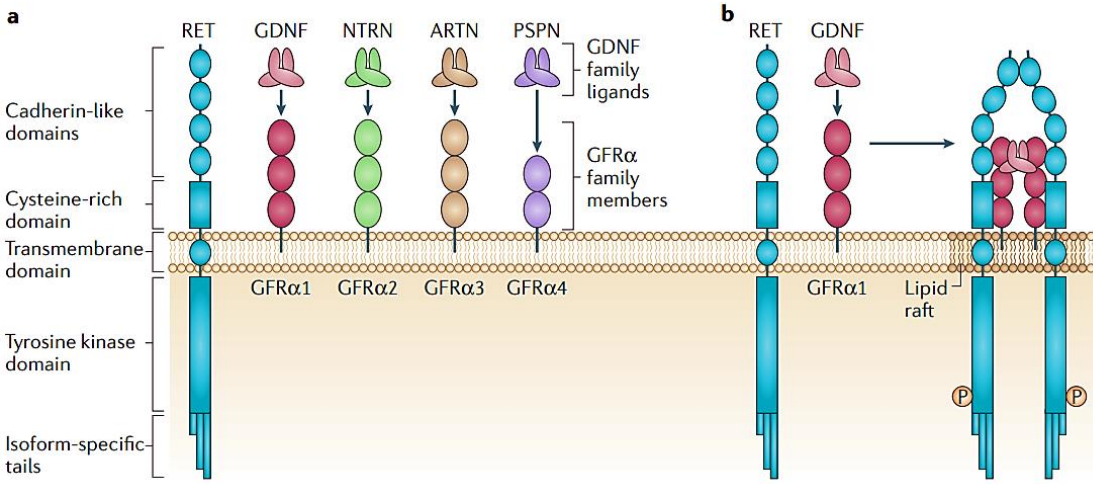

Figure 3. Molecular structure of RET receptor tyrosine kinase and its co-receptors, GFRα family members with their GDNF family ligands. RET has not direct binding ligand, so its activation is triggered by the binding of GDNF family ligands with GFRα family members. GFRα is the co-receptor of RET, the ligand-bound GFRα will heterodimerize with RET, thereby trigger autophosphorylation (P) and activate the downstream targets (Mulligan, 2014).

RET is a member of the receptor tyrosine kinase family, which plays a critical role in cancer invasion and metastasis. The binding of GDNF family ligands (GDNF, NTRN, ARTN and PSPN) to GFRA family co-receptors of RET (GFRα1, GFRα2, GFRα3 and GFRα4) triggers dimerization of RET and its co-receptor

GFRα (Figure 3), thereby leading to kinase activation and stimulation of downstream signaling pathways, thus influencing cancer cell survival, proliferation, migration and metastasis (Mulligan, 2014). The activation of RET and its downstream signaling pathway has been widely shown to facilitate cancer cells invasion and metastasis. For instance, RET was shown to trigger migration and metastasis of estrogen receptor positive breast cancer cells by activating FAK-STAT3 signaling pathway in a cytokine IL-6 dependent manner (Gattelli et al., 2013). Besides, the activation of RET promotes pancreatic tumor cell migration and perineural invasion by activating Ras-Raf-MEK-ERK and the phosphatidylinositol 3-kinase pathways (Veit et al., 2004)

In addition to ligand-induced RET activation, gain-of-function mutations of RET, which lead to constitutive activation, are also discovered in several types of human cancers. For instance, KIF5B-RET fusion was frequently observed in patients with lung adenocarcinoma and the tumor cells expressing this fusion are sensitive to RET inhibitor (Kohno et al., 2012). Moreover, another chimeric oncogene RET/PTC triggers the formation of an autocrine loop involving osteopontin and its cell surface receptors CD44 by transcriptionally activating osteopontin gene, thereby influencing cell–cell and cell–matrix interactions and promoting invasion, migration and metastasis of thyroid carcinoma cells (Castellone et al., 2004; Guarino et al., 2005).

1.2.3.2 The role of p38 MAPK signaling pathway in EMT and metastasis

Activation of RET activates p38 MAPK signaling pathway (Fonseca-Pereira et al., 2014; Ibiza et al., 2016; Zhao et al., 2009), which regulates EMT and cancer metastasis through different mechanisms. It has been shown that MAPK p38 signaling pathway regulates EMT and metastasis in both TGFß-dependent and -independent ways (del Barco Barrantes and Nebreda, 2012; Derynck and Zhang, 2003; Moustakas and Heldin, 2005). Moreover, p38 MAPK stabilize Twist1 protein by phosphorylating it and enabling its capability to trigger EMT and metastasis (Hong et al., 2011). Furthermore, activated p38 contributes to

RKIP depletion-induced EMT by enhancing phosphorylation of GSK3β, in turn enhancing the protein level of β-catenin, Snail and Slug (Al-Mulla et al., 2011). In addition, p38α activates hypoxia-inducible factor 1α (HIF1α) under the condition of hypoxia, thereby inducing EMT and metastasis (Emerling et al., 2005).

Other than EMT, p38 MAPK signaling pathway regulates cancer metastasis also by affecting other steps of the process, such as by inducing invasion, extravasation and formation of pre-metastatic niche (del Barco Barrantes and Nebreda, 2012). For instance, activated p38 MAPK induces ECM remodeling by increasing the expression of MMP1, MMP3 and MMP13, thereby promoting cancer cell invasion (del Barco Barrantes and Nebreda, 2012; Johansson et al., 2000; Park et al., 2011b). Futhermore, the interaction between colon cancer cells and endothelial cells triggers p38 MAPK activation in both types of cells, in turn increasing transendothelial permeability, thus facilitating cancer cells extravasation (Tremblay et al., 2006). In addition, activation of p38 MAPK pathway also contributes to CXCR4 and VEGFR1 mediated recruitment of BMDCs, which facilitates cancer cell metastasis by promoting pre-metastatic niche formation (Hiratsuka et al., 2011).

1.2.3.3 Other cell signaling pathways that regulate EMT and cancer metastasis

TGFß /SMAD is one of the most well-known signaling pathways contributing to EMT and metastasis. TGFß enhances cancer invasion and metastasis by stimulating the expression and secretion of MMP-2 and MMP-9 (Hagedorn et al., 2001). Binding of TGFß to its receptors activates their intracellular target SMADs, which finally translocate into nuclei and regulate transcription of EMT and cancer metastasis related genes (Feng and Derynck, 2005; Massague, 2012). Besides, it has been shown that EMT transcription factors cooperate with SMADs in response to TGFß stimulation (Lamouille et al., 2014). For instance, Snail collaborates with SMAD3-SMAD4 to repress transcription of E-cadherin gene, thus inducing EMT and cancer metastasis (Vincent et al., 2009).

In addition, TGFß mediated SMADs activation also directly induces the expression of a variety of EMT transcription factors, including Snail (Hoot et al., 2008), Slug (Morita et al., 2007), Zeb (Shirakihara et al., 2007), Twist (Kang et al., 2003).

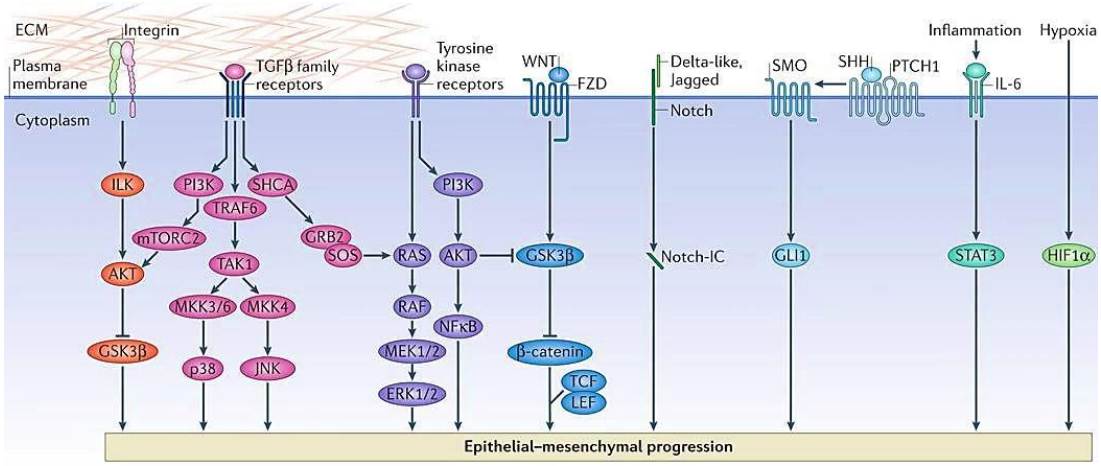

Figure 4. Cell signaling pathways implicated in EMT (Lamouille et al., 2014).

In addition to its direct role in repressing E-cadherin expression, TGFß signaling pathway also indirectly contributes to EMT by activating other cell signaling pathways (Figure 4). For example, TGFß leads to activation of PI3K/AKT signaling pathway, thus results in activation of both mTOR1 and mTOR2. Both mTOR1 and mTOR2 stabilize Snail expression, thereby repressing E-cadherin expression and trigger EMT (Bachelder et al., 2005; Lamouille et al., 2012). In addition, activation of PI3K/AKT signaling pathway enhances expression of filopodia, which greatly elevates motility of cancer cells (Yang et al., 2004). Moreover, Notch signaling pathway also plays an important role in promoting cancer metastasis through enhancing secretion of Interleukin 6 (IL-6) by Notch ligand Jagged1 (Guo et al., 2014; Sethi et al., 2011).

Other factors that act through receptor tyrosine kinases (RTKs) have also been shown to induce EMT by activating specific downstream signaling pathways (Figure 4). For example, hepatocyte growth factor (HGF) induces Snail expression by activating ERK MAPK pathway and by stimulating the binding of

early growth response 1 (EGR1) to the promoter of Snail gene (Grotegut et al., 2006). In addition to Snail, Slug expression can be also induced by HGF (Savagner et al., 1997). Besides, epidermal growth factor (EGF) induces Snail (Lu et al., 2003) or Twist (Lo et al., 2007) expression which results in loss of E-cadherin, thereby triggering EMT. Furthermore, insulin-like growth factor 1 (IGF1) activates its receptor and downstream signaling pathway, which in turn increases Snail expression, thus repressing E-cadherin expression and inducing EMT (Kim et al., 2007). Moreover, WNT signaling pathway also plays a key role in promoting EMT and metastasis. The binding of WNT ligands with Frizzled receptors prevents GSK3ß from phosphorylating ß-catenin, thereby stabilizing the function of ß-catenin. Once stabilized, ß-catenin regulates the expression of Snail gene *(Lamouille et al., 2014; Niehrs, 2012)*. In addition, platelet-derived growth factor (PDGF) induces nuclear localization of ß-catenin, thereby reducing E-cadherin level, thus promoting EMT (Yang et al., 2006).

1.2.4 Other regulators of EMT and cancer metastasis

The genetic control and biochemical determinants underlying the acquisitions of invasive and metastatic phenotype of cancer cells have been intensively investigated, and many factors have been validated to facilitate metastasis.

1.2.4.1 Chemokines and their receptors

Chemokines are small molecular proteins that interact with the G-protein-coupled chemokine receptors. It has been shown that chemokines play key roles in promoting cancer metastasis (Muller et al., 2001; Sarvaiya et al., 2013). For instance, CXCL12 and its receptor CXCR4 have been widely shown to initiate and mediate metastasis in a variety of human cancers, including lung (Phillips et al., 2003; Su et al., 2005), breast (Li et al., 2004; Liang et al., 2004; Wendt et al., 2008) colorectal cancer (Speetjens et al., 2009; Wendt et al., 2006) and so on. Cancer cells tend to highly express CXCR4, which leads them migrate to the organs with high level of CXCL12, including lung, brain, lymph

nodes, liver, and bone marrow (Bruce et al., 1970; Muller et al., 2001; Sarvaiya et al., 2013). In addition, CCR7-CCL19/CCL21 axis (Muller et al., 2006; Takanami, 2003) as well as CCR9-CCL25 (Amersi et al., 2008; Johnson-Holiday et al., 2011; Singh et al., 2011), CCR10-CCL27/CCL28 (Muller et al., 2001; Simonetti et al., 2006), CXCR3-CXCL9, CXCL10, CXCL11 (Cambien et al., 2009; Pradelli et al., 2009) and CXCR5-CXCL13 axis (Airoldi et al., 2008; Lopez-Giral et al., 2004) have also been shown to facilitate cancer metastasis.

1.2.4.2 Angiogenesis

Angiogenesis increases the chance for cancer cells to intravasate by providing larger vascular areas (Moserle and Casanovas, 2013). Besides, vascular endothelial growth factor (VEGF), which is essential for angiogenesis (Carmeliet, 2005), facilitates cancer cells intravasation and extravasation by increasing vascular permeability (Bates, 2010; Liu et al., 2002; Moserle and Casanovas, 2013). Furthermore, it has been shown that VEGFR1-expressing bone marrow-derived hematopoietic progenitor cells migrate to tumor-specific pre-metastatic sites and pave the way for the incoming cancer cells by forming the pre-metastatic niche and promoting vascularization (Kaplan et al., 2005).

1.2.4.3 Extracellular matrix (ECM) remodeling

A successful metastasis requires metastatic cancer cells to survive, colonize and proliferate at a distant site (Hunter et al., 2008; Mehlen and Puisieux, 2006), therefore, interaction between the disseminated cancer cells and the new microenvironment is of great importance. ECM is a non-cellular structure composed of diverse proteins, such as collagen, proteoglycans, glycoproteins and so forth.

As an important element of metastatic niche, ECM remodeling and the changing in cell-ECM interaction are critical to the initiation and progression of EMT (Lamouille et al., 2014) and play key roles in the invasion and metastatic colonization of cancer cells in the distant sites (Hoye and Erler, 2016). For

instance, integrin α3ß1 is indispensable for TGFß mediated EMT, by coordinating cross-talk between E-cadherin/β-catenin and TGFß/Smad signaling pathways (Kim et al., 2009). Additionally, the expression of integrin α5ß1 and its interaction with fibronectin are induced by the TGFß-stimulated EMT (Maschler et al., 2005; Mise et al., 2012). Furthermore, the interaction of Collagen type I with ß1-containing integrins facilitates pancreatic cancer cells invasion and metastasis via disrupting E-cadherin mediated cell-cell adhesion (Koenig et al., 2006). Moreover, the binding of integrin αvß6 to the TGFß isoforms activates TGFß-mediated EMT and cancer cell metastasis (Sheppard, 2005).

MMP-3, MMP-7 and MMP-9 are known to cleave E-cadherin into small fragments, thereby inhibiting E-cadherin and promoting EMT in an EGFR signaling pathway dependent manner (David and Rajasekaran, 2012; Maretzky et al., 2005; Najy et al., 2008; Noe et al., 2001). In addition to the cleaving function on E-cadherin, MMP3 upregulates Snail by elevating the cellular level of reactive oxygen species (ROS), which plays a key role in stimulating expression of Snail gene (Radisky et al., 2005). In addition, MMP9 also cooperates with Snail to induce EMT (Lin et al., 2011).

1.2.4.4 Hypoxia

Hypoxia, a well-known feature of tumor microenvironment, is emerging as a key factor in the regulation of cancer metastasis. Hypoxia activates HIF signaling, thereby facilitating cancer metastasis by various mechanism.

Hypoxia and HIF signaling activation facilitate cancer cells resistance to cytotoxic T lymphocyte-mediated immune attack (Palazon et al., 2014; Rankin and Giaccia, 2016) and natural killer cell-mediated antitumor responses (Baginska et al., 2013; Messai et al., 2014), thereby contributing to cancer cell survival and metastasis. Furthermore, HIF1α induces Snail and Twist expression by directly binding to their promoter (Higgins et al., 2007; Liu et al., 2014; Yang et al., 2008), thereby facilitating EMT and cancer metastasis.

It has been shown that hypoxia, on the one hand, facilitates metastasis via regulating ECM remodeling in the metastatic niche, on the other hand, regulates ECM by elevating the MMPs expression in cancer cells (Gilkes et al., 2014). Moreover, hypoxia results in modification of collagen matrix, thus leads to recruitment of bone marrow–derived cells (Gilkes et al., 2014; Rankin and Giaccia, 2016), which finally stimulate cancer cell metastasis via various mechanism, including secreting chemokines which recruit and guide cancer cell, as well as stimulating cancer cell extravasation (Gao et al., 2008; Kaplan et al., 2005; Rankin and Giaccia, 2016; Wong et al., 2011a).

In addition, hypoxia induces expression of VEGF-A, thereby stimulate angiogenesis and cancer metastasis (Joyce and Pollard, 2009; Maxwell et al., 1997).

1.2.4.5 Epigenetic control of EMT

Increasing amount of studies have been indicating that epigenetic regulation of E-cadherin level as well as EMT transcription factors expression and function play pivotal roles in modulating EMT process, thus regulating cancer cells migration and metastasis (Sun and Fang, 2016). The mechanism by which epigenetic events influence EMT and cancer metastasis will be discussed detailedly in Chapter 1.5.

1.3 Changes in nuclear structure in cancer cells

Despite of well-understood cellular and molecular changes taking place in cancer progression and metastasis, the clinical diagnosis of cancer still largely based on the cancer specific morphological changes, especially the alterations of nuclear structure (Zink et al., 2004). The most frequent observed morphological alterations of nuclear structure in cancer cells consist of changes in nuclear matrix, irregular nuclear shape and size, changes in the quantity and the size of nucleoli as well as in the chromatin structure and organization (Zink et al., 2004) (Figure 5).

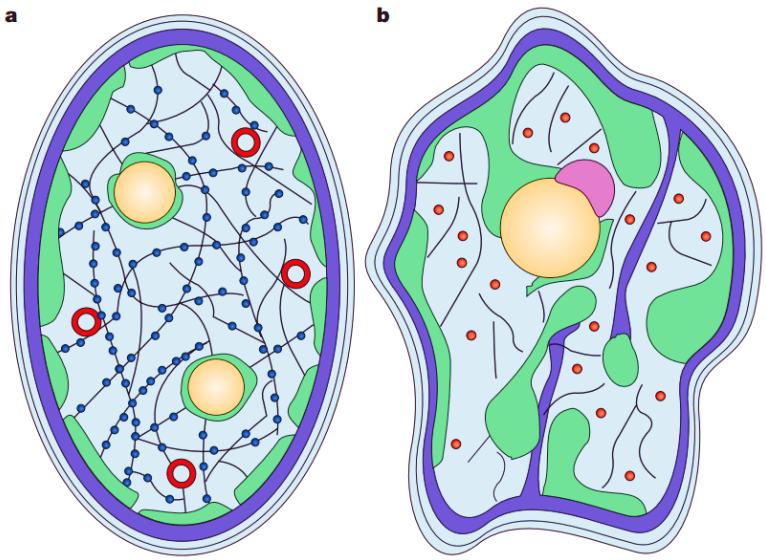

Figure 5. Nuclear structure in normal and cancer cells (Zink et al., 2004). a. Nucleus of normal cell. b. nucleus of cancer cell. Purple, nuclear lamina; green, heterochromatin; yellow, nucleoli; red, promyelocytic leukaemia (PML) body; pink, perinucleolar compartment (PNC)

1.3.1 Nuclear shape and size in cancer cells

Change of nuclear shape is an important morphological alteration observed frequently in cancer progression. In contrast to the normal nucleus with a regular rounded or oval shape, the nucleus of a cancer cell becomes odd with irregular shape and begin to fold (Zink et al., 2004) (Figure 5). In fact, changes in nuclear shape has been used as an important diagnostic feature in identifying various cancer cells. For example, checking the nuclear shape with Pap smear has been widely applied in early detection of cervical cancer (Webster et al., 2009). In addition, deformed nuclei with malleable appearance are also regarded as a key feature for diagnosing SCLC (Zink et al., 2004). In contrast to the frequent observation in cancer cells, the exact role of altered nuclear shape in cancer cells and its potential cause are still poorly understood. Some studies claim that altered nuclear shape associates with chromatin reorganization and genomic instability, thereby affecting gene expression and cancer progression (He et al., 2008; Oberdoerffer and Sinclair, 2007). In

addition, others suggest that altered nuclear shape contributes to cancer metastases by reducing nuclear stiffness, which enables cancer cells to penetrate the tissues (Dahl et al., 2008; Webster et al., 2009). In respect to the cause of altered nuclear, aberrant expression and architecture of nuclear lamina are considered as the principle determinants of nuclear shape alteration (Goldman et al., 2002).

1.3.2 Changes in nuclear matrix in cancer cells

Nuclear matrix, a filamentous protein network in nucleoplasm, functions as skeleton to provide the framework for maintaining the overall size, shape and spatial arrangements of the nucleus. Moreover, nuclear matrix acts as scaffold to support diverse biochemical processes including, transcription, RNA splicing, DNA replication and so on. As a nuclear ribonucleoprotein network, nuclear matrix is composed of more than 200 nuclear matrix proteins including lamins, nuclear mitotic apparatus protein (NUMA), B23, hnRNP and so forth (Fey et al., 1986; Mancini et al., 1996; Mattern et al., 1996; Zink et al., 2004). During cancer progression, the protein composition of nuclear matrix is changed. For instance, p114, which binds to the matrix attachment region (MAR) of DNA sequence, is detected specifically in human breast cancer, but not in normal breast tissues. Therefore, it is proposed to be a reliable diagnostic marker for breast cancer (Yanagisawa et al., 1996). In addition, some other nuclear matrix proteins are also specifically found in certain types of cancer tissues, such as PC1 in prostate tumor (Partin et al., 1997), a fusion protein between nuclear matrix protein NUMA and retinoic acid receptor-α (RARα) in acute promyelocytic leukemia (Sukhai et al., 2004) as well as BLCA-4 in bladder cancer (Konety et al., 2000).

1.3.3 Alteration of nucleoli and perinucleolar compartment (PNC)

Alteration of nucleolus is also frequently observed in cancer cell. Cancer nucleoli are significantly enlarged in Hodgkin' disease and large cell carcinoma,

and has developed as a key diagnostic trait (Frost, 1986; Zink et al., 2004). At the periphery of the nucleolus, there is an irregularly shaped dynamic structure physically associated with nucleolus called perinucleolar compartment (PNC), which is enriched with RNA-binding proteins and short RNAs transcribed by RNA polymerase III (Huang et al., 1997; Pollock and Huang, 2010). PNC specifically exists in cancer cells but is rarely present in normal cells, therefore PNC is suggested as potential prognostic marker for cancer (Huang et al., 1997; Kamath et al., 2005; Norton et al., 2008). Furthermore, the presence of PNC widely correlates with metastatic capacity of various human cancers, including prostate cancer (Norton et al., 2008; Pettaway et al., 1996), colorectal cancer (Norton et al., 2008) and breast cancer (Samant et al., 2000).

1.3.4 Promyelocytic leukemia (PML) bodies

Promyelocytic leukemia (PML) nuclear body is a nuclear matrix associated multiprotein complex. These small structures of 0.2–1 μm in diameter exist in the nuclei of most cells with a number of 10-30 per nucleus (Boisvert et al., 2000; Zink et al., 2004). PML bodies are assembled by tumor suppressor PML protein together with dozens of other proteins, such as retinoblastoma protein (Rb) and p53 (Zhong et al., 2000). It has been shown that PML bodies are the sites of p53 post-translational modification (Bernardi and Pandolfi, 2003; Fogal et al., 2000; Pearson et al., 2000), and PML bodies play key roles in both p53-dependent and –independent apoptosis (Bernardi and Pandolfi, 2003; Wang et al., 1998). Moreover, PML bodies also play important roles in genomic stability and DNA repair (Bernardi and Pandolfi, 2003). Reduction or depletion of PML level is observed in several types of human cancers, including prostate, colon, breast, lung cancer and lymphomas (Chan et al., 1998; Gurrieri et al., 2004; Zhang et al., 2000). In addition, PML depletion is also associated with malignant invasion and progression of prostate cancer and breast cancer (Koken et al., 1995).

1.3.5 Changes in chromatin organization

Alterations in chromatin organization are another important features of malignant transformation. It has been widely shown that individual chromosomes occupy discrete nuclear regions, called chromosome territories (CTs). Furthermore, CTs display a radial positioning, with gene-poor CTs which usually present more close to nuclear periphery, whereas gene-rich CTs are nearer to the nuclear center (Boyle et al., 2001; Croft et al., 1999; Zink et al., 2004). In the nuclei of cancer cells, the radial chromatin order appears to be partially lost (Cremer et al., 2003).

The most well-investigated chromosomal aberration in cancer cells is chromosomal translocation, which has been applied as an important diagnostic trait (Zink et al., 2004). For instance, t (14; 18) (q32; q21) translocation is an important diagnostic marker for follicular lymphomas. Moreover, t (11; 14) (q13; q32) translocation is a maker of mantle-cell lymphoma (1997; Zink et al., 2004). In addition, changes in chromatin texture, caused by either chromatin condensation or decondensation, are also frequent observed in cancer cells, and suggested to be of diagnostic significance (Frost, 1986; Lukasova et al., 2004). The easiest observations of chromatin texture alterations are chromatin coarsening and exaggerative open chromatin (Zink et al., 2004). Activation of HRAS oncogene is one of the causes for chromatin coarsening, which leads to heterochromatin aggregation and correlates with metastatic potential of cancer cells (Fischer et al., 1998). In addition, exaggerated open chromatins, resulted from loss of heterochromatin aggregates, also frequently present in various types of cancer cells (Frost, 1986).

1.4 Nuclear envelope and nuclear lamins

1.4.1 Structure and components of the nuclear envelope

Nuclear envelope is composed of inner and outer nuclear membranes, nuclear lamina and nuclear pore complexes (NPCs). It plays an essential role in

separating the contents of the nucleus from the cytoplasm, providing the structural framework of the nucleus and maintaining the nuclear structure (Chow et al., 2012; Coutinho et al., 2009) (Figure 6).

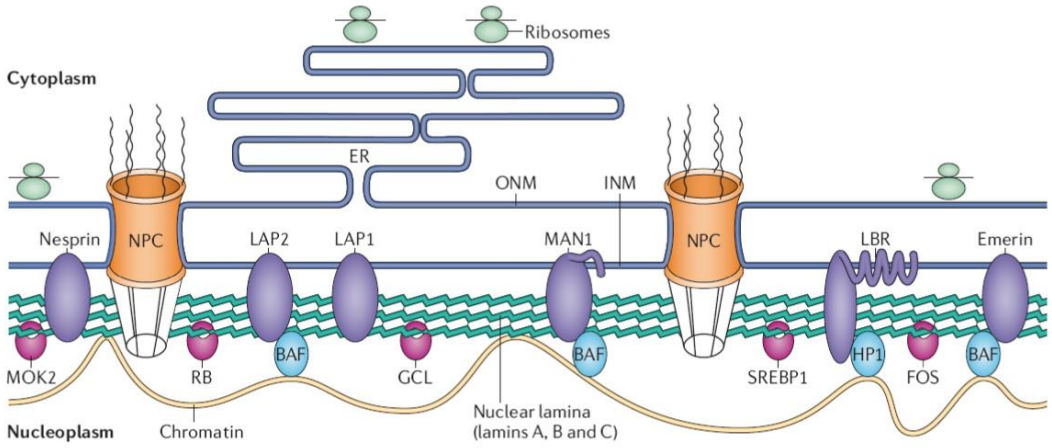

Figure 6. Structure of nuclear envelope (Coutinho et al., 2009).

The outer nuclear membrane is continuous with the membrane of the rough endoplasmic reticulum (ER) with numerous ribosomes attached to the surface. Moreover, the perinuclear space between the inner and outer nuclear membranes is also directly connected with the lumen of the endoplasmic reticulum. In contrast, the inner nuclear membrane associates with a variety of nuclear specific proteins. The outer and inner nuclear membranes are fused into a highly curved membrane at the sites of NPCs, which are composed of approximately 30 different proteins, termed nucleoporins (Doucet and Hetzer, 2010). NPCs act as selective channels that function together with soluble receptors to guide exchange of molecules (including proteins and RNA) between the nucleus and cytoplasm. The selective proteins and RNA trafficking mediated by NPCs are essential to the establishment of inner nuclear composition and regulation of gene expression, and also play a role in regulating cancer progression and metastasis (Chow et al., 2012; Strambio-De-

Castillia et al., 2010; Wente and Rout, 2010). For instance, nucleoporin NUP155 was shown to interact with HDAC4 and enhance its inhibitory effect on the expression of target genes (Kehat et al., 2011). Furthermore, nucleocytoplasmic shuttling of Smad2, mediated by nucleoporins NUP214 and NUP153, is of critical importance in regulation of gene expression mediated by TGFß/SMAD signaling pathway (Xu et al., 2002). Besides, NUP153 also facilitates nuclear translocation of activated ERK1-ERK2 by direct interaction (Shindo et al., 2016). Moreover, depletion of nucleoporin NUP358 increases the cAMP-mediated cell adhesion in ovarian cancer cells (Gloerich et al., 2011). In addition, overexpression of nucleoporin NUP88 is widely observed in various cancers, and is considered as a cancer biomarker because of its association with aggressive cancer phenotype and poor prognosis (Agudo et al., 2004; Martinez et al., 1999; Zhang et al., 2007).

1.4.2 Nuclear lamins

The structural support to the nucleus is provided by fibrous meshwork of intermediate filaments which locate underlying the inner nuclear membrane, called nuclear lamina. The structural elements of nuclear lamina are lamins, which form polymers to constitute nuclear lamina. Nuclear lamins are subdivided into two different types, A- and B- type, based on their structural and protein features, expression pattern as well as biochemical and dynamic properties (Dechat et al., 2010; Dittmer and Misteli, 2011). A- type lamins are made up of two major isoforms, lamin A and lamin C, which result from alternative splicing of *LMNA* gene (Lin and Worman, 1993). In contrast, lamin B1 and lamin B2, which are the two main B- type lamins, are encoded by *LMNB1* gene and *LMNB2* gene, respectively (Peter et al., 1989; Vorburger et al., 1989). As illustrated in Figure 7, the protein structure of these two types of lamins generally resemble in the N-terminal head, central α-helical rod domain as well as C-terminal tail containing immunoglobulin domain and a conserved CAAX box (Dittmer and Misteli, 2011), which is the one responsible of nuclear

localization of lamins and establishment of protein-protein interactions (Kalinowski et al., 2013; Rusinol and Sinensky, 2006).

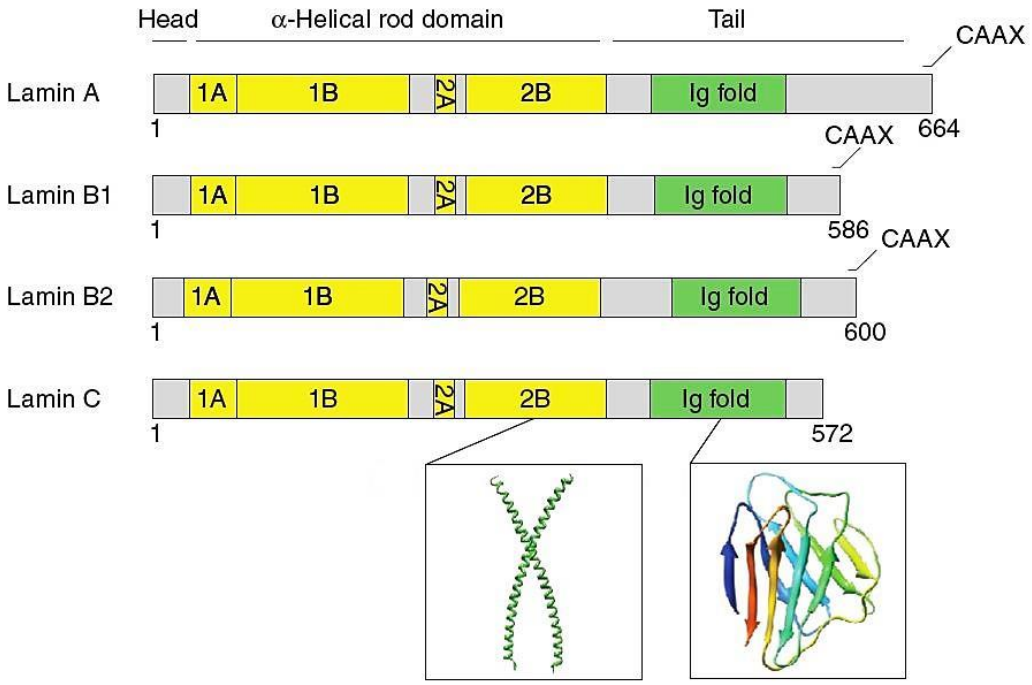

Figure 7. Protein structure of nuclear lamins (Dittmer and Misteli, 2011).

In mammals, B-type lamins are constitutively expressed in all somatic cells, whereas A-type lamins are developmentally regulated and expressed in a tissue- and cell type-specific manner (Dechat et al., 2010; Dittmer and Misteli, 2011). For instance, A-type lamins are absent in most neural and neuroendocrine cells as well as hematopoietic cells (Broers et al., 1997; Rober et al., 1990).

It is widely acknowledged that A- and B-type lamins form separate filamentous networks and both networks overlap and interact with each other (Dechat et al., 2010). In addition, rising evidences show that both types of lamin structures appear to compensate each other. For example, depletion of lamin B1 in Hela cells enhances the mesh size of A-type lamins network (Shimi et al., 2008). In consistence, another study also shows an enlarged A-type lamins meshwork after mutating lamin B1 (Vergnes et al., 2004).

In respect to their subnuclear localization, although the majority of lamins are

present in the nuclear periphery, some of them locate within the nucleoplasm (Dittmer and Misteli, 2011; Hozak et al., 1995). Nuclear peripheral lamins, which are integrated into the nuclear lamina, are relatively stable. In contrast, the nucleoplasmic A-type lamins are thought to be more dynamic and mobile. B-type lamins in the nucleoplasm appear to be static and immobile (Broers et al., 1999; Dechat et al., 2008; Moir et al., 2000b; Shimi et al., 2008).

1.4.3 Function of nuclear lamins

1.4.3.1 The role of lamins in regulating nuclear shape and mechanical properties

Lamins are of critical importance to regulate nuclear shape and mechanical stability. Two independent studies have shown nuclear deformation in mouse embryonic fibroblasts (MEFs) isolated from *Lmna*-/- mice (Houben et al., 2007; Lammerding et al., 2004). Similar observation was also made by another study showing that loss of A-type lamins results in nuclear deformation in both human ES cells and epithelial cells (Pajerowski et al., 2007). The deformed nuclei caused by lamin A/C depletion are more fragile and show decreased mechanical stiffness compared with *Lmna* +/+ nuclei (Broers et al., 2004). Besides, mutation of A-type lamins also leads to irregular nuclei (Bechert et al., 2003; Favreau et al., 2003; Vigouroux et al., 2001). In addition to A-type lamins, B-type lamins also form stiff meshwork which provides nuclei with structural strength enabling the nuclei to resist deformation (Panorchan et al., 2004a; Panorchan et al., 2004b).

1.4.3.2 The role of lamins in DNA replication, damage and repair

Several studies have shown the role of lamins in regulation of DNA replication. For example, lamins colocalize with replication-associated protein, such as proliferating cell nuclear antigen (PCNA), at DNA replication foci (Kennedy et al., 2000; Moir et al., 1994; Shumaker et al., 2008). Moreover, depletion (Meier et al., 1991; Newport et al., 1990) or dominant-negative mutations (Moir et al.,

2000a; Shumaker et al., 2008; Spann et al., 1997) of B-type lamins disable the cells to replicate their DNA.

In addition, lamins regulate DNA repair. It has been reported that cells expressing progerin, which is a truncated version of lamin A responsible of Hutchinson Gilford Progeria Syndrome (HGPS), have a high level of DNA damage by increasing the level of double-strand break marker γ-H2AX and inhibiting the recruitment of DNA repair factor p53-binding protein (53BP1) at the sites of DNA damage (Liu et al., 2005). Moreover, lamin A activates SIRT6 in response to DNA damage, thereby facilitating SIRT6-mediated DNA repair (Ghosh et al., 2015). Furthermore, lamin B1 stabilizes RAD51, an essential key factor in the homologous recombination response taking place at the DNA double-strand breaks induced by ionizing radiation, in turn contributing to DNA repair (Liu et al., 2015a).

1.4.3.3 The role of lamins in gene expression

Increasing evidences support that lamins play key role in regulating gene expression by influencing transcription and a number of signaling pathway. On the one hand, lamins interact with various transcription factors and sequester them away from chromatin, thereby repressing the transcription of their target genes (Heessen and Fornerod, 2007). For example, lamin B1 associates with transcription factor Oct-1 at the nuclear periphery, thereby preventing Oct-1 from activating the transcription of its target genes (Malhas et al., 2009). Furthermore, the sequestration of c-Fos at the nuclear envelope through direct interaction with lamin A/C was shown to suppress the DNA-binding thus the transcriptional activity of Activating Protein 1 (AP-1) (Ivorra et al., 2006). On the other hand, lamins also act as platforms for signaling molecules. For instance, A-type lamins facilitate dephosphorylation of pRb by recruiting nuclear phosphatase PP2A, thereby restoring the stability of pRb (Van Berlo et al., 2005). Moreover, lamins influence wnt and TGFβ signaling pathway(Liu et al., 2003; Vaughan et al., 2001) by interacting with emerin.

Additionally, lamins regulate gene expression by affecting RNA polymerase II activity. Downregulation of lamin B1 in Hela cells leads to inhibition of RNA polymerase II activity, thereby repressing the RNA synthesis (Tang et al., 2008). Besides, disrupting the lamin organization with dominant negative A-type lamins also represses RNA polymerase II activity (Spann et al., 2002).

1.4.3.4 The role of lamins in epigenetic regulation

Lamins play a crucial role on an epigenetic level by modifying chromatin structure, in turn influencing gene expression. Nuclear lamins are thought to be global regulators of chromatin via directly tethering heterochromatin to nuclear envelope. Depleting or mutating nuclear lamins results in loss of peripheral heterochromatin (Galiova et al., 2008; Nikolova et al., 2004; Shimi et al., 2008; Sullivan et al., 1999). These lamin-associated changes in heterochromatic organization are reflected by alterations in histone modification, including reduced levels of heterochromatin markers histone H3 lysine 9 trimethylation (H3K9me3), histone H3 lysine 27 trimethylation (H3K27me3) as well as elevated level of histone H4 lysine 20 trimethylation (H4K20me3) (Scaffidi and Misteli, 2006; Shimi et al., 2008; Shumaker et al., 2006). Furthermore, ectopical overexpression of lamins in myoblasts leads to alteration of chromatin organization along with enhanced level of H3K4me3, a marker of transcriptional activation (Hakelien et al., 2008).

Human genome regions that interact with the nuclear lamins are referred to as lamina-associated domains (LADs) (Guelen et al., 2008). These domains are enriched with heterochromatic markers and labelled as gene-poor and transcriptionally repressive (Guelen et al., 2008; Peric-Hupkes et al., 2010). However, several other studies also claimed that lamins do not completely repress the expression of all the genes within LADs (Finlan et al., 2008; Kumaran and Spector, 2008; Reddy et al., 2008; Zheng et al., 2015). Moreover, Kim et al. demonstrated that B-type lamins binding profiles are associated with gene silencing but such interaction between B-type lamin and the silenced gene

is not necessarily required in mouse embryonic stem cells and differentiated trophectoderm cells (Kim et al., 2011).

1.4.4 Nuclear lamins as cancer biomarkers

A number of studies have been analyzed the expression of lamins in different cancers (Sakthivel and Sehgal, 2016). By examining a variety of lung cancer cell lines and specimens, Broers *et al*. revealed that B-type lamins is considerably downregulated in NSCLC, especially adenocarcinomas. In contrast, lamin A/C levels are significantly reduced in both SCLC cell lines and specimens (Broers et al., 1993). Another studies revealed that lamin A/C level is dramatically enhanced in oncogene v-rasH-expressing SCLC cell lines as well as v-rasH driven large cell carcinoma-like tumors. Importantly, the increased level of lamin A/C is positively associated with enhanced malignancy of lung cancer (Kaufmann et al., 1991). In consistence, another independent study also demonstrated that lamin A/C is overexpressed in adenocarcinoma cell line A549 in comparison with normal lung fibroblast cell line MRC-5 (Rubporn et al., 2009).

Moreover, high level of lamin A/C has been shown to correlate with poor prognosis and survival of colorectal cancer patients, and proposed to be a significant risk indicator for colorectal cancer (Willis et al., 2008). The interaction between lamin A/C and S100A6, an interacting partner of ß-catenin, is implicated in colorectal cancer development and progression (Kilanczyk et al., 2012). However, paradoxically, another study showed that low level of lamin A/C associates with increased colon cancer recurrence (Belt et al., 2011).

Lamin B1 upregulation is also observed in the prostate cancer and correlates with cancer differentiation level (Coradeghini et al., 2006). Moreover increased phosphorylation of B-type lamins in prostate cancer cell associates with altered structure of nuclear envelope, thus leading to changes in genes expression, which may ultimately contribute to a more aggressive cancer phenotype (Barboro et al., 2012; Sakthivel and Sehgal, 2016). Aside from B-type lamins,

A-type lamin levels have been shown to correlate with prostate cancer cell growth, invastion and migration via affecting PI3K/AKT/PTEN signaling pathway. Therefore, lamin A/C was prosposed to be a potential oncogenic biomarker and novel therapeutic target for prostate cancer (Kong et al., 2012). In support of this, another study revealed that the level of A-type lamins are positively correlated with Gleason score of prostate cancers. Therefore, lamin A was proposed to be a potential biomarker for discriminating between low- and high-grade prostate cancers (Skvortsov et al., 2011).

Lamin A/C expression is reduced in keratinocytic tumors, especially in basal cell carcinoma and poorly differentiated cutaneous squamous cell carcinoma. In contrast, B-type lamins are downregulated in most well-differentiated cutaneous squamous cell carcinoma and keratoacanthomas. Therefore the levels of nuclear lamins are based on the differentiation level and transformation of skin, which may serve as a diagnostic trait of keratinocytic cancer (Oguchi et al., 2002). By correlating the proliferation rate of basal cell carcinomas cells with lamins expression, another study showed that loss of lamin A is associated with higher growth rate, whereas absence of lamin C is correlated with slow growth rate. It suggests that lamin A may negatively affect proliferation of basal cell carcinomas (Venables et al., 2001).

By screening and correlating the mRNA level of both A- and B-type lamins in breast cancer and tumor adjacent non-cancerous tissues with clinicopathological data, Wazir et al. revealed that higher level of A-type lamins was correlated with better survival and clinical outcome. In contrast, reduced lamin B1 level associates with higher tumor grade and worse clinical outcome (Wazir et al., 2013). Moreover, loss of lamin A/C were also found in breast cancer cells along with aberrations in nuclear morphology and aneuploidy (Capo-chichi et al., 2011).

In addition, Wong et al. revealed a significant upregulation of lamin B1 in hepatocellular carcinoma tissue and found a highly sensitive and specific way

to detect early hepatocellular carcinoma by checking the circulating lamin B1 mRNA level in patients' blood samples (Wong and Luk, 2012). Similar study also showed that elevated lamin B1 level serves as an useful clinical marker for early detection of hepatocellular carcinoma, and positively correlates with tumor stages, tumor sizes, and number of nodules (Sun et al., 2010).

The elevated lamin B1 level is correlated with poor prognosiss and increased metastatic incidence. Importantly, lamin B depletion reduces the proliferation, invasion and tumorigenicity of pancreatic cancer cells (Li et al., 2013). Moreover, decreased levels of both nuclear A- and B-type lamins are found and proposed to be potential biomarkers of early stages of gastrointestinal malignancy and gain of cytoplasmic lamin A/C level is observed and may serve as an indicator for more malignant stages of gastric cancer (Moss et al., 1999; Sakthivel and Sehgal, 2016). In addition, loss of A-type lamins enhances aggressiveness and drug resistance of human neuroblastoma (Maresca et al., 2012).

Table 1. Role of nuclear lamins in different types of cancers

Type of cancer	**alteration of lamins**	**references**
Lung cancer	Reduced A-type lamins level in SCLC Reduced B-type lamins level in NSCLC	(Broers et al., 1993; Kaufmann et al., 1991; Rubporn et al., 2009)
Colorectal cancer	Both elevated and reduced lamin A/C level	(Belt et al., 2011; Kilanczyk et al., 2012; Willis et al., 2008)
Prostate cancer	Elevated lamin A or lamin B1 level	(Barboro et al., 2012; Coradeghini et al., 2006; Helfand et al., 2012; Kong et al., 2012; Skvortsov et al., 2011)
Skin cancer	Reduced A- or B-type lamins	(Oguchi et al., 2002; Venables et al., 2001)
Breast cancer	Reduced A- or B-type lamins	(Capo-chichi et al., 2011; Wazir et al., 2013)
Hepatocellular cancer	Elevated lamin B1 level	(Sun et al., 2010; Wong and Luk, 2012)

Type of cancer	alteration of lamins	references
Pancreatic cancer	Elevated lamin B1 level	(Coradeghini et al., 2006; Li et al., 2013)
Gastric cancer	Elevated A- or B-type lamins	(Moss et al., 1999)
Neuroblastoma	Reduced A-type lamins	(Maresca et al., 2012)

1.4.5 Nuclear lamins and cell migration

Willis et al. observed an enhanced cell motility and invasiveness by ectopically expressing the lamin A in colorectal cancer cells. Moreover, they found that lamin A upregulates the T-plastin, an actin bundling protein, and lead to downregulation of E-cadherin, thereby facilitating cancer migration and invasion (Willis et al., 2008). However, in contradiction to this study, Lu et al. showed that increased level of lamin A/C impedes lung cancer cell motility by triggering actin remodeling (Lu et al., 2009).

Furthermore, loss of A-type lamins has been shown to significantly induce the cell migration by reducing the nuclear lamina stiffness (Harada et al., 2014). In addition, lamin B1 facilitates the migration of epicardial cells by influencing the expression of genes related to cell adhesion and the extracellular matrix function (Tran et al., 2016).

1.5 Epigenetic regulation of chromatin in cancer

Alterations of chromatin organization and structure are frequently observed in human cancers, therefore emphases have been made on the role of chromatin remodeling and modification in driving cancer initiation and metastasis. It is widely known that genomic DNA wrap around a discrete protein octamer, made up of histone proteins H2A, H2B, H3 and H4, to form the nucleosome core particles, which are fundamental units of chromatin (Kornberg, 1974; Kornberg and Thomas, 1974). Additionally, nucleosomes are further folded into an ordered and compacted chromatin with the help of linker histone H1 and other

non-histone proteins (Laybourn and Kadonaga, 1991). The altered affinity between chromatin proteins and DNA as well as its resulting changes in chromatin architecture are of great importance for gene expression and other biological processes (Nair and Kumar, 2012).

1.5.1 Chromatin remodeling in cancer

Gene transcription requires not only the general transcription machinery and transcription factors but also the alteration of local structural dynamics of chromatin to enable the accesses of various factors to the genes (Khan et al., 2015; Nair and Kumar, 2012). The compactness and accessibility of chromatin intimately associate with transcriptional activity. The less condensed chromatin is usually transcriptionally active, because the open structures facilitate the DNA accessibility to the transcription factors. Chromatin accessibility is regulated by ATP-dependent chromatin remodeling enzymes (chromatin remodelers), which are capable of modifying the chromatin architecture. To date, four families of chromatin remodelers have been well identified to alter chromatin structures by regulating the nucleosome mobility and positioning, including SWI/SNF (BAF), ISWI, CHD/NuRD and INO80 family (Langst and Manelyte, 2015). The role of chromatin remodelers in tumorigenesis and cancer metastasis has been intensively studied. For example, loss of BRM and BRG1, which are the subunits of SWI/SNF complex, were shown to facilitate cancer progression and metastasis by downregulating tumor suppressor genes and upregulating oncogenes and metastasis-promoting genes (Marquez-Vilendrer et al., 2016). Another study highlighted the role of Smarcd3/Baf60c, subunits of SWI/SNF family, in promoting the EMT of breast cancer cells by inducing the Wnt5a signaling pathway (Jordan et al., 2013). Moreover, metastatic tumor antigen 1 (MTA1), a core-subunit of NuRD complex, is upregulated in various human cancers and correlates with higher tumor grade, aggressiveness and poor prognosis (Lai and Wade, 2011). MTA1 is also implicated in several receptor tyrosine kinase-driven signaling pathway, such as HER2, estrogen

receptor (ER), thus influencing cancer progression and metastasis (Mazumdar et al., 2001; Molli et al., 2008).

1.5.2 Posttranslational modifications of histones

Posttranslational modifications of histones have been shown to modulate the overall affinity of nucleosome histones with DNA, alter nucleosome mobility, thus regulating chromatin relaxation and condensation (Nair and Kumar, 2012). The most well-known modifications of histones are methylation (me), acetylation (ac), ubiquitination (ub) as well as phosphorylation (ph) on certain amino acid (Berger, 2007; Kouzarides, 2007) (Figure 8). Histone methylation occurs at different degree depending on how many methyl groups are added onto the amino acid residue, including monomethyl (me), dimethyl (me2), trimethyl (me3). Furthermore, different sites of histone amino acid residues can be modified, such as histone H3 lysine (K) 4 (H3K4), H3K9, H3K27 or arginine (R) site 2 (H3R2), H3R8 and so on (Figure 8).

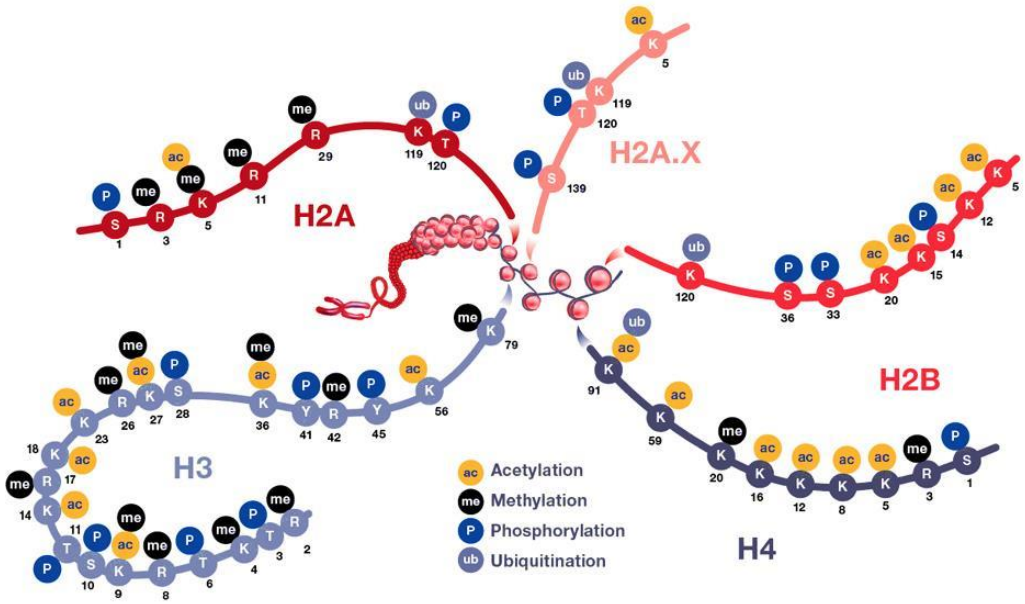

Figure 8. Posttranslational modification of histones. (www.thermofisher.com)

Histone modifications are dictated by various enzymes including those which add a specific modification (referred to as “writers”) as well as enzymes which

remove a specific modification (referred to as “eraser”) (Khan et al., 2015; Nair and Kumar, 2012). Histone acetyltransferases (HATs), histone methyltransferases (HMTs) and histone kinases are the examples of “writers” which add acetyl, methyl and phosphoryl groups, respectively. Whereas histone deacetylases (HDACs), histone demethylases (HDMs) and histone phosphatases are examples of “erasers” which remove acetyl, methyl and phosphoryl groups, respectively (Khan et al., 2015).

1.5.3 Role of histone modification in gene expression

Histone modifications influence gene expression in different ways (Table 2). For instance, histone acetylation associates with gene transcriptional activation (Hebbes et al., 1988; Verdin and Ott, 2015). Whereas histone methylation acts diversely as activator or repressor to gene expression depending on which amino acid residue is methylated and how many methyl groups are added onto the certain amino acid residue. For example, H3K4me3 and H3K36me3 associate with transcriptional activation, whereas, H3K9me3, H3K27me3 and H4K20me3 are correlated with transcriptional repression (Barski et al., 2007; Zentner and Henikoff, 2013).

Histone posttranslational modification influences the affinity between histone proteins and DNA by altering the steric effects and/or charge interactions, in turn resulting in the change of chromatin architecture. For instance, H4K16 acetylation induces chromatin relaxation by impeding the formation of higher order chromatin structure thereby resulting in an open chromatin and facilitating transcriptional activation (Shogren-Knaak et al., 2006). On the other hand, histone modification alters the interaction between chromatin and chromatin binding proteins. For instance, H3K9me3 is recognized by heterochromatin protein 1 (HP1), which play a key role in inducing the formation of compact chromatin structure thereby reducing the accessibility of chromatin, which leads to transcriptional repression of target genes (Bannister et al., 2001).

1.5.4 Role of histone modification in cancer initiation and progression

Various histone modifications have been proposed to be of diagnostic and prognostic value in human cancers and play a critical role in cancer progression and (Table 2). For instance, H3K9me3 silences several tumor suppressor genes by forming a heterochromatic structure, in turn impeding transcriptional initiation (Nguyen et al., 2002). Furthermore, the decreased level of H2B monoubiquitination (H2Bub) during breast cancer progression and metastasis is essential to estrogen receptor-α (ERα) regulated gene transcription in breast cancer cells by promoting transcriptional elongation of target genes and maintaining chromatin dynamics overall (Prenzel et al., 2011). In addition, loss of H3K27me3 is correlated with shorter overall survival time of cancer patients and is proposed to be a prognostic indicator for poor clinical outcome in patients with breast, ovarian, and pancreatic cancers (Wei et al., 2008). Besides, bivalent configuration of H3K4me3 and H3K27me3 is responsible for poising genes which are enriched in PI3K and TGFβ signaling pathways, thus leading to epigenetic silencing in ovarian cancer cells. Cancer specific bivalent marks are also proposed to potentially influence the cancer progression as well as the subsequent development of drug resistance (Chapman-Rothe et al., 2013).

Table 2. The role of histone modifications in human cancer (adapted from Khan, S.A *et al*. 2015) (Khan et al., 2015).

Modification	Writers	Erasers	Function	Cancer types
H3K9ac	GCN-5	SIRT-1; SIRT-6	Transcription initiation	Lung, breast, varian
H3K18ac	CBP/p300		Transcription initiation and repression	Lung, prostate, breast, esophagus
H4K5ac	CBP/P300; HAT1; TIP60; HB01		Transcription activation	Lung
H4K8ac	TIP60; HB01		Transcription activation	Lung
H4K16ac	TIP60; hMOF	SIRT-1; SIRT-2	Transcription activation	Colorectal, Lung, breast

Modification	Writers	Erasers	Function	Cancer types
H3K4me	SETD1A, 1B; ASH1L; MLL1, 2, 3, 4; SETD7	KDM1A; DM1B, 5B; NO66	Transcription activation	Prostate, kidney
H3K4me2	SETD1A, 1B; MLL1, 2, 3, 4; SMYD3	KDM1A, 1B, 5A, 5B, 5C, 5D; NO66	Transcription activation	Prostate, lung, kidney, breast, pancreatic, liver
H3K4me3	SETD1A, 1B; ASH1L; MLL1, 2, 3, 4; SMYD3; PRMD9	KDM2B, 5A, 5B, 5C, 5D; NO66	Transcription elongation	Kidney, liver, prostate
H3K9me	SETDB1; G9a; EHMT1; PRDM2	KDM3A, 3B; KDM3B; PHF8; JHDM1D	Transcription initiation	Myeloma, kidney, pancreas, prostate
H3K9me2	SUV39H1; SUV39H2; SETDB1; G9a; EHMT1; PRDM2	KDM3A, 3B, 4A, 4B, 4C, 4D; PHF8; KDM1A; JHDM1D	Transcription initiation and repression	Prostate, pancreas
H3K9me3	SUV39H1; SUV39H2; SETDB1; PRDM2	KDM3B, 4A, 4B, 4C, 4D	Transcription initiation and repression	Colorectal, myeloma, lung, prostate, breast, leukemia, stomach
H3K27me	EZH2; EZH1	JHDM1D	Transcription activation	Kidney
H3K27me3	EZH2; EZH1	KDM6A; KDM6B	Transcription repression	Breast, pancreatic, ovarian, prostate, stomach, liver
H4K20me3	SUV420H1; SUV420H2		Transcription repression	Colorectal, myeloma, prostate, breast, lung, breast, lymphoma, colon, ovarian

1.5.5 Role of histone modifications in EMT and cancer metastasis

Histone modifications also play a key role in promoting EMT and cancer metastasis through a variety of mechanisms (Sun and Fang, 2016).

1.5.5.1 Histone acetylation in EMT and cancer metastasis

Histone acetylation has been shown to facilitate EMT and thus cancer metastasis by directly affecting the transcription of EMT markers or EMT transcription factors. For instance, H4K16 acetylation, mediated by histone acetyltransferase hMOF, is essential to maintain the expression of E-cadherin in breast cancer cells (Kapoor-Vazirani et al., 2008). Other than histone

acetyltransferase, histone deacetylases (HDACs) are recruited to E-cadherin promoter by EMT transcription factors, thus repressing the transcription of E-cadherin gene, thereby triggering EMT and cancer metastasis. The recruitment of HDAC1/ 2 by Snail (Peinado et al., 2004) as well as the recruitment of HDAC1/2 (Aghdassi et al., 2012) or SIRT1 by Zeb1 (Byles et al., 2012) are responsible of the transcriptional repression of E-cadherin in cancer cells.

1.5.5.2 Histone methylation in EMT and cancer metastasis

In addition to acetylation, histone methylation also serves as modulator of EMT and cancer metastasis through affecting the expression of EMT related genes. For instance, DOT1L, which catalyzes H3K79me3, cooperates with the c-Myc-p300 complex to transcriptionally activate Snail and Zeb1/2, in turn inhibiting the transcription of E-cadherin gene and thus facilitating EMT and metastasis (Cho et al., 2015). Furthermore, global elevation of H3K4me3 and H3K36me3 was observed in TGFβ-mediated EMT, suggesting a genome-wide reorganization of these two permissive methylation marks (McDonald et al., 2011). Moreover, histone arginine methyltransferase PRMT1 promotes EMT and metastasis by catalyzing asymmetric H4R3me2 at the promoter of *ZEB1*, thus transcriptionally activating *ZEB1* (Gao et al., 2016). Besides, Snail recruits histone demethylase KDM1A to the promoter of *CDH1* (E-cadherin gene), thus reducing the H3K4me2 levels, thereby repressing the *CDH1* transcription. In this way, loss of H3K4me2, mediated by KDM1A, is essential to Snail mediated EMT in breast cancer (Lin et al., 2010a).

Aside from permissive histone methylation, the repressive ones also influence EMT and cancer metastasis in various ways. For instance, Snail recruits methyltransferase G9a (Dong et al., 2012; Liu et al., 2015b) or Suv39h1 (Dong et al., 2013) to *CDH1* promoter, in turn catalyzing H3K9me3 and thus repressing the transcription of *CDH1*. Moreover, H3K27me3 is also a key regulator of EMT and cancer metastasis, its role will be discussed in detail in Chapter 1.5.7. In addition, the arginine methyltransferase PRMT5 is also

recruited by Snail to *CDH1* promoter, thereby catalyzing symmetric H4R3me2 and thus transcriptionally repressing E-cadherin expression (Hou et al., 2008). Furthermore, in breast cancer cells, arginine methyltransferase PRMT7 forms a complex with YY1 and HDAC3 and is recruited to *CDH1* promoter thus silencing the gene expression of E-cadherin by inducing H4R3me2 and histone deacetylation (Yao et al., 2014).

1.5.5.3 Coordinated histone modification in EMT and cancer metastasis

Numerous studies have revealed that multiple histone modifiers form complexes to collaboratively regulate transcription of EMT related gene (Suganuma and Workman, 2008; Sun and Fang, 2016) (Figure 9). For example, Zeb1/2 bind to *CDH1* promoter, and recruit HDAC1/2 and G9a/GLP. HDAC1/2 and G9a/GLP trigger H3K9 deacetylation and H3K9 methylation respectively. Meanwhile, LSD1 is also recruited by Zeb1/2, in turn demethylating H3K4me1/2 and impeding the H3K9 re-acetylation (Shi et al., 2004; Shi et al., 2003; Wang et al., 2001) (Figure 9a). H3K9 methylation recruits HP1 protein which induces a more closed and compact chromatin structure. HP1 further recruits DNA methyltransferase 1(DNMT1) for DNA methylation (Smallwood et al., 2007) (Figure 9b). Altogether, these different changes of histone modifications act to repress the transcription of E-cadherin, thereby inducing EMT and cancer metastasis.

Moreover, other studies revealed that methyl-H3K9-binding protein MPP8 is recruited and bind to G9a/GLP or Suv39-induced methyl-H3K9 (Figure 9c). MMP8 recruits DNMT3A for CpG methylation and class III HDAC SIRT1 for H4K16 deacetylation, which act together to repress the transcription of E-cadherin genes (Kokura et al., 2010; Sun et al., 2015) (Figure 9d).

Additionally, Snail interacts with Sin3a and polycomb repressive complex 2 (PRC2), which induce histone deacetylation and H3K27me3, respectively

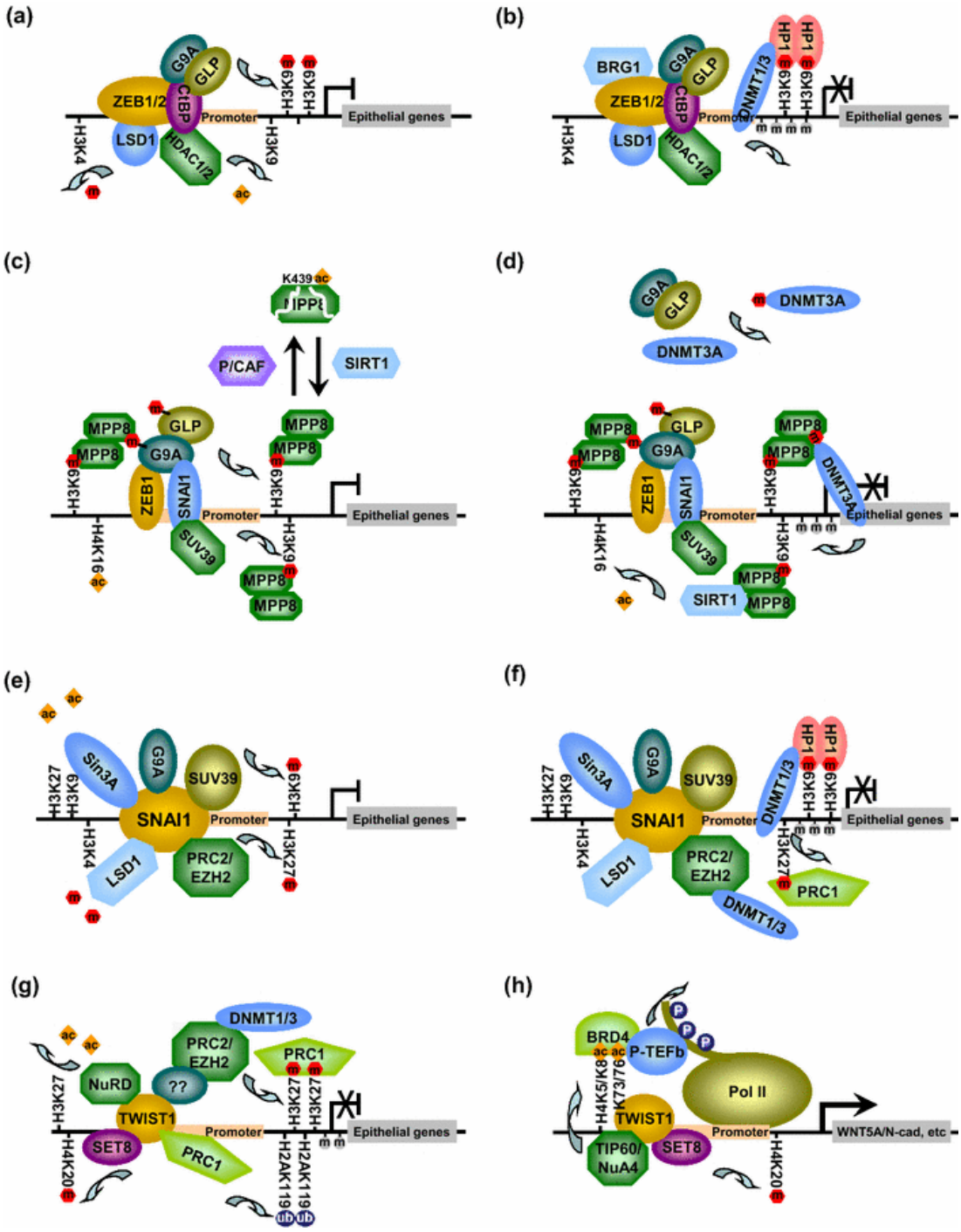

Figure 9. Coordination between different EMT transcription factor and histone modifier in regulating transcription of EMT associated genes (from Sun L & Fang J. 2016) (Sun and Fang, 2016).

(Herranz et al., 2008; Peinado et al., 2004). In this way, E-cadherin gene is transcriptionally repressed. In addition, Snail also recruits G9a and SUV39H1 at *CDH1* promoter to catalyze H3K9me2 and H3K9me3, in turn impeding the

transcription of *CDH1* (Dong et al., 2013; Dong et al., 2012). DNMT1/3 is further recruited by both PRC2 and H3K9 methylation-associated HP1 to catalyze CpG methylation of *CDH1* promoter (Dong et al., 2012; Herranz et al., 2008; Wong et al., 2011b) (Figure 9f). Besides, Snail also recruits LSD1 to demethylate H3K4 at the promoter of *CDH1* for transcriptional repression (Lin et al., 2010b). All the modifications mentioned above are critical for Snail-dependent E-cadherin silencing and induction of EMT (Figure 9e, f).

Aside from Zeb and Snail, Twist also affects the histone code by interacting with various histone modifiers (Figure 9g, h). For instance, Twist has been shown to recruit NuRD complex to deacetylate H3K27 for transcriptional repression (Fu et al., 2011). Moreover, PRC1 and PRC2 are recruited by Twist, in turn repressing the E-cadherin transcription by catalyzing H3K27me3 at its promoter (Yang et al., 2010). Furthermore, Twist also interacts with histone methyltransferase SET8, which play a key role in repressing gene transcription by inducing H4K20me1. Intriguingly, apart from the repressive role of Twist in gene transcription, Twist also play a role in promoting EMT by activating the Wnt signaling pathway (Shi et al., 2014) (Figure 9h). It has been reported that the TIP60-mediated di-acetylation of Twist at K73/K76 as well as H4K5/K8 di-acetylation activate the transcription of WNT5A by recruiting BRD4, P-TEFb and RNA polymerase II to the promoter of WNT5A gene. In this way, Twist functions as a supporter to promote EMT and tumorigenesis of breast cancer (Shi et al., 2014) (Figure 9h).

1.5.6 The role of Polycomb group complexes and H3K27me3 in cancer initiation and progression

H3K27me3 is mainly catalyzed by the polycomb repressive complex 2 (PRC2), therefore major focus has been put on the role of this complex, especially its catalytic subunit enhancer of zeste 1 and 2 (EZH1 and EZH2), in cancer progression and metastasis (Hock, 2012; Kim and Roberts, 2016; Koppens and van Lohuizen, 2016; Pasini and Di Croce, 2016).

PRC2 consists of four core subunits, including the methyltransferase EZH1 or EZH2, EED, SUZ12 and RBAP46/48 (Kim and Roberts, 2016). EZH1 and 2 are responsible of PRC2-mediated H3K27me3 (Margueron et al., 2008; Shen et al., 2008), while its physical interaction with EED and SUZ12 is indispensable for stabilizing its catalytic activity (Cao and Zhang, 2004; Pasini et al., 2004). In addition to PRC2, PRC1 is another type of polycomb repressive complex, which is constituted by CBX, RING1B, HPH and BMI. PRC1 is recruited to H3K27me3 sites through recognition by the CBX subunit, then catalyzes the monoubiquitination of H2A (H2Aub), which works together with H3K27me3 to induce chromatin compaction and repress gene expression (Min et al., 2003; Wang et al., 2004) (Figure 10).

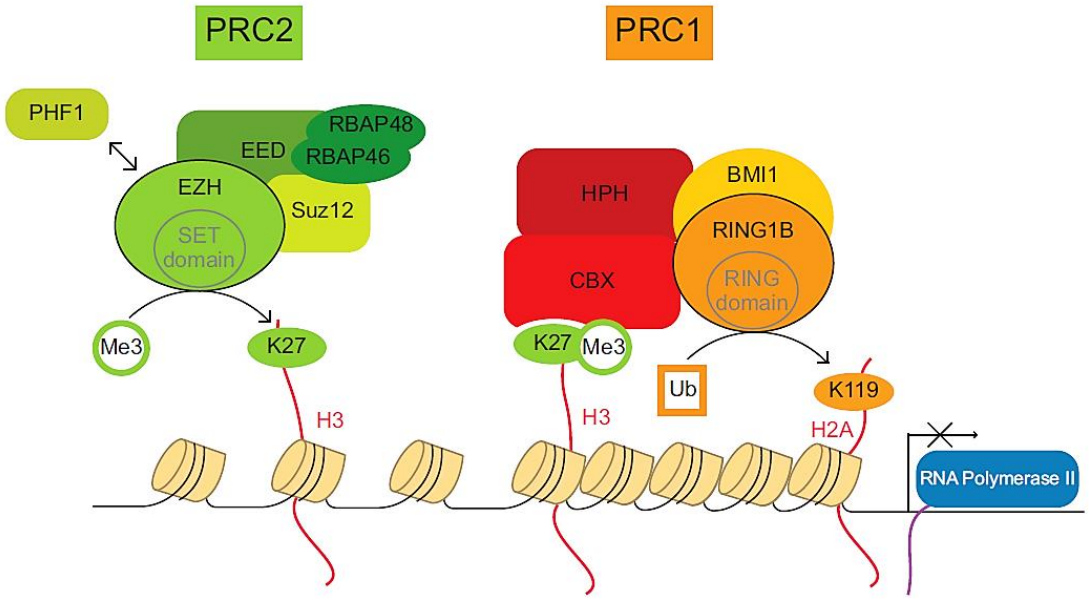

Figure 10. The components of polycomb repressive complexes (PRCs) and their enzymatic activities in regulating genes transcriptions (from Vissers JH *et al*. 2012) (Vissers et al., 2012).

The role of PRC in cancer has been widely studied and appears to be context and cancer type- specific. On the one hand, PRC2 repress the expression of various tumor suppressor genes by catalyzing H3K27me3, which contributes to cancer progression.

In agreement with this, a number of studies revealed that EZH2 is overexpressed in various types of human cancers, and correlated with aggressive cases and cancer progression (Hock, 2012). Moreover, pharmacologically or genetically disrupting EZH2 is sufficient to impede the proliferation and survival of EZH2-expressing cancer cells (Tan et al., 2007; Wilson et al., 2010). Futhermore, the H3K27me3 demethylase JMJD3 (also known as KDM6B), is underexpressed in human cancers (Agger et al., 2009; Barradas et al., 2009). Moreover, EZH2-H3K27me3 facilitates cancer metastasis by transcriptionally repressing tumor suppressor gene DLC1 (Au et al., 2013).

However, on the other hand, PRC2 also acts as tumor suppressor in various types of human cancers, by transcriptionally repressing several oncogenes. For example, loss of EZH2 in T-acute lymphoblastic leukemia (T-ALL) is correlated with aggressiveness (Simon et al., 2012) by derepressing the Notch signaling pathway (Ntziachristos et al., 2012). Furthermore, disruption of EZH2 was shown to trigger T-ALL (Simon et al., 2012). In addition, the increased level of JMJD3 in Hodgkin's lymphoma and T-ALL was shown to derepress target oncogenes by reducing the H3K27me3 level, in turn facilitating pathogenesis (Anderton et al., 2011; Simon et al., 2012).

1.5.7 The role of Polycomb group complexes and H3K27me3 in EMT and cancer metastasis

In addition to its role in cancer formation and progression, PRC and PRC-mediated H3K27me3 play important role in modulating EMT and cancer metastasis. Yu et al. revealed that EZH2 level is increased significantly and is accompanied with decreased E-cadherin level in lymph node metastatic breast cancer in comparison with primary tumors, suggesting a supporting role of PRC2 in EMT and metastasis (Yu et al., 2012). Moreover, EZH2 and EZH2-mediated H3K27me3 are critical in Snail-mediated E-cadherin repression and EMT in pancreatic cancer (Herranz et al., 2008). Additionally, in gastric cancer

cells, PRC2 induces H3K27me3 at *CDH1* promoters, thereby facilitating metastasis (Xia et al., 2015). Furthermore, the H3K4me3-to-H3K27me3 switch occurs at the promoters of various EMT markers, including E-cadherin. In contrast, the H3K27me3-to-H3K4me3 switch occurs at the promoter of upregulated mesenchymal markers, such as N-cadherin (Malouf et al., 2013).

Apart from the promoting role of PRC and H3K27me3 in inducing EMT and cancer metastasis, several studies also highlighted a suppressive role of PRC and PRC-mediated H3K27me3 in EMT and cancer metastasis. Cardenas et al. revealed the decreased levels of EZH2 and H3K27me3 at the promoter of *ZEB2* genes in the context of TGFß-mediated EMT in ovarian cancer cells. It leads to transcriptional activation of *ZEB2* gene, in turn reducing the E-cadherin level and triggering EMT and metastasis (Cardenas et al., 2016). Similarly, another study found that H3K27me3 presents at the promoter of *SNAI1* gene, thus reducing the Snail expression and thereby impeding Snail-mediated EMT. In contrast, JMJD3 activates Snail expression by removing the H3K27me3 mark from the *SNAI* promoter, thereby facilitating EMT and cancer metastasis (Ramadoss et al., 2012). Consistently, H3K27me3 is also present at the promoter of *SNAI2* gene and is responsible for the transcriptional silencing of *SNAI2* gene. However, removing of H3K27me3 mark by JMJD3 increases the level of Slug and thereby triggering EMT and cancer metastasis (Li et al., 2015). Thus, the role of PRC2 and H3K27me3 appear to be highly context and cell-type specific.

2. Objectives

Lung cancer is the number one cause of cancer-related death worldwide. Therefore, improving diagnostic, prognostic and therapeutic efficiency of lung cancer is of utmost importance. Clarifying the molecular determinants and mechanisms driving lung cancer formation, development, malignancy and metastasis are of great benefit to the early detection, prognosis and therapeutic treatment of lung cancer.

Lung cancer cells are characterized by alteration of nuclear morphology and structure. Nuclear lamins, the major determinant of nuclear structure, especially lamin A/C, have been proposed as a lung cancer marker by several studies. Besides, lamin B1 also contributes to nuclear stiffness and integrity (Panorchan et al., 2004a; Panorchan et al., 2004b) and loss of lamin B1 facilitates lung cancer migration and metastasis possibly through reducing nuclear stiffness (Harada et al., 2014). Indeed, previous study in our lab correlated the lower level of lamin B1 with higher lung cancer tumor grade and found that lamin B1 depletion enhanced mouse lung epithelial cell migration.

The objective of present study is to focus on the following aspects: 1. To determine the specific function of nuclear lamins in lung cancer initiation, development and metastasis; 2. To investigate the role of lamins on cell morphology, nuclear architecture and gene expression profiles; 3. To study the role of lamins in cell proliferation, migration and invasion as well as the underlying mechanism; 4. To study the role of nuclear lamins in regulating gene positioning and chromoatin decondensation.

3. Results

3.1 Expression of lamins in lung cancer patients

3.1.1 Lamin B1 levels are decreased in lung cancer specimens

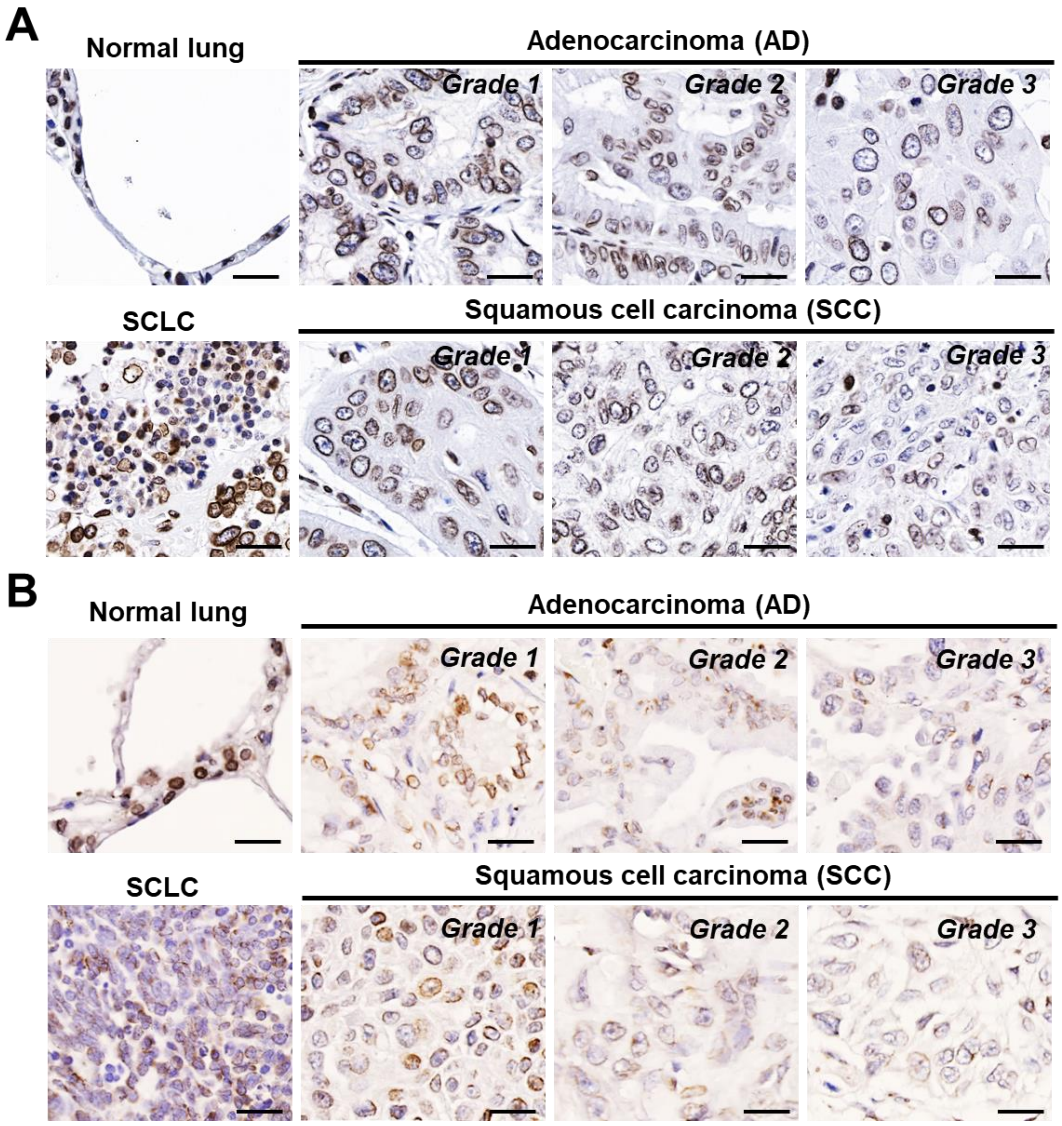

Figure 11. Lamin B1 shows decreased expression in lung cancer patients. Immunohistochemistry analysis of representative tissue samples from different types and grades of lung tumors specimens from a tissue microarray stained with two different anti-lamin B1 antibodies: (**A**) Sigma-Aldrich, HPA050524 (**B**) Santa Cruz, sc-6216. AD, adenocarcinoma; SCC, squamous cell carcinoma; SCLC, small cell lung cancer. Scale bars, 25 μm.

Previous studies in the group indicated that lower levels of lamin B1 were

associated with higher grade, poorly differentiated adenocarcinoma and squamous cell carcinoma. In order to determine whether aberrant level of lamin B1 may contribute to lung cancer initiation, progression and metastasis, we performed immunohistochemistry (IHC) on a human lung cancer tissue microarray with two different lamin B1 specific antibodies. Interestingly, the results revealed significantly lower level of lamin B1 in small cell lung cancer (SCLC) as well as a progressive loss of lamin B1 expression in high-grade adenocarcinoma (AD), squamous cell carcinoma (SCC), which are prognostically worse in comparison to lower grade tumors (Figure 11 and Figure 12). Grade I cancer cells expressed higher levels of lamin B1, evaluated by H-score of IHC staining, whereas in grade II and especially in grade III tumors, much fewer cells expressed lamin B1, typically at substantially lower levels (Figure 12).

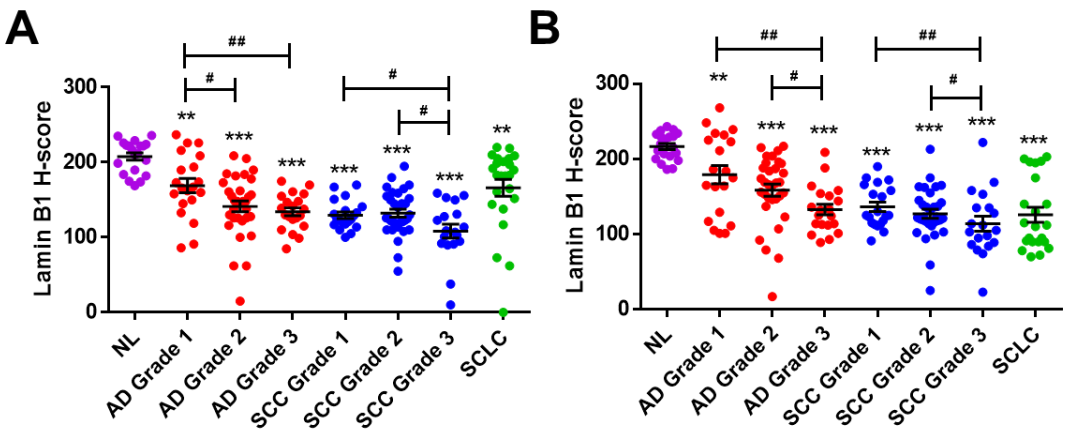

Figure 12. Statistical analysis of relative intensity (H-score) of lamin B1 IHC staining using different anti-lamin B1 antibodies in lung tumors of different types and grades as well as normal lung tissue. (**A**) Sigma-Aldrich, HPA050524 (**B**) Santa Cruz, sc-6216. n=70 AD (20 Grade 1, 30 Grade 2, 20 Grade 3); n=69 SCC (16 Grade 1, 33 Grade 2, 20 Grade 3); n=22 SCLC and n=20 NL. NL, normal lung tissue; AD, adenocarcinoma; SCC, squamous cell carcinoma; SCLC, small cell lung cancer. **, $p<0.01$ vs. NL; ***, $p<0.001$ vs. NL; #, $p<0.05$; ##, $p<0.01$

3.1.2 Lamin A/C levels remain unchanged in NSCLC, but decreases in SCLC specimens

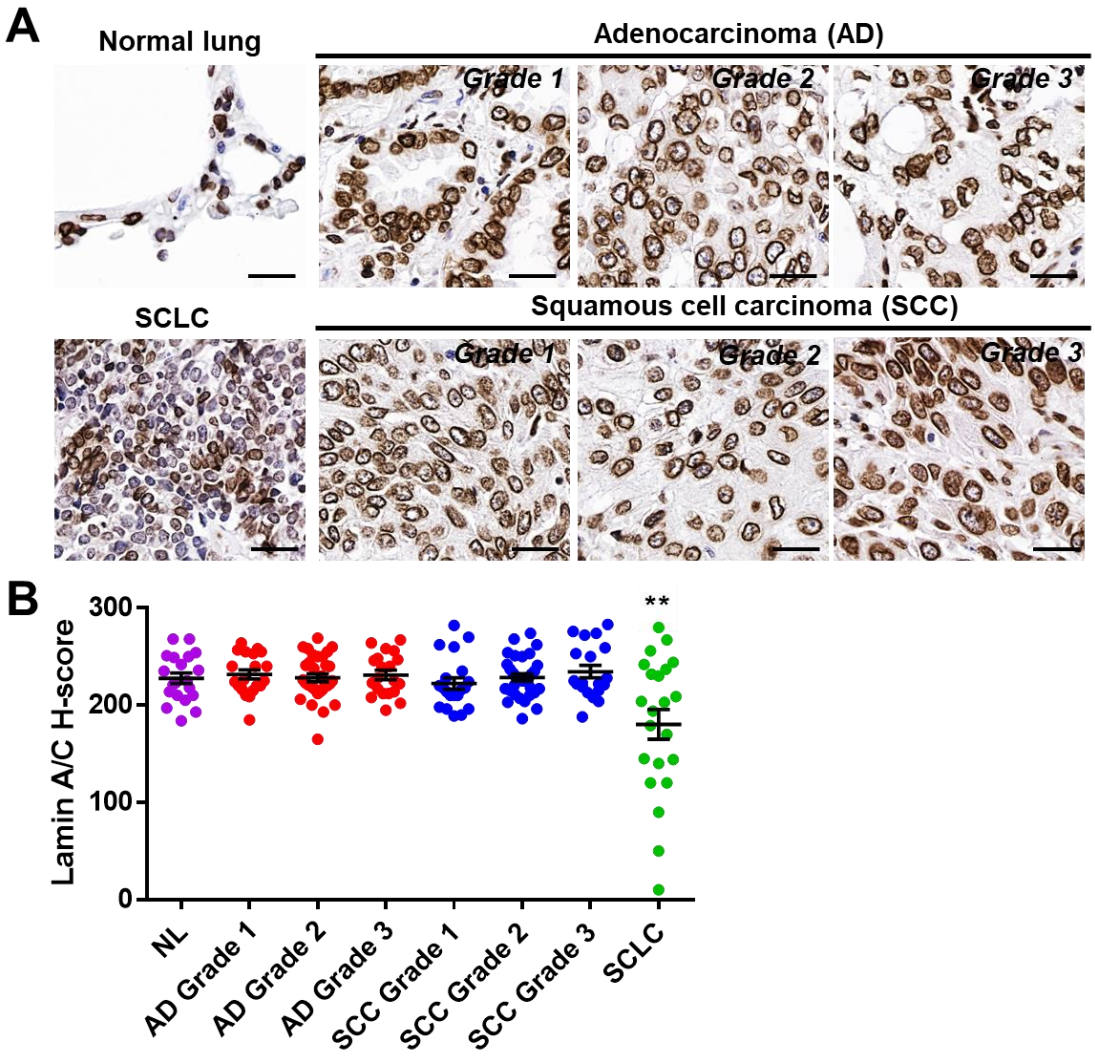

Figure 13. Expression of lamin A/C in lung cancer patients. (**A**) Immunohistochemistry of representative tissue samples from different types and grades of lung tumors from a tissue microarray stained with an anti-lamin A/C antibody. Scale bars, 25 µm. NL, normal lung tissue; AD, adenocarcinoma; SCC, squamous cell carcinoma; SCLC, small cell lung cancer. (**B**) Relative staining intensity (H-Score) for lamin A/C in lung tumors of different types and grades. n=70 for AD (n=20 Grade 1, n=30 Grade 2, n=20 Grade 3); n=69 for SCC (n=16 Grade 1, n=33 Grade 2, n=20 Grade 3), n=22 for SCLC and n=20 for NL. **p < 0.01.

In contrast, lamin A/C IHC staining in human lung cancer tissue microarray

with anti-lamin A/C antibody shows no differences in terms of lamin A expression between normal lung tissue and all subtypes and grades of NSCLC, except for a decrease in SCLC (Figure 13). These observations, in consistence with the previous study in our lab, suggest that the lower level of lamin B1 expression associates with higher lung cancer grades.

3.1.3 Cells in tumor microenvironment highly express lamin B1

In contrast to the low lamin B1 levels in cancer cells, we observed that non-cancerous cells in the tumor microenvironment express high levels of lamin B1. However, lamin A/C levels were high in cancer cells, whereas the non-cancerous cells express no lamin A/C (Figure 14).

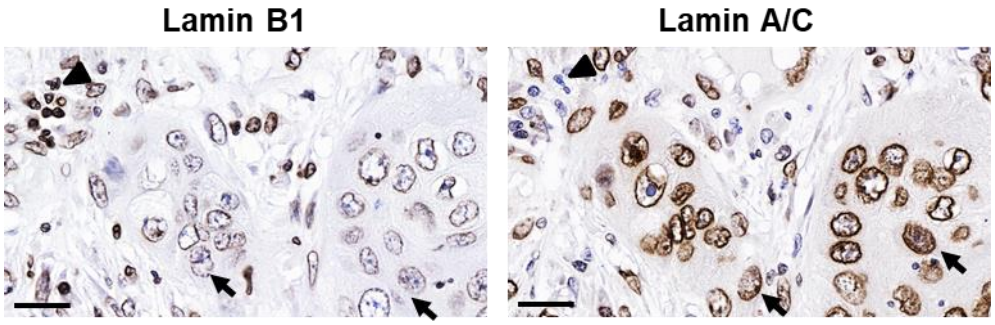

Figure 14. Non-cancerous cells in tumor microenvironment express high level of lamin B1 but no lamin A/C. Immunohistochemistry of consecutive lung cancer tissue samples using anti-lamin B1 antibody (Sigma-Aldrich, HPA050524) and lamin A/C antibody, showing high levels of lamin A/C and low levels of lamin B1 in lung cancer cells (arrows). Stroma cells (arrowheads) show high levels of lamin B1 and no lamin A/C. Scale bars, 25 μm.

Moreover, in Grade II and in particular in Grade III tumors we observed clusters of cells highly positive for lamin B1 and stained positive for the immune/inflammatory marker CD45 (Figure 15). Thus, lamin B1 levels are significantly reduced in tumor cells of lung cancer patients, but high in immune cells, which have been shown to exhibit stage-dependent accumulation in human lung tumors (Banat et al., 2015).

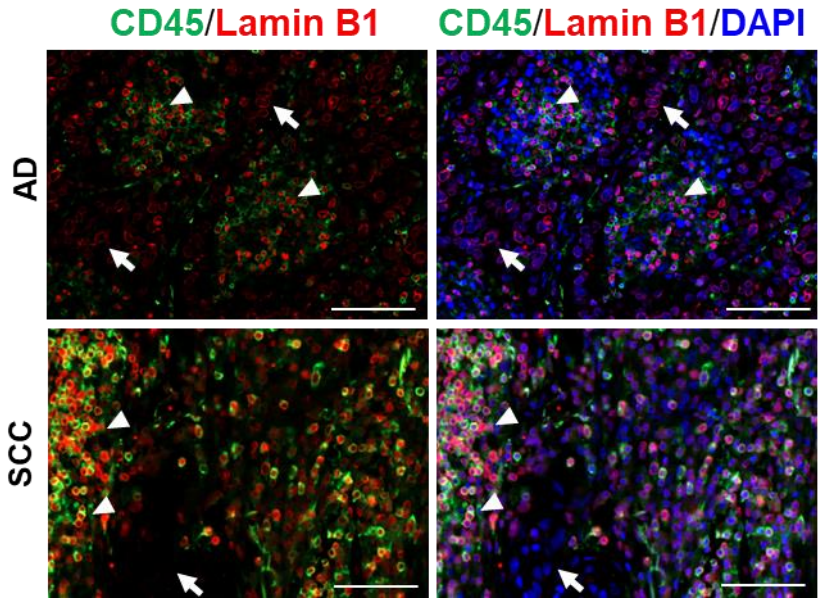

Figure 15. Lamin B1 is highly expressed in immune cells. Co-immunostaining with CD45 and lamin B1 antibodies of representative Grade III adenocarcinoma (AD) and Grade III squamous cell carcinoma (SCC) samples showing that cells highly positive for lamin B1 are CD45 positive immune/inflammatory cells. Scale bars, 50 µm.

3.1.4 Lamin B1 expression is decreased in lung cancers cell lines

Futhermore, the decrease of lamin B1 levels in lung cancer compared to non-malignant lung cells/ tissues was confirmed by Western blot analysis of mouse lung epithelial (MLE12) cells and normal human bronchial epithelium B2B (BEAS-2B) cells, compared to the highly aggressive, metastatic mouse Lewis lung carcinoma (LLC1) cells, as well as H69 human small-cell lung cancer cells (Figure 16 A). Interestingly, LLC1 cells showed abnormal nuclear shape and lamin B1 localization in comparison to MLE12 cells (Figure 16 B). Together, these findings support the notion that loss of lamin B1 may play a role in promoting lung cancer initiation, progression and malignancy.

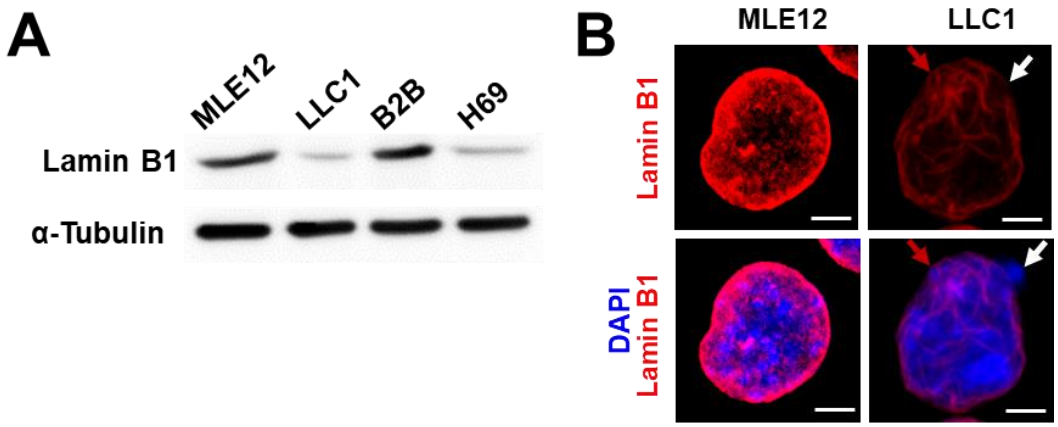

Figure 16. Lamin B1 levels are decreased in lung cancers cell lines. (**A**) Immunoblot analysis of total cell lysates of mouse lung epithelial (MLE12) cells, mouse Lewis lung carcinoma (LLC1), human bronchial epithelium B2B (BEAS-2B) and H69 human small-cell lung cancer cells, showing decreased lamin B1 levels in mouse and human lung cancer cell lines. (**B**) Confocal images of immunostaining for lamin B1 in MLE12 and LLC1 cells. Scale bars, 5 μm. White arrows show nuclear blebs and local lamin B1 loss in LLC1 cells, whereas red arrows point to abnormalities in lamin B1 staining. To more clearly visualize the staining pattern in the LLC1 cells, which had a weaker lamin B1 signal, we acquired the LLC1 images with higher exposure compared to the MLE12 cells.

3.2 Lamin B1 depletion promotes EMT, anchorage-independent growth, cell migration and invasion

3.2.1 Loss of lamin B1 in mouse lung epithelial cells leads to EMT

To further gain insight into the mechanism by which lamin B1 loss promotes cancer cells migration and metastasis, we depleted lamin B1 in mouse lung epithelial (MLE12) cells and the highly aggressive, metastatic Lewis lung carcinoma (LLC1) cells by lentivirally driven shRNA-mediated silencing (Figure 17 A and B). In consistence with previous data in our group, we observed that control MLE12 cells maintained a rounded, epithelial appearance in culture, however lamin B1 knockdown MLE12 cells develop a spindle-shaped morphology (Figure 17 C), which resemble morphologically mesenchymal cells.

These dramatic changes of lamin B1 knockdown cells share morphological similarities to those occurring during EMT, which is a crucial event during tumor progression and metastasis.

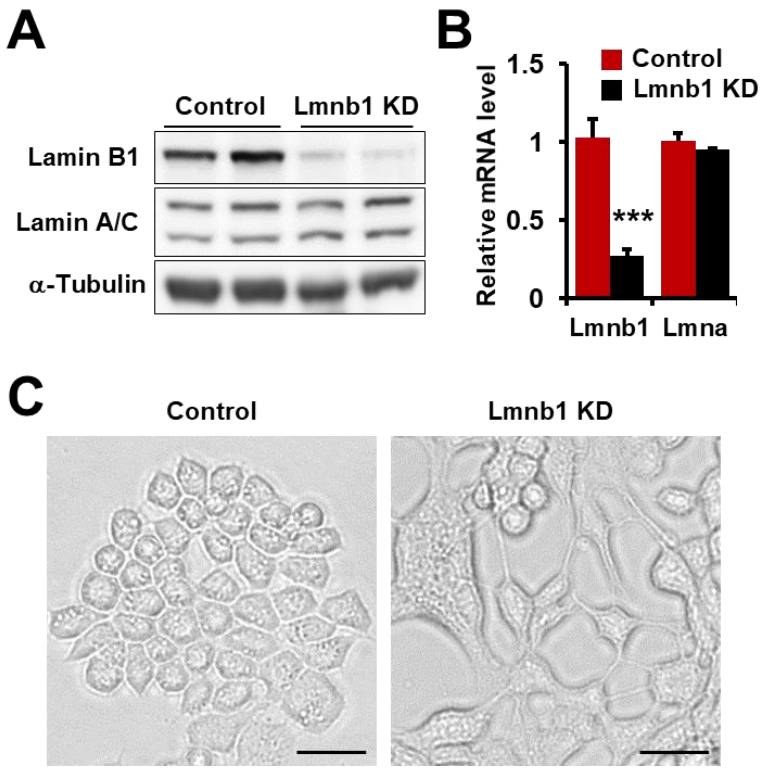

Figure 17. Loss of lamin B1 lead to morphological changes of MLE12 cells. (**A**) Immunoblot analysis of total cell lysates of MLE12 cells expressing control shRNA or shRNA against lamin B1 using lamin B1 and lamin A/C antibodies. α-Tubulin served as loading control. (**B**) qPCR analysis of Lmnb1 and Lmna expression in MLE12 expressing control shRNA or shRNA against lamin B1 (right panel) (n=6). (**C**) Representative microscopic images of control and lamin B1 knockdown MLE12 cells, showing morphological changes after lamin B1 silencing. Scale bars, 25 μm.

EMT is characterized by loss of epithelial markers and gain of mesenchymal markers, thus, in order to investigate if these is the case in lamin B1 knockdown cells, we checked the expression of several EMT makers in both control and lamin B1 knockdown MLE12 cells by immunofluorescent staining and western blotting analyses. As shown by both analyses, lamin B1 knockdown cells exhibit significant reduction of epithelial marker E-cadherin in comparison to control

cells (Figure 18). In addition, the level of mesenchymal markers, such as fibronectin, vimentin and N-cadherin, increase dramatically after lamin B1 silencing (Figure 18). These findings demonstrate that loss of lamin B1 is capable of inducing EMT and thereby results in a dramatic morphological change of lamin B1-depleted cells.

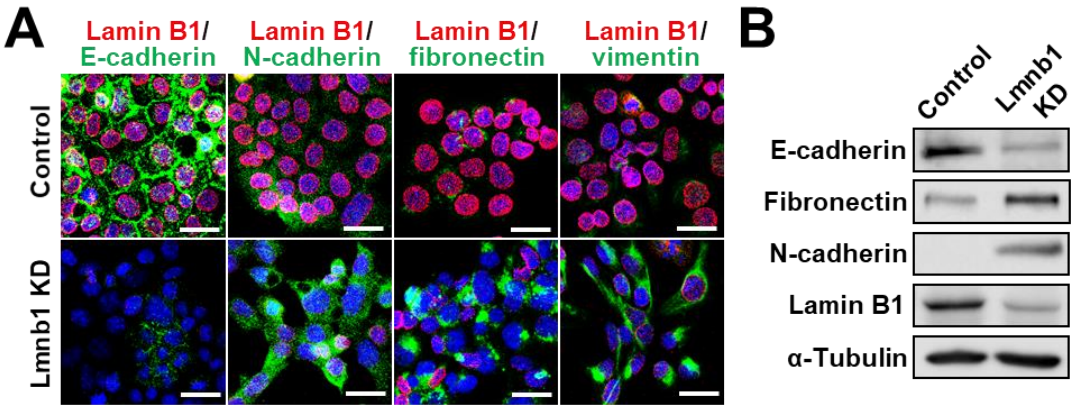

Figure 18. Expression of EMT markers in control and lamin B1 knockdown MLE12 cells analyzed by immunofluorescent stainings (**A**) and Western blot analyses (**B**). Scale bars, 20 µm.

3.2.2 Lamin B1 depletion promotes cell migration and invasion

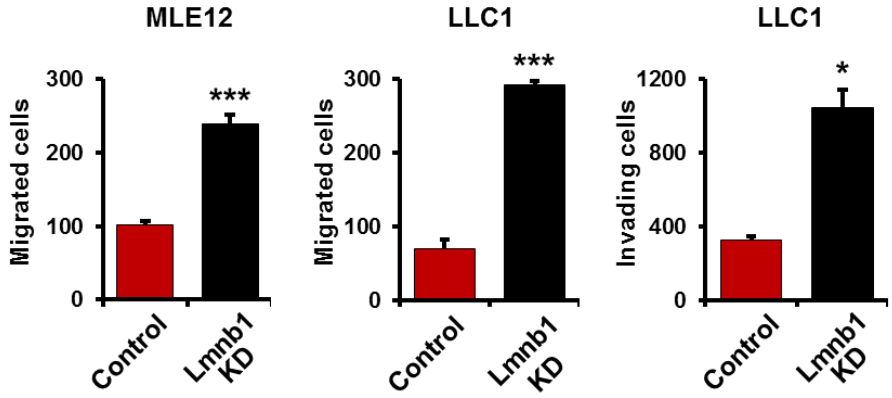

Figure 19. Boyden chamber migration (left and middle panel) and invasion (right panel) assay on control and lamin B1-silenced MLE12 (left panel) and LLC1 cells (middle and right panel). Data are shown by mean ± SEM. *, $p < 0.05$ vs control; ***, $p < 0.001$ vs control.

EMT associates with increased migratory and invasive abilities during cancer progression and metastasis, thus we evaluated the migratory and invasive capacities of control and lamin B1 knockdown MLE12 and LLC1 cells by performing the Boyden chamber-based migration and invasion assays. As expected, lamin B1-depleted cells possessed significantly higher migratory and invasive capacities in comparison with control cells (Figure 19).

3.2.3 Lamin B1 depletion enhances cell anchorage-independent growth

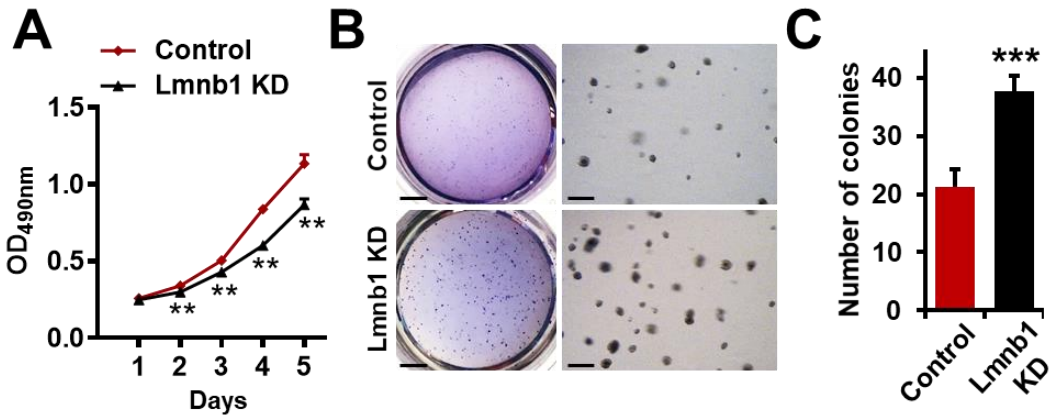

Figure 20. Loss of lamin B1 hinders proliferation of MLE12 cells in 2D adherent monolayer cultures but promotes anchorage-independent growth. (**A**) MTT assay to determine the effect of lamin B1 loss on cell proliferation (n=8). (**B**) Soft agar assay to assess the anchorage independent cell growth of control and lamin B1 knockdown MLE12 cells. Higher magnifications (right panels) show the increased colony size upon lamin B1 loss (n=6). Scale bars of left panels, 4 mm; Scale bars of right panels, 0.5 mm. (**C**) Quantification of the number of colonies per field in the soft agar assay. ***, $p < 0.001$ vs control.

The role of lamin B1 in cell proliferation appears to be complex and cell type specific (Butin-Israeli et al., 2012). Thus, we next tested the role of lamin B1 silencing on cell proliferation and anchorage-independent growth. Interestingly, while lamin B1 silencing led to decreased cell proliferation in 2D adherent monolayer cultures (Figure 20 A), the capacity of MLE12 cells to form colonies in soft agar as a measure of anchorage-independent growth, one of the

hallmarks of malignant transformation(Hanahan and Weinberg, 2011), was markedly increased after downregulation of lamin B1 (Figure 20 B). Furthermore, the individual colony size was increased by lamin B1 depletion (Figure 20 B). Taken together, these data suggest that loss of lamin B1 play a key role in promoting EMT, anchorage-independent growth, cell migration and invasion.

3.3 Lamin B1 depletion leads to upregulation of migration-related genes

To further gain insights into the mechanisms mediating the role of lamin B1 in EMT and cell migration, we performed RNA-Seq from control and lamin B1-depleted MLE12 cells. Consistent with a well-known repressive function of lamin B1 on gene expression (Reddy et al., 2008), we observed a significantly high number of upregulated genes after lamin B1 depletion (Figure 21). Only 72 genes were downregulated in lamin B1 knockdown cells, whereas 169 genes are found to be upregulated upon loss of lamin B1 with a Log2 Fold Change > 1. Importantly, among these upregulated genes, 24 genes are well-annotated cancer related genes, which are widely implicated in cancer initiation, progression, development, migration, metastasis and cancer related pathway, by KEGG database (http://www.genome.jp/kegg/, genes are listed in Figure 21 A and C). Furthermore, we performed a Gene Ontology (GO) analysis to get a better understanding of the functional characteristics and the potentially involved biological processes of the upregulated genes upon lamin B1 depletion. Intriguingly, output of the analysis revealed over-representation for GO terms linked to migration and related signaling among the genes upregulated upon lamin B1 knockdown (Figure 21 B), which supports our finding that lamin B1 depletion play a key role in modulating cells migration by altering the expression of key molecules involved in cell migration and signal transduction.

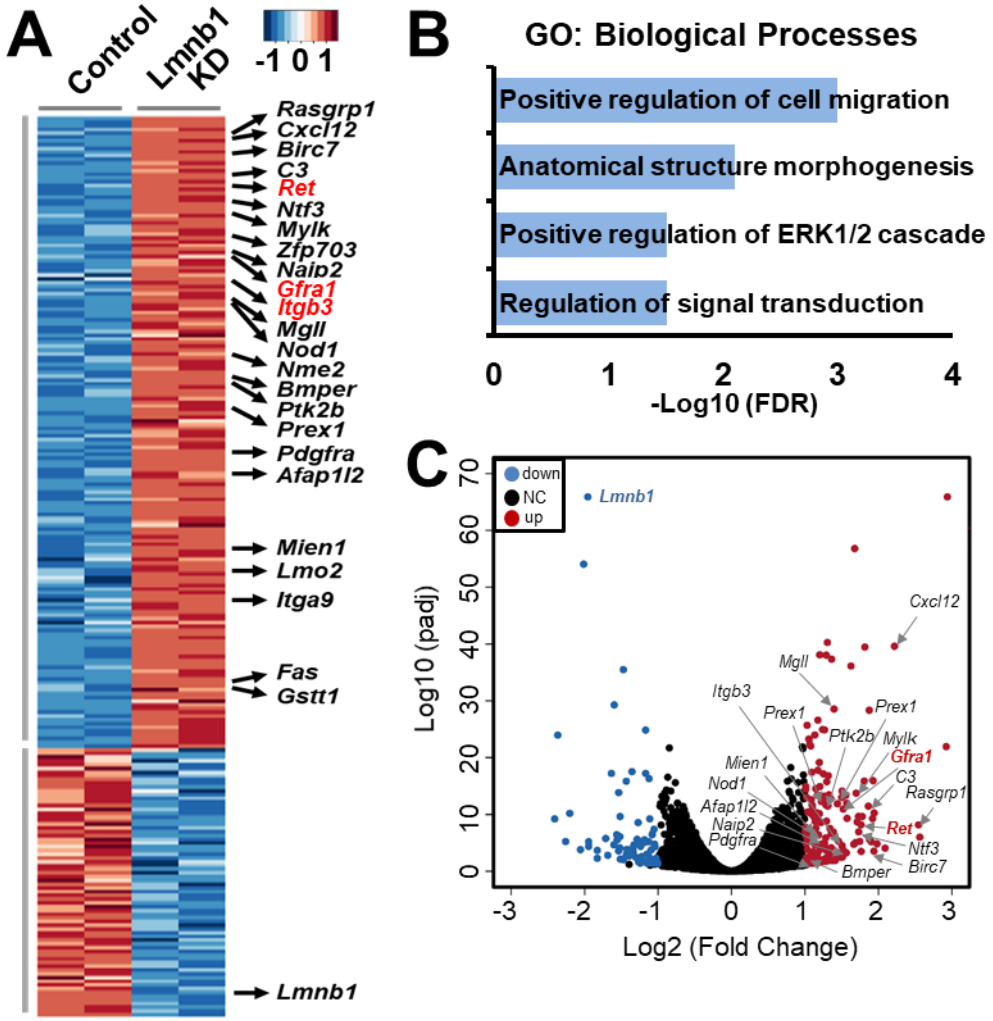

Figure 21. Loss of lamin B1 leads to upregulation of genes link to migration and related signaling. (**A**) Heat-map representation of RNA-seq analysis of control and lamin B1 knockdown MLE12 cells, showing a large number of genes involved in cancer development among the genes upregulated upon lamin B1 loss of function. (**B**) GO terms enriched among genes upregulated upon lamin B1 knockdown. (**C**) Volcano plot showing log2 fold change plotted against log10 adjusted P value for lamin B1 knockdown versus control MLE12 samples. Red dots represent genes upregulated and blue dots represent genes downregulated (adjusted $P<0.05$, fold change ≤ 0.5, ≥ 2) upon lamin B1 loss of function. Genes involved in cell migration and signaling are indicated.

3.4 Upregulation of the RET plays a key role in mediating the EMT and malignant phenotype upon lamin B1 loss

3.4.1 The receptor tyrosine kinase RET is upregulated upon lamin B1 depletion

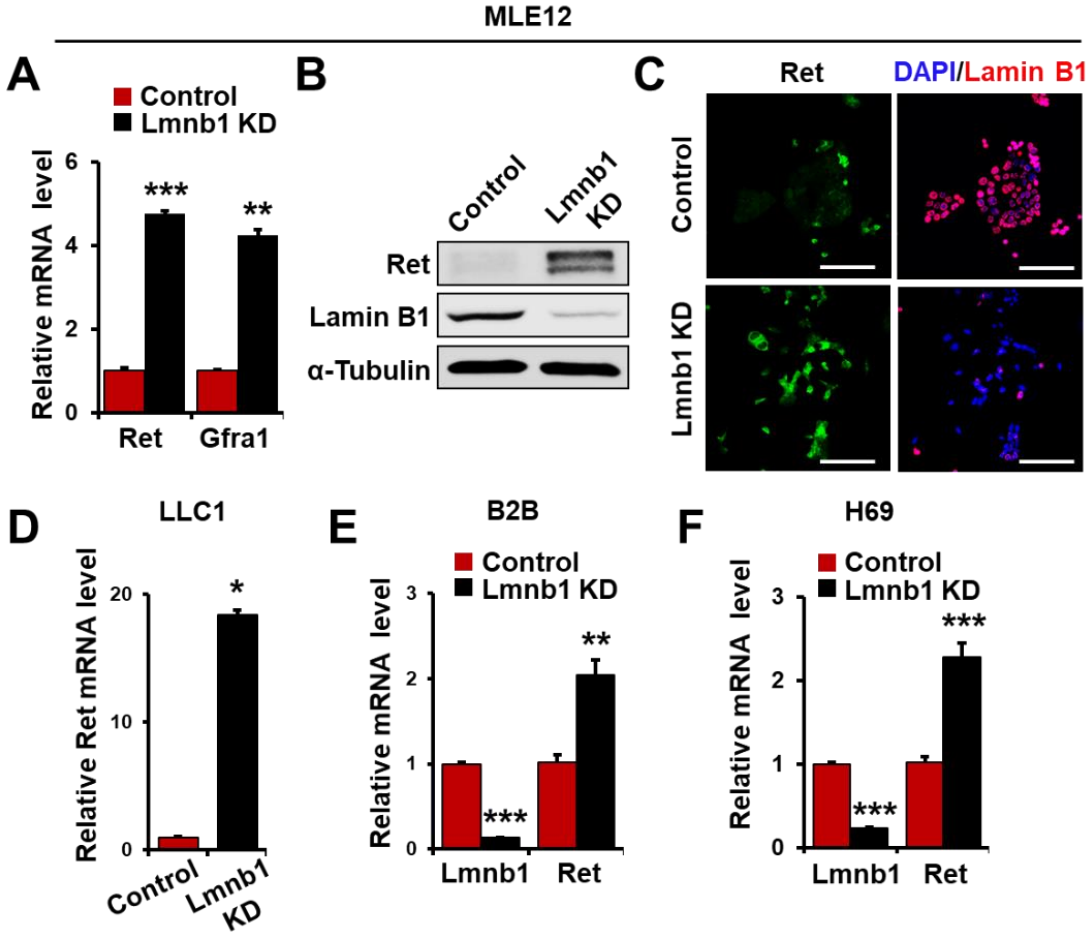

Figure 22. Expression of RET in control and lamin B1-depleted MLE12, LLC1, B2B and H69 cells. (**A**) qPCR validation of RET and Gfra1 upregulation upon lamin B1 depletion in MLE12 cells. Western blot (**B**) analysis and immunefluorescent staining (**C**) of RET in control and lamin B1 knockdown MLE12 cells. Scale bars, 100 μm. (**D**-**F**) Increased mRNA level of RET in lamin B1-silenced LLC1 (**D**), B2B (**E**) and H69 (**F**) cells compared with control shown by qPCR analysis. (**A**, **D**-**F**): data are shown by mean ± SEM. *, p<0.05 vs. control; **, p<0.01 vs. control; ***, p<0.001 vs. control.

Among all the upregulated genes upon lamin B1 depletion which are associated

with cell migration, particularly interesting was the upregulation of RET (rearranged during transfection) proto-oncogene and its co-receptor Gfra1 (GDNF family receptor alpha-1). First of all, we confirmed the increased expression of RET and Gfra1 in lamin B1-depleted MLE12 cells by qPCR, western blot and immunofluorescent staining analyses (Figure 22 A-C). In addition, similar results were also observed in lamin B1-silenced LLC1 cells in comparison to control (Figure 22 D) as well as in normal human lung bronchial epithelial cell line BEAS-2B (B2B, Figure 22 E) and human small cell lung cancer cell line NCI-H69 (H69, Figure 22 F) showing that loss of lamin B1 leads to significant increase of RET mRNA level.

3.4.2 Targeting RET inhibits the migration and invasion of lamin B1-depleted cells

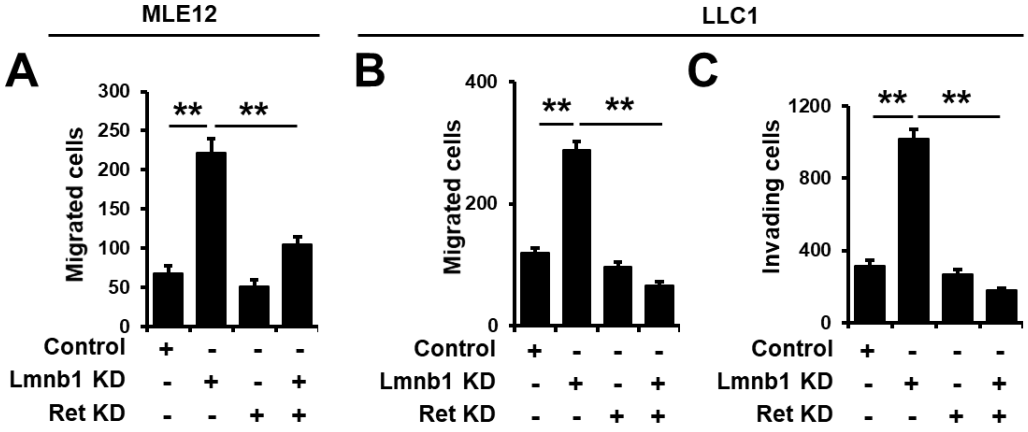

Figure 23. Boyden chamber migration (**A** and **B**) and invasion (**C**) assay with control, lamin B1 knockdown (Lmnb1 KD), RET knockdown (RET KD) and lamin B1/RET double knockdown MLE12 (**A**) and LLC1 (**B** and **C**) cells. Data are shown by mean ± SEM. **, $p < 0.01$

RET is a member of the receptor tyrosine kinase family that is activated by the glial-derived neurotrophic factor (GDNF) family of ligands. These peptides bind the RET co-receptors from the GFRA family. Ligand binding leads to complex formation between RET and its ligand-bound co-receptors, resulting in kinase

activation and stimulation of downstream signaling pathways affecting cell proliferation and migration (Mulligan, 2014).

To further investigate the role of RET upregulation in mediating EMT and the increased migration of lamin B1 knockdown cells, we knockdown RET in control and lamin B1-depleted MLE12 and LLC1 cells by lentivirally driven shRNA-mediated silencing. Importantly, we observed that RET knockdown lead to a significant decrease in the cell migratory and invasive capacities of lamin B1-depleted cells (Figure 23).

Moreover, inhibitory targeting RET via treating the lamin B1-depleted MLE12, LLC1, B2B and H69 cells with RET selective inhibitor vandatanib also lead to a significant reduction of the migratory ability (Figure 24).

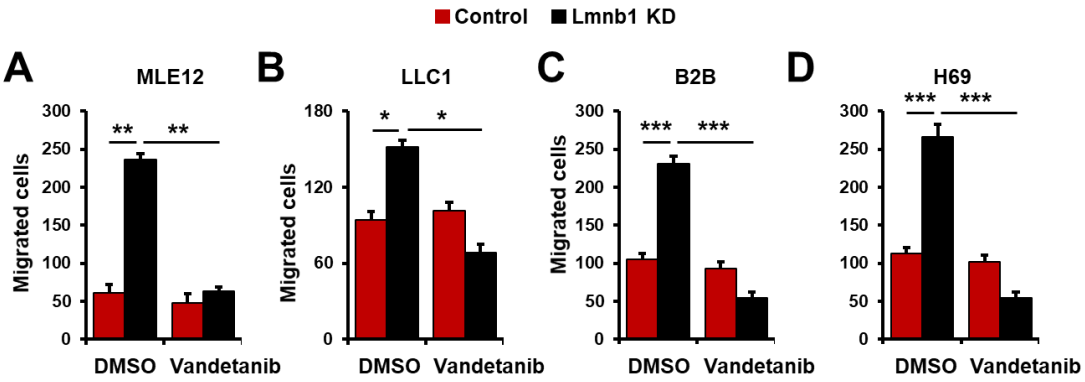

Figure 24. Boyden chamber migration assay with control, lamin B1 knockdown (Lmnb1 KD) MLE12 (**A**), LLC1 (**B**), B2B (**C**) and H69 (**D**) cells treated with DMSO or 20 nM Vandetanib. Data are shown by mean ± SEM. *, $p < 0.05$; **, $p < 0.01$; ***, $p < 0.001$.

These findings suggest that inhibition of RET can reverse the increased migratory and invasive abilities upon lamin B1 depletion which suggests that lamin B1 depletion modulates cancer cells migration and invasion in a RET-dependent manner. In contrast to lamin B1 depletion, silencing of lamin A/C did not have any effect on RET expression and cell migration, suggesting a specific role of lamin B1 in regulating EMT in mouse lung epithelial cells (Figure 25).

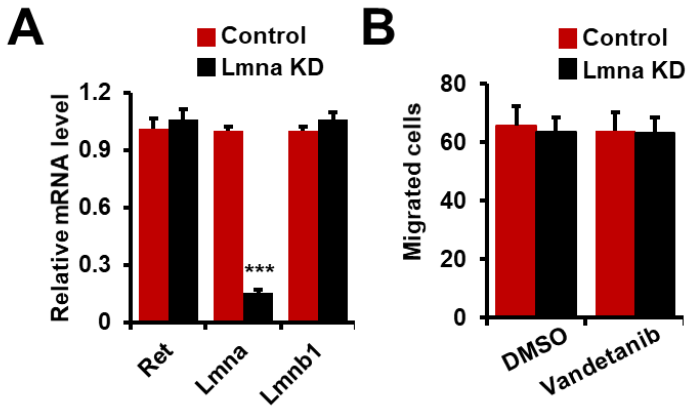

Figure 25. Silencing lamin A/C did not affect RET expression and cell migration. (**A**) qPCR analysis of RET, Lmnb1, Lmna expression in MLE12 expressing control shRNA or shRNA against lamin A/C. (**B**) Boyden chamber migration assay with control and lamin A/C KD MLE12 cells, treated either with DMSO or with 20 nM vandetanib (n=4).

3.4.3 RET upregulation promotes lamin B1 depletion mediated EMT

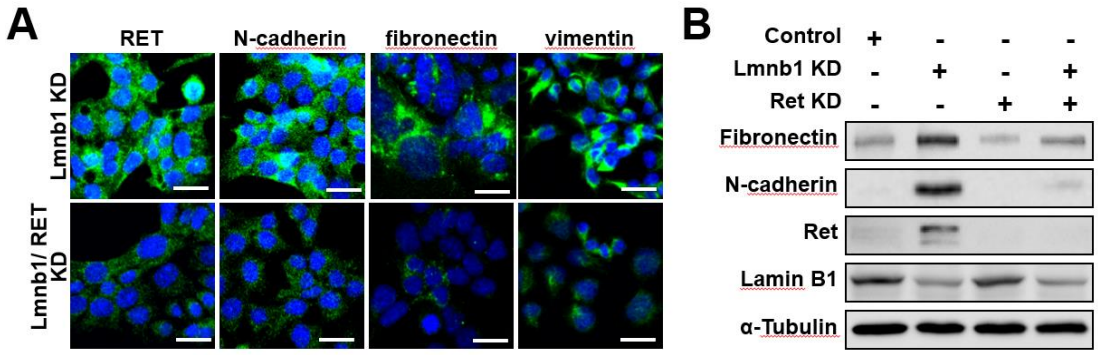

Figure 26. Expression of EMT markers in control, lamin B1 knockdown (lamin B1 KD), RET knockdown (RET KD) and lamin B1/RET double knockdown MLE12 cells shown by immunofluorescent stainings (**A**) and Western blot analysis (**B**). Scale bars, 20 µm.

Considering the EMT phenotype of lamin B1-depleted cells, we assumed that upregulation of RET may also play a role in regulating lamin B1 depletion-mediated EMT and may thereby facilitate cancer cell migration and metastasis. In order to corroborate the assumption, we checked the level of EMT markers

in lamin B1 knockdown and lamin B1/RET double knockdown MLE12 cells to investigate the effect of RET loss on lamin B1 depletion-mediated EMT. Intriguingly, we observe a dramatic reduction of mesenchymal markers in lamin B1/RET double knockdown MLE12 cells in comparison to lamin B1 knockdown MLE12 cells (Figure 26), implying a functionally involvement of RET upregulation in lamin B1 depletion-mediated EMT process.

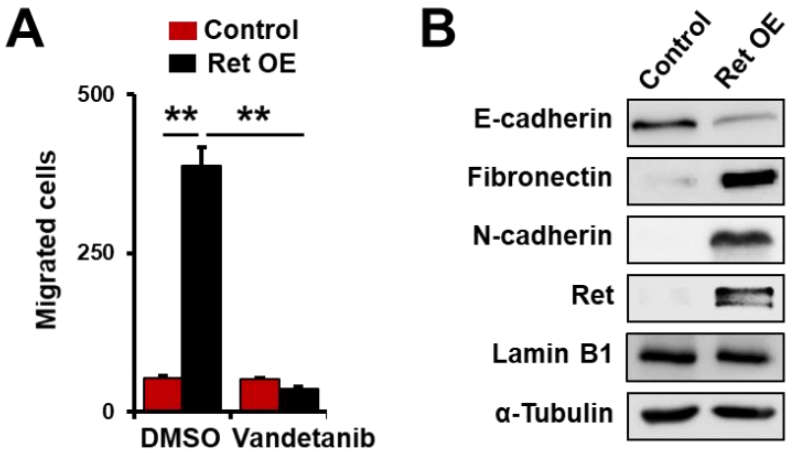

Figure 27. Effect of RET ectopic overexpression on cell migration and EMT. (**A**) Boyden chamber migration assay with control and RET-overexprssing MLE12 cells (RET OE) treated with DMSO or 20 nM Vandetanib. Data are shown by mean ± SEM. **, $p < 0.01$. (**B**) Expression of EMT markers in control and RET OE MLE12 cells assessed by western blot analysis.

Moreover, ectopic overexpression of RET in MLE12 cells also led to significantly increase the migratory ability and was dramatically reversed by RET inhibitor treatment (Figure 27A). Furthermore, the ectopic RET overexpression reduced the level of epithelial marker E-cadherin and at the same time induceed the expression of mesenchymal markers (Figure 27B). Taken together, these data suggest that RET is a key downstream target of lamin B1, which mediates EMT and the increased migratory and invasive phenotype upon lamin B1 loss.

3.4.4 P38 MAPK signaling pathway is activated upon RET overexpression in lamin B1-depleted cells

Several studies have uncovered a role of RET in stimulating numerous signaling pathways affecting cell migration, including p38, JNK and ERK. Therefore we investigated whether these pathways were affected in lamin B1 depleted mouse lung epithelial cells. To this end, first we examined whether components of the MAPK signaling pathway are activated upon RET overexpression in lamin B1-depleted cells.

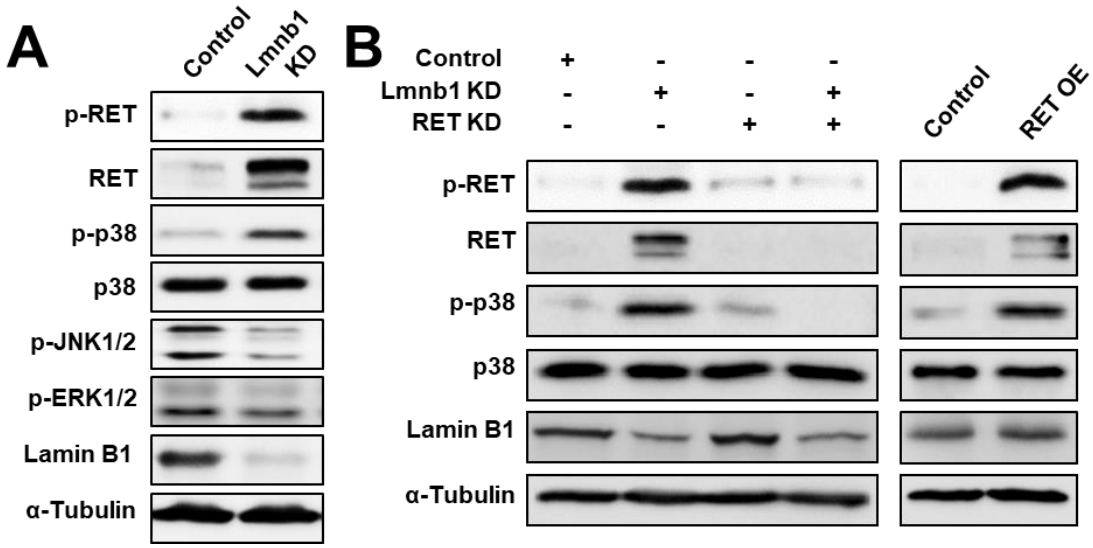

Figure 28. Role of RET upregulation in activating MAPK signaling pathway upon lamin B1 depletion(**A**) Western blot analyses for activated p38, JNK and ERK1/2 of control and lamin B1 knockdown MLE12 cells. (**B**) Western blot analyses for p38 and activated phospho-p38 in control, lamin B1 KD, RET KD, lamin B1/RET double KD, RET overexpressed (OE) MLE12 cells.

Immunoblot analysis for activated phosphorylated p38 (p-p38), phosphorylated JNK1/2 (p-JNK1/2) and phosphorylated ERK1/2 (p- ERK1/2) revealed a marked increase of p-p38 level, indicating p38 activation, in lamin B1-depleted MLE12 cells. The levels of p-ERK1/2, indicating ERK1/2 activation, were not changed and p-JNK1/2, indicating JNK1/2 activation, was even decreased (Figure 28 A). Importantly, depletion of RET in lamin B1-silenced cells lead to a

significant decrease in p-p38 (Figure 28 B). In addition, the level of p-p38 in RET-overexpressing MLE12 cells is higher than the one in the control (Figure 28 B).These data indicate that p38 as a downstream target of RET can be activated by RET upregulation.

3.4.5 RET/p38 axis is responsible for the increased migratory phenotype upon lamin B1 loss

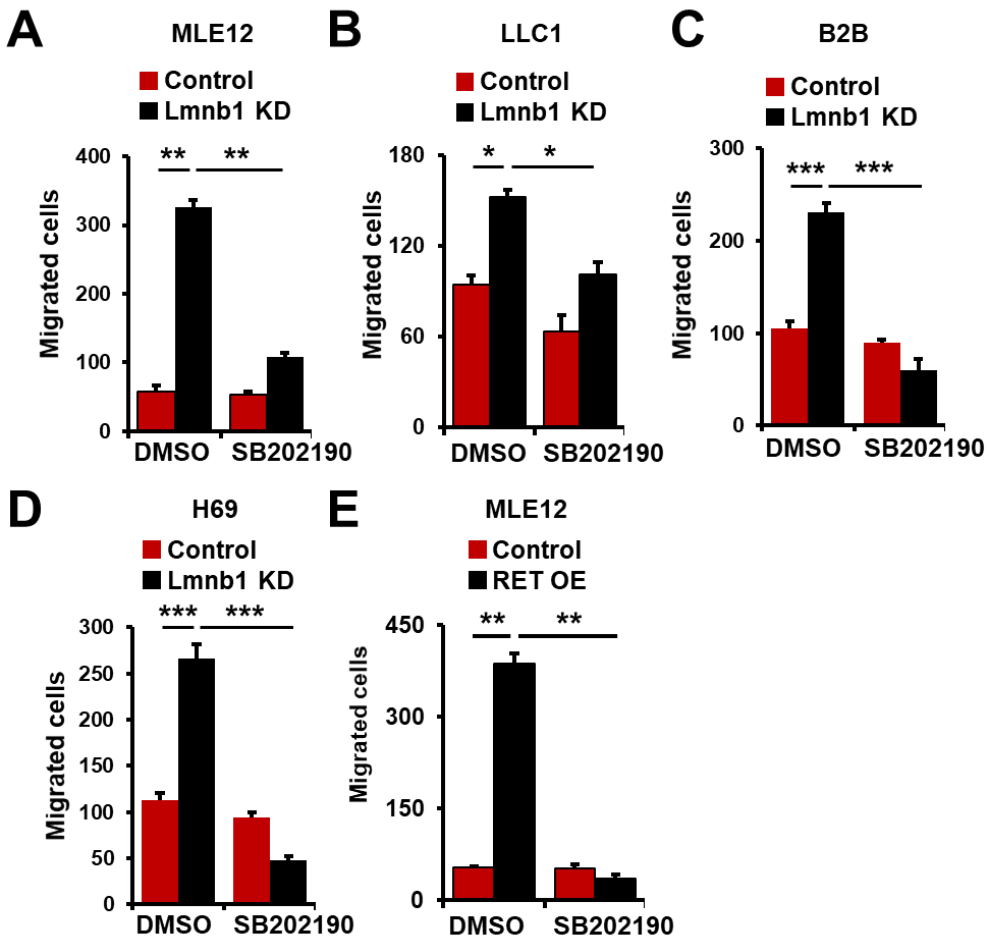

Figure 29. Effect of p38 inhibition on the increased migratory ability upon lamin B1 loss. Boyden chamber migration assay with control and Lmnb1 KD MLE12 (**A**), LLC1 cells (**B**), B2B (**C**) and H69 (**D**) as well as control and RET overexpressed (OE) MLE12 (**E**) treated with DMSO or 30 µM SB202190. Data are shown by mean ± SEM. *, $p < 0.05$; **, $p < 0.01$; ***, $p < 0.001$

In order to investigate the role of the RET/p38 axis in mediating the increased migratory and invasive phenotype upon lamin B1 loss, we made use of a p38

selective inhibitor SB202190. Interestingly, treatment of lamin B1-silenced MLE12, LLC1, B2B and H69 cells with SB202190 induced a dramatic decrease in the migratory capacity (Figure 29 A-D). Moreover, the high migratory ability of RET-overexpressing MLE12 cells is dramatically reduced by p38 inhibitor treatment (Figure 29 E). These data indicate that the activation of p38 signaling pathway is induced by RET upregulation upon lamin B1-depletion and plays a key role in cancer cell migration and metastasis.

Taken together, these data suggest that activation of RET/p38 signaling is responsible for the high migratory phenotype of lamin B1-depleted lung epithelial cells.

3.4.6 RET upregulation play a key role in promoting migration and metastasis of lamin B1-depleted cells *in vivo*

Next, we further analyzed the role of RET in lamin B1 depletion-mediated cancer cell migration and metastasis by *in vivo* approaches. To this end, we examined the role of RET on metastatic dissemination of lamin B1-depleted lung epithelial cells by intravenously injecting the control, lamin B1 knockdown (Lmnb1 KD), RET knockdown (RET KD) and lamin B1/RET double knockdown LLC1 cells in C57BL/6 mice. After 20 days we dissected the lung of each mouse to analyze the size and to count the number of tumor nodules. Importantly, the results showed that the loss of lamin B1 induces cell metastatic ability and tumor growth, evident by the dramatic increase of the metastatic area, number of tumor nodules and tumor volume of mice injected with lamin B1 knockdown cells in comparison to control counterpart. These observations support our *in vitro* data showing that loss of lamin B1 facilitates the cancer cell migration (Figure 30). Furthermore, silencing of RET inhibited tumor growth and metastatic ability of lamin B1-depleted cells, evident by the significant decrease in terms of the metastatic area, number of tumor nodules and tumor volume of mice injected with lamin B1/RET double knockdown compared to lamin B1 knockdown LLC1 cells (Figure 30).

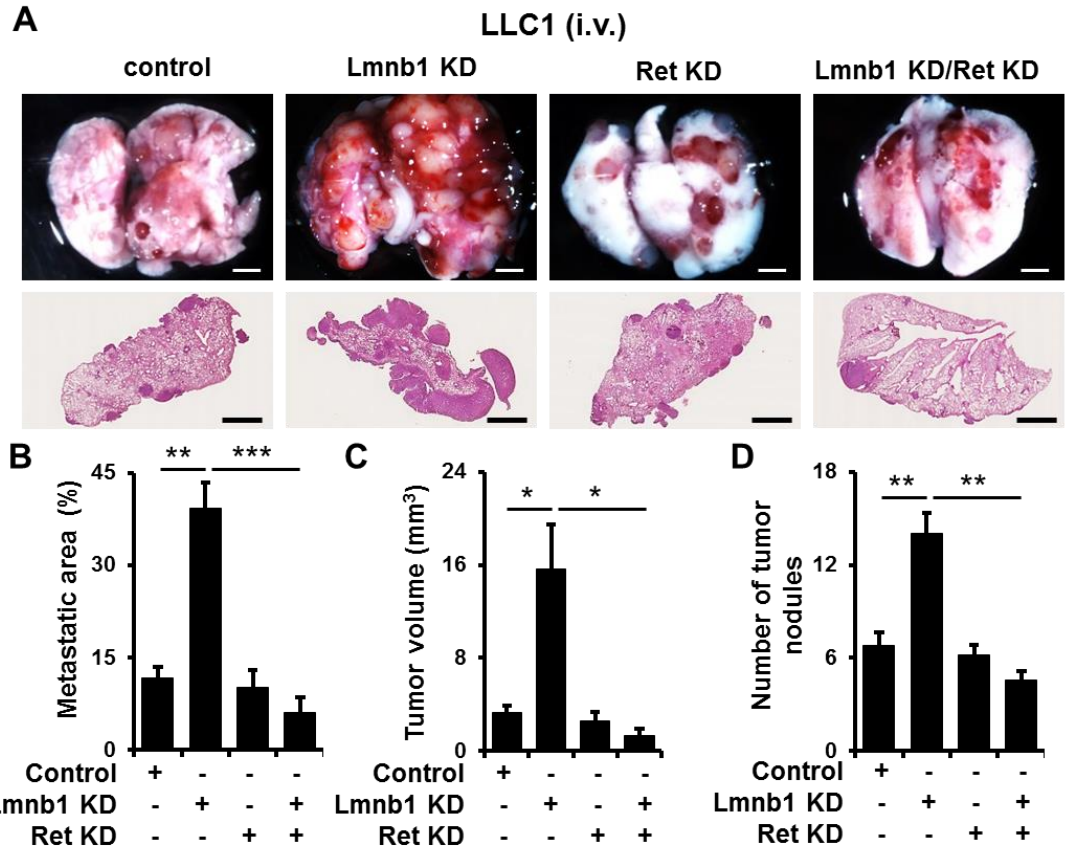

Figure 30. Lamin B1 depletion promotes formation of metastatic tumor lesions through a RET dependent mechanism. (**A-D**) Control, lamin B1 KD, RET KD and lamin B1/RET double KD LLC1 cells were injected intravenously into the tail vein of C57BL/6 mice for 20 days (n=6 each). Mice were sacrificed and examined for tumor metastases in the lungs. Macroscopic appearance (**A**, upper panels) and H&E staining (**A**, lower panels) of representative lungs. (**B-D**) Quantification of the metastatic area (**B**), microscopic tumor volume (**C**) and metastatic nodules (**D**) of mice injected with control, lamin B1 KD, RET KD and lamin B1/RET double KD LLC1 cells.

Moreover, we also analyzed the role of RET and lamin B1 on tumor growth and spontaneous metastasis *in vivo* by subcutaneously injecting the control, lamin B1 knockdown, RET knockdown and lamin B1/RET double knockdown LLC1 cells in C57BL/6 mice (Figure 31). Interestingly, the tumor volume of mice transplanted with lamin B1 silenced LLC1 cells was similar compared to controls at day 20 after injection, although subcutaneous tumors were

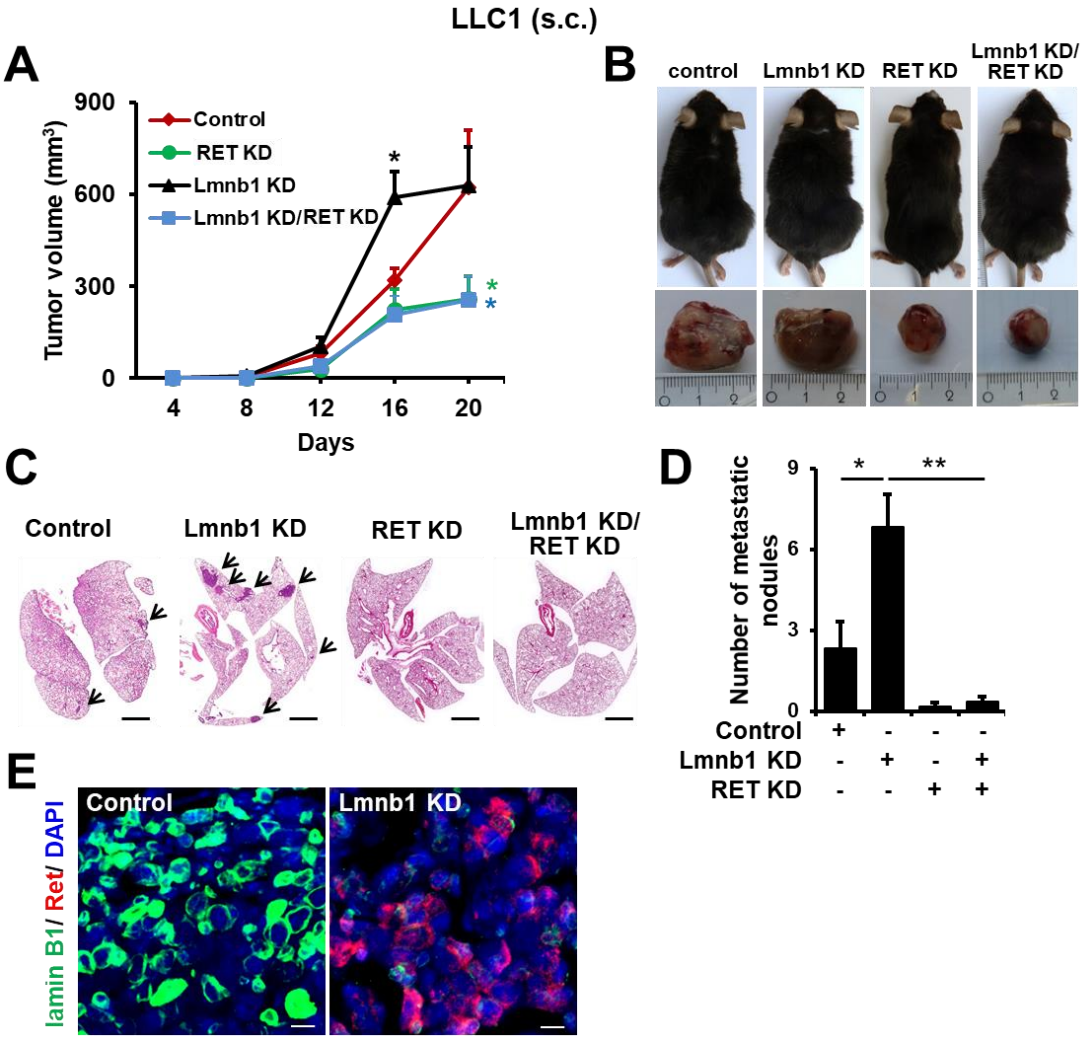

Figure 31. Lamin B1 knockdown promotes tumor growth and metastasis via a RET dependent mechanism. Control, lamin B1 KD, RET KD and lamin B1/RET double KD LLC1 cells were injected subcutaneously into the flanks of C57BL/6 mice for 20 days (n=6). (**A**) Quantification of the macroscopic tumor volume at different days after injection. (**B**, upper panels) representative image of the mice at day 20 post-injection. Mice were sacrificed and the subcutaneous tumors were removed (**B**, lower panels). (**C** and **D**) Spontaneous metastasis in lungs. H&E staining of representative lungs (**C**) and quantification of the number of metastatic nodules in the lungs (**D**) of mice injected with control, lamin B1 KD, RET KD and lamin B1/RET double KD LLC1 cells (n=6). Scale bars, 2 mm. (**E**) Co-staining with RET and lamin B1 antibodies of metastatic nodules in the lungs of mice injected with control or lamin B1 KD LLC1 cells. Scale bars, 10 µm. Data are mean ± SEM. *p< 0.05, **p< 0.01.

significantly larger in mice injected with lamin B1 knockdown LLC1 cells at day

16 (Figure 31 A and B). In contrast, RET depletion in control and lamin B1 knockdown cells resulted in significant decrease in tumor volume. Importantly, a much higher number of spontaneous metastases with larger tumor volume were found in the lungs of mice injected with lamin B1-depleted LLC1 cells compared to controls, whereas almost no metastasis was observed in mice injected with RET knockdown and lamin B1/RET double knockdown LLC1 (Figure 31 C and D). Consistently with the RET upregulation upon lamin B1 loss observed in cell culture studies, the metastatic nodules in the lungs of mice injected with lamin B1-depleted LLC1 showed high RET expression (Figure 31 E). Taken together, these data indicate that loss of lamin B1 plays a key role in mediating the EMT and malignant phenotype *in vivo* via upregulation of the proto-oncogene RET.

3.5 RET levels negatively correlate with lamin B1 levels in lung cancer patients

3.5.1 The levels of RET are increased in lung cancer patients

To address the clinical significance of our findings, we investigated whether there is a correlation between lamin B1 and RET levels in lung cancer patients. To this end, we first analyzed RET expression in a human lung tissue microarray by performing immunohistochemical staining with RET specific antibody. As it is shown in Figure 32, RET is almost undetectable in normal lung tissue, but is significantly upregulated in different types of lung cancer specimen (Figure 32).

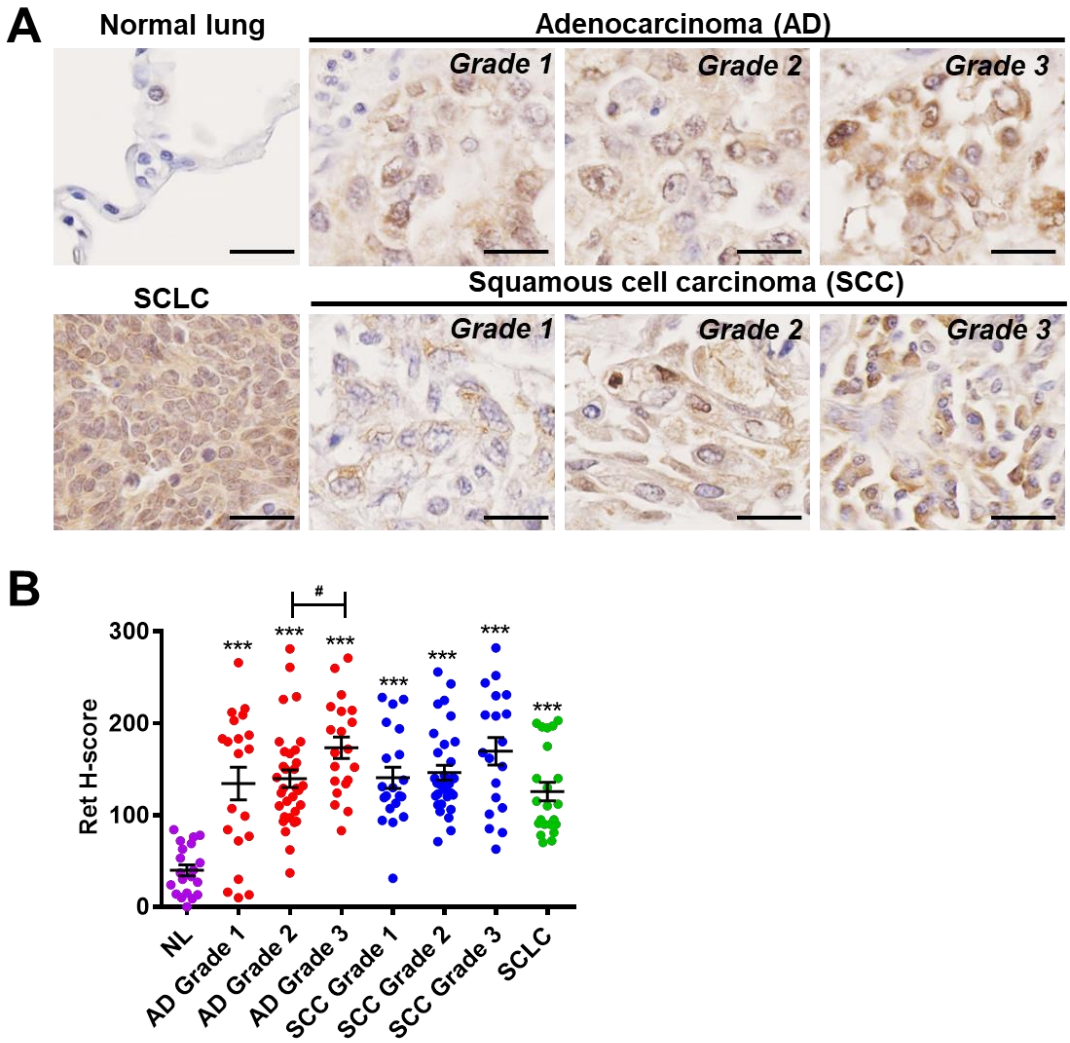

Figure 32. RET levels are increased in lung cancer specimens in comparison to normal lung tissue. (**A**) Immunohistochemistry of representative tissue samples from different types and grades of lung tumors, from a tissue microarray, stained with an anti-RET antibody. AD, adenocarcinoma; SCC, squamous cell carcinoma; SCLC, small cell lung cancer. Scale bars, 25 µm. (**B**) Relative RET staining intensity (H-Score) in lung tumors of different types and grades. n=70 AD (20 Grade 1, 30 Grade 2, 20 Grade 3); n=69 SCC (16 Grade 1, 33 Grade 2, 20 Grade 3), n=22 SCLC and n=20 NL. ***p < 0.001 vs NL. #p < 0.05.

3.5.2 RET levels negatively correlate with lamin B1 expression in lung cancer specimens

Moreover, we correlated the H-score of RET staining and lamin B1 staining in each individual human specimens. Intriguingly, the RET H-score in the tumors

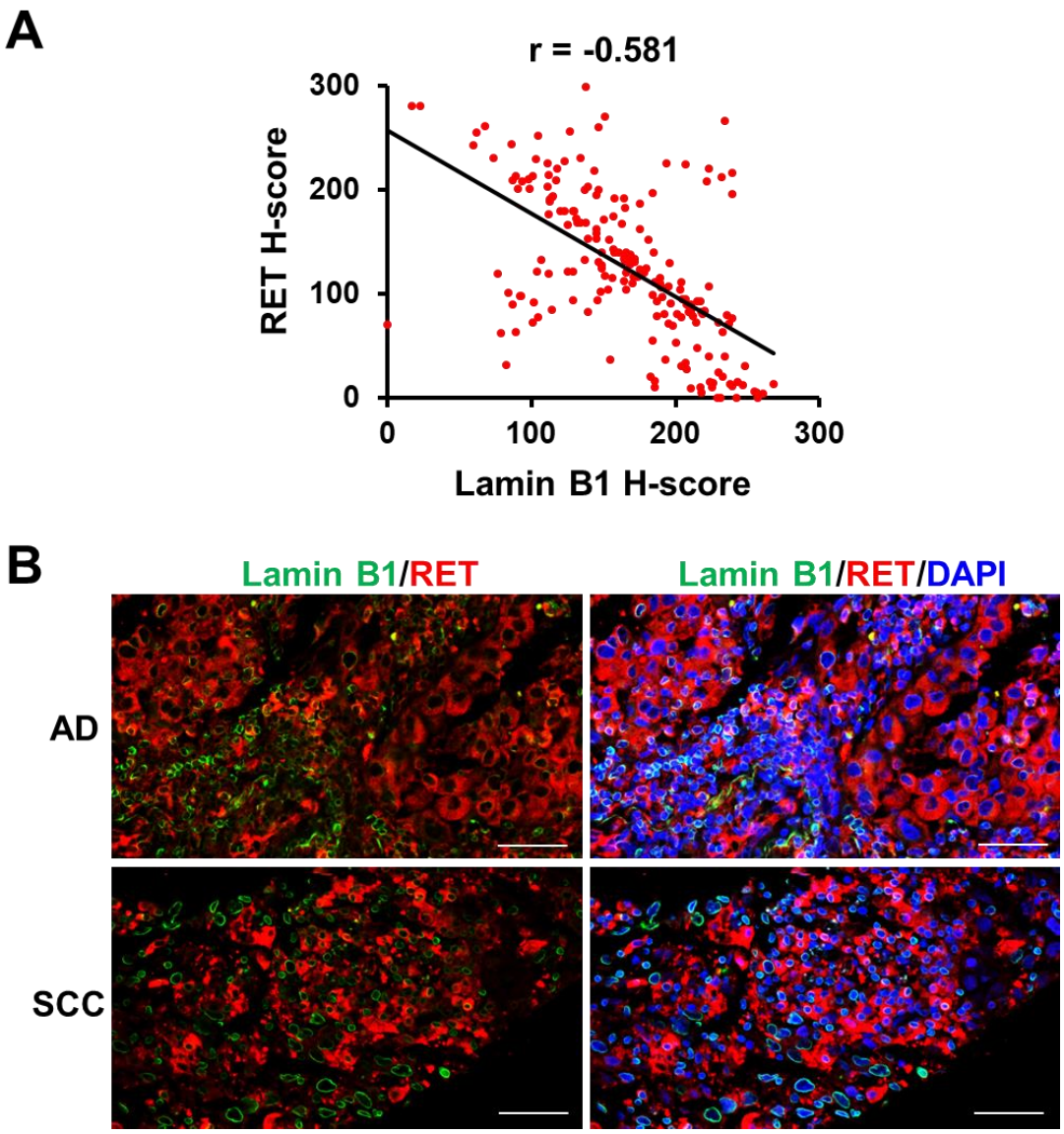

Figure 33. Lamin B1 and RET expression show inverse correlation in lung cancer patients. (**A**) Pearson correlation between the relative staining intensity for lamin B1 and RET; r, Pearson correlation coefficient. (**B**) Co-immunostaining of representative adenocarcinoma and squamous cell carcinoma Grade 3 samples with RET and lamin B1 antibodies showing that cells highly positive for lamin B1 express low levels or RET and vice versa. Scale bar, 50 μm.

was found to significantly negatively correlates with the lamin B1 H-score with a Pearson correlation coefficient r = -0.632, supporting a link between lamin B1 loss and RET upregulation in lung cancer patients (Figure 33 A). Furthermore,

we also observed a mutually exclusive pattern of lamin B1 and RET staining in lung cancer specimens (Figure 33 B). These data suggest a clinical significance and therapeutical potential of lamin B1 depletion and the consequential RET upregulation.

3.6 Lamin B1 recruits the EZH1/2 histone methyltransferase to silence RET expression

3.6.1 *RET* gene locates in lamina-associated domain with its promoter highly enriched with H3K27me3

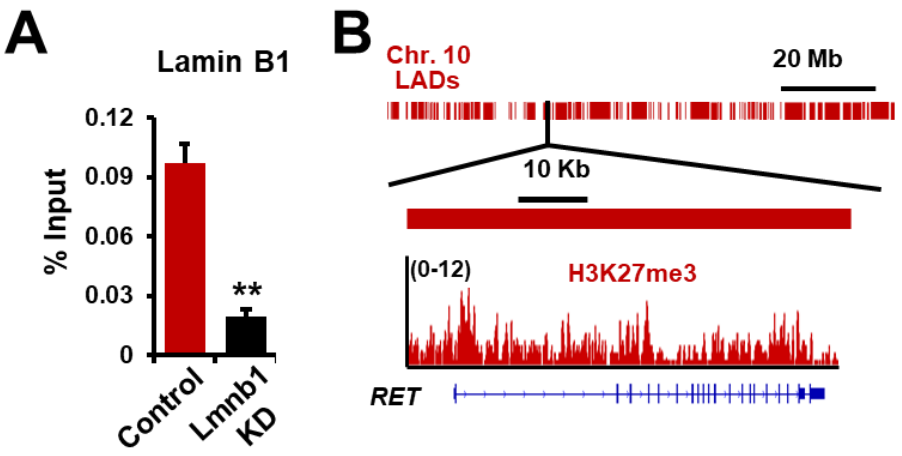

Figure 34. *RET* locates in LADs. (**A**) ChIP-qPCR analysis of lamin B1 binding at the *Ret* promoter (n=4). Data are shown as mean ± SEM. **, $p < 0.01$. (**B**) Schematic representation of the *RET* gene and its localization in LADs (top). Genome tracks of H3K27me3 of human lung tissue, showing that the *RET* promoter is decorated with H3K27me3 mark.

It has been shown that genomic regions that interact with nuclear lamins are transcriptional repressed and enriched with repressive heterochromatin marks (van Steensel and Belmont, 2017). Therefore, we investigated whether *Ret* gene directly interacts with lamin B1. ChIP-qPCR analysis revealed that lamin

B1 directly binds to *Ret* promoter in MLE12 cells (Figure 34 A) and this interaction was disrupted upon lamin B1 depletion. Similar to our finding in MLE12 cells, analysis of lamin B1 and H3K27me3 ChIP-seq data of human lung tissue (Shah et al., 2013; Thurman et al., 2012) revealed that RET gene is located in a large lamina-associated domain (LAD) and is decorated by H3K27me3 at its promoter (Figure 34 B), suggesting similar mechanism of RET regulation in humans.

3.6.2 Lamin B1 depletion leads to repositioning of *RET* and *Gfra1* genes

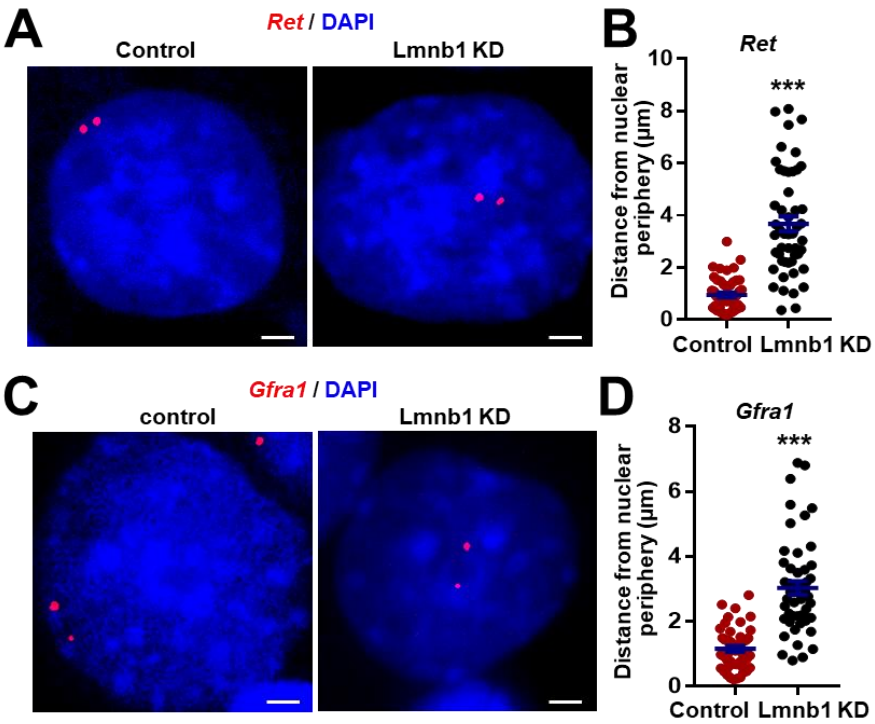

Figure 35. Lamin B1 Loss alters gene positioning. Representative DNA FISH images of *RET* (**A**) and *Gfra1* (**C**) genes (Red) in control or Lmnb1 KD MLE12 cells. Cell nuclei were labeled by DAPI. Scale bars are 2 µm. Quantification of distance of *RET* (**B**) and *Gfra1* (**D**) genes to nuclear periphery in each individual nucleus of control or Lmnb1 KD MLE12 cells. (n=50) ***: $p < 0.001$.

A number of studies revealed that spatial positioning of genes at nuclear periphery play a repressive role in regulating gene expression (Finlan et al.,

2008; Reddy et al., 2008; van Steensel and Belmont, 2017). Dissociation between gene and nuclear lamina leads to repositioning of gene away from the nuclear periphery, thus activates gene expression (Poleshko et al., 2017). To gain further insights into the molecular mechanism mediating the role of lamin B1 in lung cancer development, metastasis and gene regulation we first analyzed the spatial gene positioning of the RET (Chr. 6) and its co-receptor Gfra1 gene loci (Chr. 19) in control and lamin B1-depleted MLE12 cells by fluorescence in situ hybridization (FISH) analysis. Intriguingly, we found that *RET* and *Gfra1* locate at the nuclear periphery in control cells, whereas loss of lamin B1 leads to repositioning of *RET* and *Gfra1* away from nuclear periphery (Figure 35).

3.6.3 Loss of lamin B1 alters morphology and location of chromosome 6

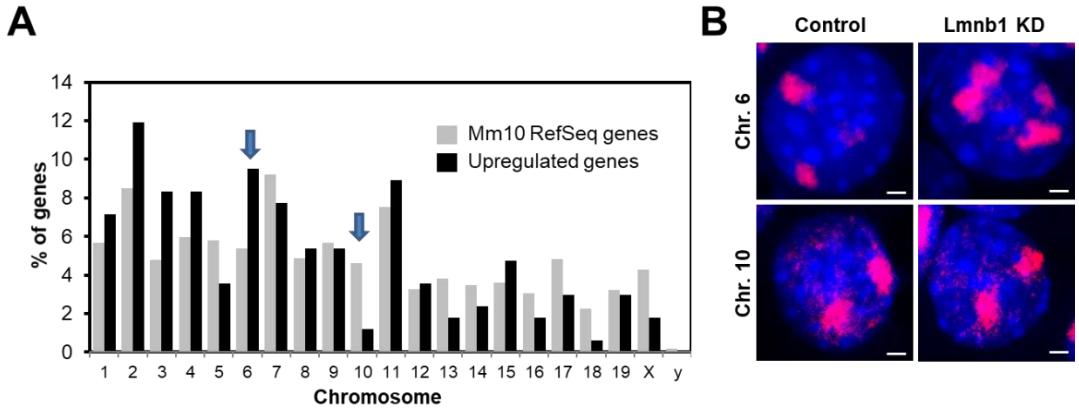

Figure 36. Lamin B1 loss affects morphology and location of Chr.6. (**A**) Distribution among chromosomes of differentially regulated genes upon lamin B1 loss of function. (**B**) FISH chromosome painting of chromosome 6 and chromosome 10 in control or Lmnb1 KD MLE12 cells.

Furthermore, we observed differences in the distribution of differentially regulated genes among chromosomes (Figure 36 A), e.g. Chr.6, showed higher percentage of upregulated genes in comparison to the % of RefSeq genes at

this chromosome, and Chr.10 showed lower percentage (Figure 36 A). Thus, we investigated the morphology and location of Chr.6 and Chr. 10 by chromosome painting. In control MLE12 cells, Chr. 6 territories were found near the nuclear lamina and were compact, whereas in lamin B1-depleted cells the nuclear territories occupied by Chr.6 were larger and more centrally localized (Figure 36 B). In contrast, no major difference was observed for Chr.10 (Figure 36 B).

3.6.4 Lamin B1 depletion reduces the enrichment of repressive histone marks at the promoter of both *RET* and *Gfra1*

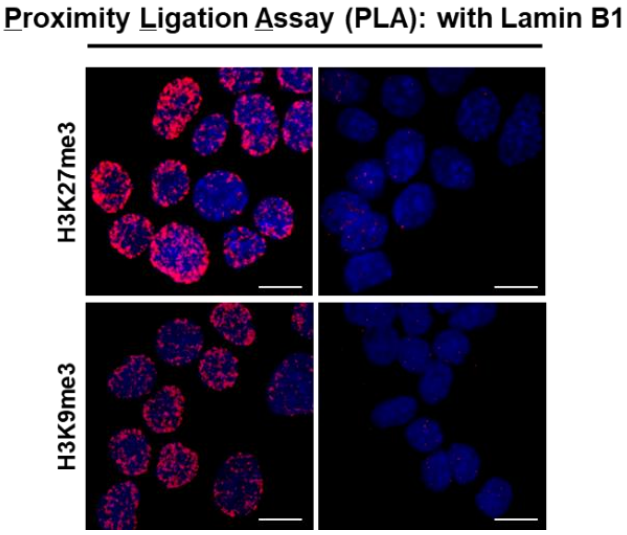

Figure 37. Proximity ligation assay (PLA) using anti-lamin B1 with either anti-H3K27me3 or anti-H3K9me3 antibodies. Scale bars, 10 µm.

Based on previous studies which have shown the role of lamins in regulating transcription by recruiting chromatin modifiers and transcription factors, we analyzed chromatin structure of control and lamin B1-depleted MLE12 cells. In support of the previous studies showing that lamina-associated domains (LADs) tightly associate with heterochromatin and enriched with repressive histone marks such as H3K9me2, H3K9me3 and H3K27me3 (van Steensel and Belmont, 2017), we observed that lamin B1 closely associates with H3K27me3 and H3K9me3 by proximity ligation assay (PLA, Figure 37).

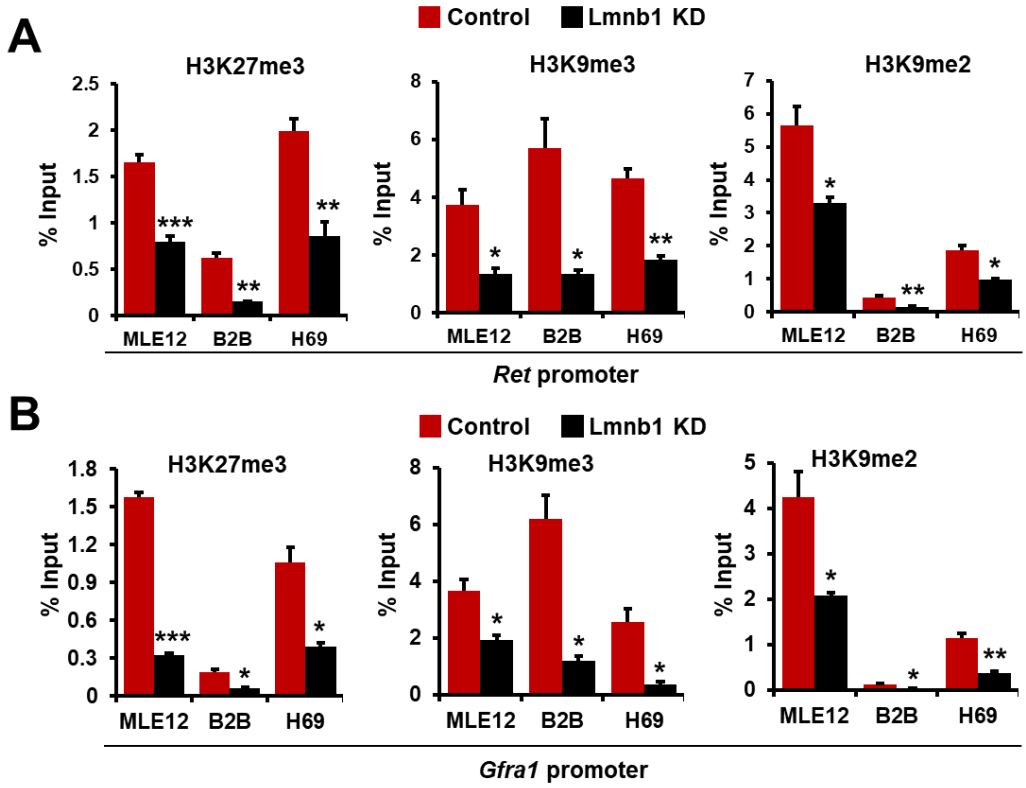

Figure 38. ChIP-qPCR analysis of H3K27me3, H3K9me3 and H3K9me2 occupancy at the *Ret* (**A**) or *Gfra1* (**B**) promoter (n=4). Data are shown as mean ± SEM. *, $p < 0.05$. **, $p < 0.01$. ***, $p < 0.001$.

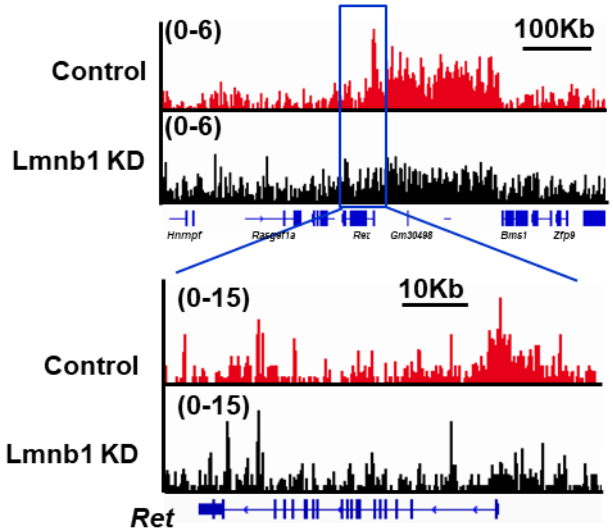

Figure 39. Genome tracks of H3K27me3 ChIP-seq in control and lamin B1 KD MLE12 cells (n=2) showing decreased levels of H3K27me3 upon lamin B1 loss.

Moreover, ChIP-qPCR analyses for H3K27me3, H3K9me3 and H3K9me2 in control and Lmnb1 KD cells reveal dramatically reduced enrichment of all these three repressive histone marks at the promoter of both *Ret* and *Gfra1* gene upon lamin B1 depletion (Figure 38).

Furthermore, genome wide ChIP-seq analysis for H3K27me3 confirmed the decreased levels of H3K27me3 at the *Ret* promoter in lamin B1-depleted lung epithelial cells (Figure 39). The *Ret* promoter is found in a broad H3K27me3 chromatin domain, which showed a global decrease of H3K27me3 upon lamin B1 loss-of-function (Figure 39).

3.6.5 Loss of lamin B1 activates *RET* transcription by increasing the binding of transcription factor Ascl1 at *Ret* promoter

Importantly, we found a significantly increased binding of transcription factor Ascl1, which has been widely shown to directly activate RET transcription and play a critical role in lung cancer development (Augustyn et al., 2014; Kosari et al., 2014), at the *Ret* promoter as well as increased accumulation of RNA polymerase II (Pol II, Figure 40 A and B).

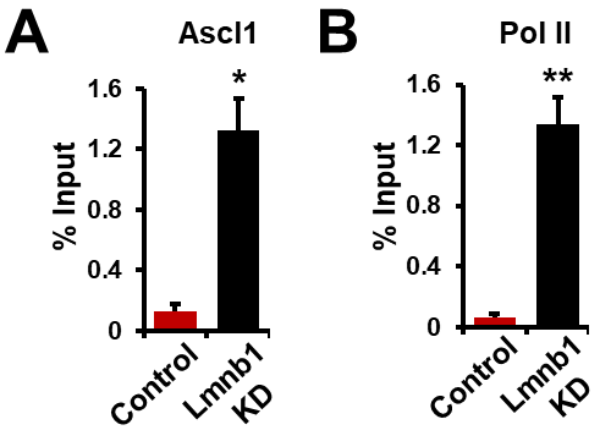

Figure 40. Lamin B1 depletion increases the binding of Ascl1 and Pol II at *Ret* promoter. ChIP-qPCR analysis of Ascl1 (**A**) and Pol II (**B**) binding at the *Ret* promoter (n=4). Data are shown as mean ± SEM. *, $p < 0.05$. **, $p < 0.01$.

3.6.6 Ascl1 does not promote *Ret* gene positioning

Thus, we analyzed the role of Ascl1 on *Ret* gene positioning and expression in lamin B1-knockdown MLE12 cells. While FISH analyses revealed that RET is more centrally localized in both lamin B1-depleted and Ascl1/lamin B1 double knockdown cells (Figure 41 A), RET expression was significantly downregulated upon Ascl1 depletion in lamin B1-silenced cells (Figure 41 B), suggesting that not only lack of tethering to the nuclear periphery leads to Ascl1-dependent *Ret* gene activation.

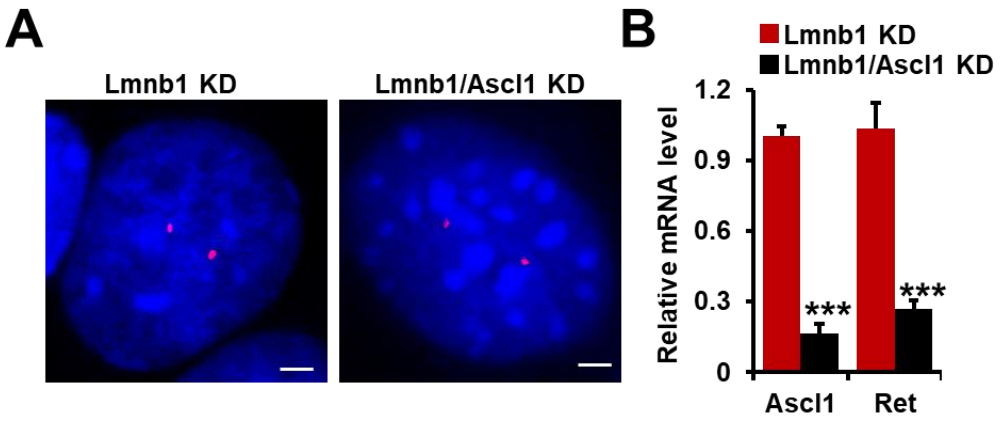

Figure 41. Ascl1 depletion in Lmnb1 KD cells reduces *RET* transcription without affecting the positioning of *Ret* gene. (**A**) Representative DNA FISH images of the *Ret* gene (red) in Lmnb1 KD or Lmnb1/ Ascl1 double KD MLE12 cells. Scale bars are 2 µm. (**B**) qPCR analysis of Ascl1 and RET expression in Lmnb1 KD or Lmnb1/ Ascl1 double KD MLE12 cells (n=6). Data are shown as mean ± SEM. ***, $p < 0.001$.

3.6.7 Lamin B1 binds to EZH1/2 and recruits EZH1/2 to chromatin

Extensive epigenetic studies have revealed that H3K27 methylation is catalyzed by the methyltransferases enhancer of zeste homologs 1 (EZH1) and 2 (EZH2), which are the core catalytic subunits of polycomb repressive complex 2 (PRC2) (Cao et al., 2002; Czermin et al., 2002). Therefore, we hypothesized that the expression of RET might be also regulated by EZH1 and EZH2. In order

to understand the role of these methyltransferases in regulating RET expression, we first analyzed their expression in lamin B1 knockdown MLE12 cells by western blot. Interestingly, although the global nuclear levels of EZH1/2 remained the same, significant lower level of EZH1/2 was found in the chromatin bound fraction of lamin B1-depleted cells (Figure 42 A). These data suggest that lamin B1 might bind and recruit EZH1/2 to chromatin, thereby facilitating EZH1/2-mediated H3K27me3.

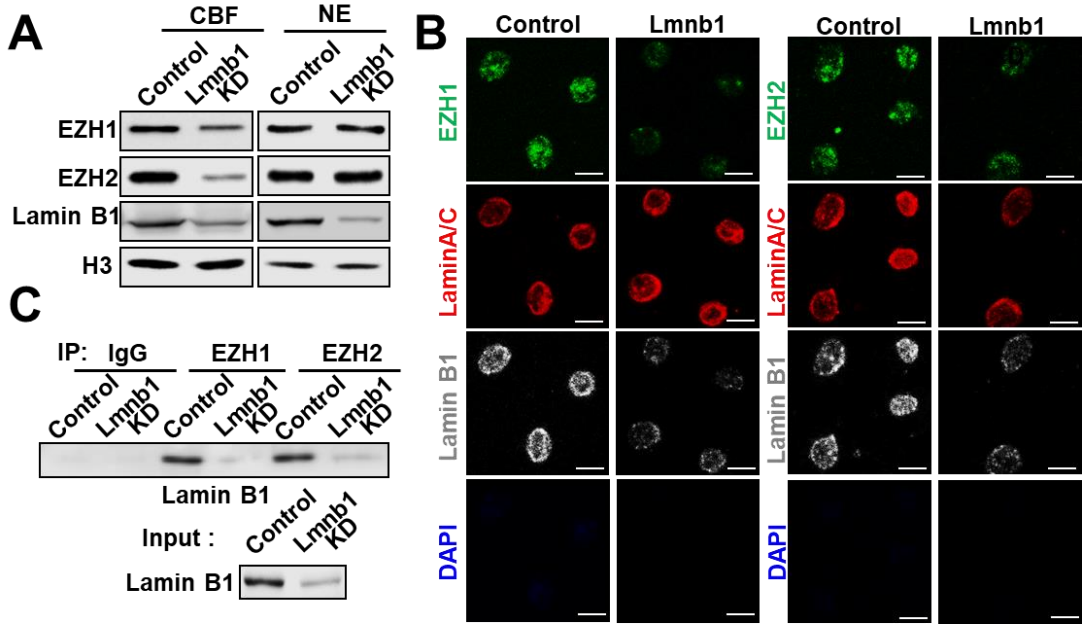

Figure 42. Lamin B1 recruits EZH1/2 to chromatin. (**A**) Western blot analysis of EZH1 and EZH2 level in nuclear extracts (NE) and chromatin bound fraction (CBF) of control and lamin B1 knockdown (Lmnb1 KD) MLE12 cells. (**B**) Immunostainings for lamin B1, lamin A/C and EZH1 or EZH2 of in situ nuclear matrix preparations of control and lamin B1 KD MLE12 cells. DNA content was assessed by DAPI staining, confirming that all chromatin has been removed. Scale bars, 5 µm. (**C**) Co-immunoprecipitation of extracts from control and lamin B1 KD cells using control, EZH1 or EZH2 antibodies and detected with anti-lamin B1 antibody.

Indeed, nuclear matrix/intermediate filament preparations demonstrated that EZH factors are retained throughout the nuclear matrix preparations from which

all chromatin detectable by DAPI staining has been removed in control mouse lung epithelial cells, but lost upon lamin B1 depletion (Figure 42 B). Thus, EZH factors are associated with the nuclear matrix through lamin B1. Moreover, co-immunoprecipitation revealed that lamin B1 binds specifically to EZH1 and EZH2 (Figure 42 C).

3.6.8 Loss of lamin B1 leads to reduced enrichment of EZH1/2 at *Ret* promoter and global decrease of H3K27me3

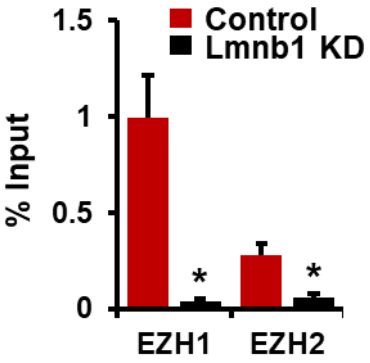

Figure 43. Lamin B1 loss reduces enrichment of EZH1/2 at *Ret* promoter. ChIP-qPCR analysis of EZH1 and EZH2 binding to the *Ret* promoter (n=4). Data are shown as mean ± SEM. *, $p < 0.05$.

Consistent with these results, EZH1 and EZH2 were not recruited to the *Ret* promoter in lamin B1 knockdown cells, whereas in control cells we detected strong association of both EZH1 and EZH2 to the promoter region of *Ret* (Figure 43).

Importantly, we observed a global decrease of H3K27me3 upon lamin B1 loss-of-function, consistent with the global decrease of chromatin-bound EZH1/2 (Figure 44 A and B).

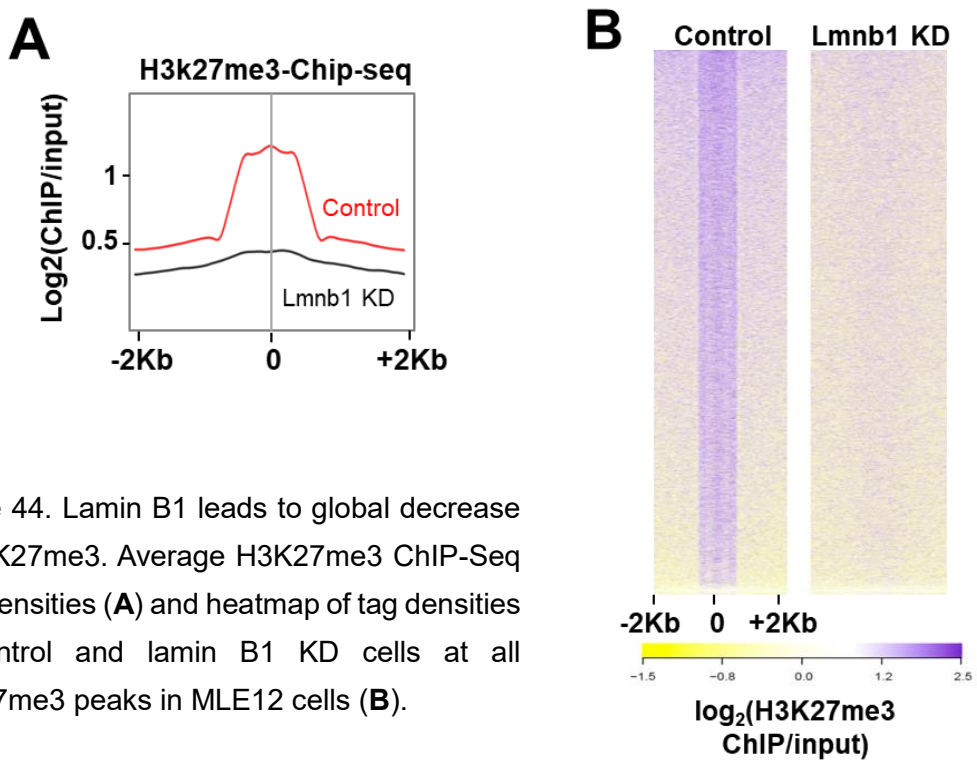

Figure 44. Lamin B1 leads to global decrease of H3K27me3. Average H3K27me3 ChIP-Seq tag intensities (**A**) and heatmap of tag densities in control and lamin B1 KD cells at all H3K27me3 peaks in MLE12 cells (**B**).

3.6.9 Targeting EZH1/2 increases RET expression and phenocopies the enhanced migratory phenotype of lamin B1-depleted cells

Next, we analyzed whether inhibition of EZH1/2 would phenocopy the increased migratory phenotype of lamin B1-depleted cells. To this end, we started by checking the efficiency of EZH1/2 inhibitor (UNC1999) treatment. Western blot analysis showed a significant decrease of H3K27me3 levels in MLE12 cells upon treatment with UNC1999 (Figure 45 A). This observation was confirmed by H3K27me3 ChIP followed by real-time PCR using specific primers, showing a dramatic reduction of H3K27me3 enrichment at the *Ret* promoter (Figure 45 B). Moreover, the reduction of H3K27me3 occupancy at *Ret* promoter mediated by UNC1999 treatment led to an increase of RET expression (Figure 45 C). Importantly, the migration capacity of MLE12 cells was also increased by UNC1999 application and could be restored to control levels by treatment with the RET inhibitor, Vandetanib (Figure 45 D), suggesting that RET functions as a downstream target of EZH1/2 to regulate cell migration

upon lamin B1 loss.

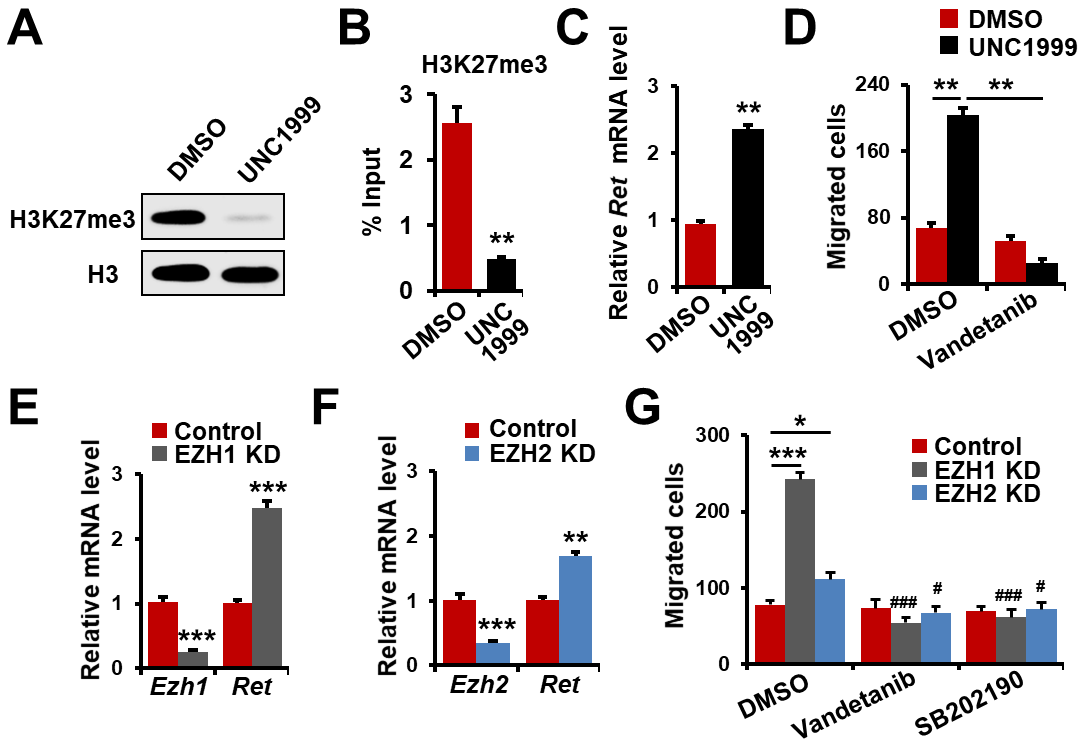

Figure 45. Inhibition of EZH1/2 activates RET expression and phenocopies the increased migratory phenotype of lamin B1-depleted cells. (**A**) Western blot analysis of global H3 and H3K27me3 levels in acid extracts of MLE12 cells treated with DMSO or the EZH1/EZH2 inhibitor UNC1999 (1 μM) for 3 days. (**B**) ChIP-qPCR analysis of H3K27me3 at the *Ret* promoter in MLE12 cells treated with DMSO or 1 μM UNC1999 (n=4). (**C**) Relative RET expression levels in MLE12 cells treated with DMSO or 1 μM UNC1999 (n=6). (**D**) Boyden chamber migration assay with MLE12 cells treated with DMSO, 1 μM UNC1999 or 1 μM UNC1999 and 20 nM Vandetanib (n=4). (**E** and **F**) Relative RET expression level in EZH1 (**E**) and EZH2 (**F**) knockdown MLE12 cells (n=6). (**G**) Boyden chamber migration assay with control, Ezh1 and Ezh2. knockdown MLE12 cells treated with DMSO, 20 nM Vandetanib or with 30 μM SB202190 (n=4). Data are mean ± SEM. *p< 0.05, **p< 0.01, ***p < 0.001 Ezh1 KD or Ezh2 KD vs control; ###p < 0.001, #p < 0.05 vs DMSO.

To further dissect the role of EZH1 and EZH2 in RET regulation and cell migration, we knockdown EZH1 and EZH2 in MLE12 cells by lentivirus-driven shRNA-mediated silencing. Intriguingly, we observed highly increased RET

expression in EZH1 depleted MLE12 cells in comparison to control cells (Figure 45 E). In contrast, EZH2 silencing only led to a moderate increase of RET expression (Figure 45 F). Likewise, EZH1 depletion tremendously induced migratory capacity of MLE12 cells (Figure 45 G). However, EZH2 merely resulted in a slight increase of cell migration (Figure 45 G). Similar to the EZH1/2 inhibitor studies, treatment with the RET inhibitor vandetanib dramatically reduced migration of both EZH1 and EZH2 knockdown cells to control levels (Figure 45 G). In addition, treatment with p38 inhibitor SB202190 also significantly decreased the migratory ability of EZH1- and EZH2 -silenced cells, comparable to control cells (Figure 45 G). Taken together, these data suggest that EZH1, instead of EZH2, play a more prominent role in mediating the malignant phenotype of lung epithelial cells with decreased lamin B1 levels.

3.6.10 Depletion or inhibition of EZH1/2 does not affect the positioning of *Ret* gene

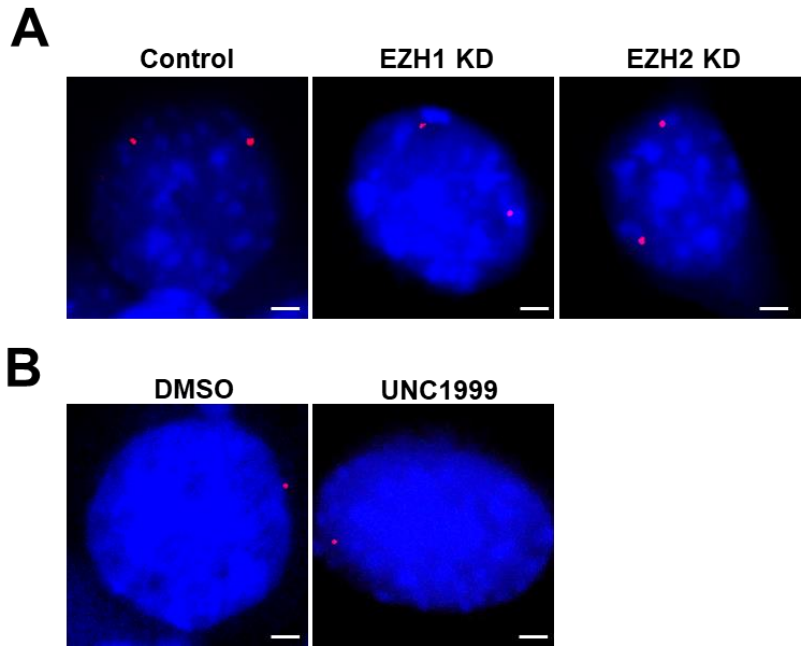

Figure 46. EZH1/2 depletion or inhibition has no effect on the localization of *Ret* gene. Representative DNA FISH images of *Ret* gene loci (red) in control, EZH1 or EZH2 KD MLE12 cells (**A**) and MLE12 cells treated with DMSO or 1 µM UNC1999 (**B**). Scale bars are 2 µm.

Next, we studied whether EZH1/2 depletion or inhibition affects *Ret* gene localization. We did not observe major changes in *Ret* positioning upon EZH1/2 loss or inhibition (Figure 46 A and B), indicating that not only lack of tethering to the nuclear periphery but also loss of EZH1/2 activity is essential for *Ret* gene activation.

3.6.11 Low levels of EZH1 are correlated with poorer prognosis of lung cancer patients

We next analyzed whether there is a correlation of EZH1 level with survival of lung cancer patients using Kaplan Meier-plotter (publicly available). Consistent with the stronger effects observed on cell migration upon EZH1 depletion, lung cancer patients expressing low levels of EZH1 had a significantly poorer prognosis than patients with higher EZH1 expression (Figure 47).

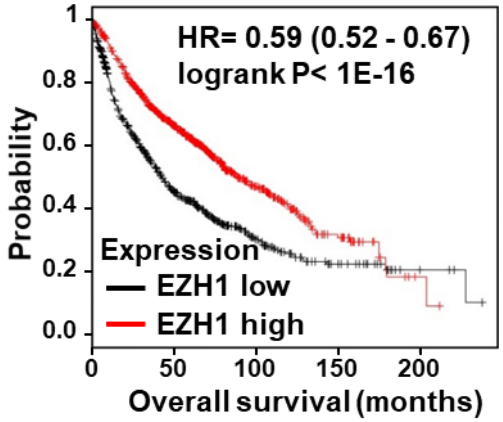

Figure 47. Overall survival curves (Kaplan-Meier plot) of lung cancer patients (Gyorffy et al., 2013) expressing high vs low levels of EZH1.

Taken together, these data support our finding that depletion of EZH1 and EZH2, especially EZH1, play a key role in upregulating RET in MLE12 cells upon lamin B1 depletion, thereby facilitating EMT, migration and metastasis. In respect to the inhibitory function of EZH1 and EZH2 in regulating RET expression, EZH1 play a relatively dominant role in comparison to EZH2.

3.7 Lamin B1 depletion induces aggressive lung tumor formation

3.7.1 Loss of one Lmnb1 allele is sufficient to induce lung tumor formation

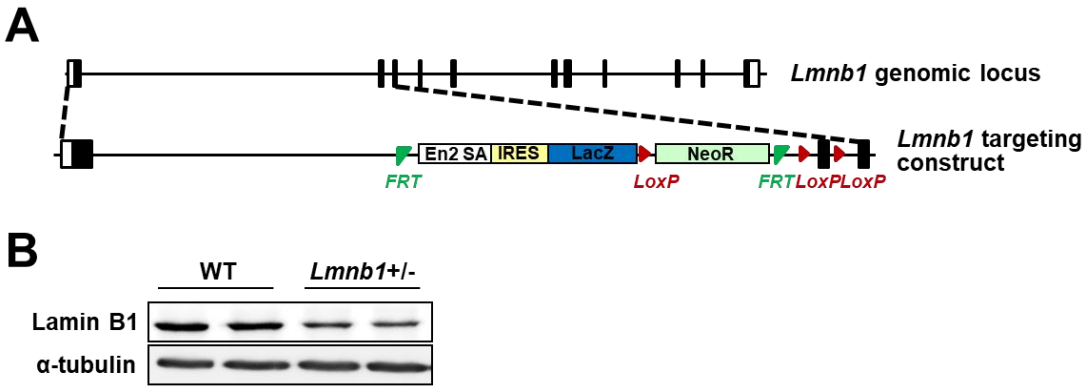

Figure 48. (**A**) Schematic representation of the *Lmnb1* genomic locus and *Lmnb1* targeting construct. (**B**) Western blot analysis of lysates from mouse embryonic fibroblasts derived from wild-type (WT) and *Lmnb1*+/- mice.

In order to further corroborate the role of lamin B1 downregulation in facilitating lung cancer formation and development, we used genetic approach with mice carrying a *Lmnb1* null allele (Figure 48 A). In consistence with published studies (Kim et al., 2011; Vergnes et al., 2004) and previous observations in our lab, *Lmnb1*-/- mice died at birth with profound lung abnormalities, whereas *Lmnb1*+/- mice, which showed lower lamin B1 protein levels (Figure 48 B), appeared normal at a young age although smaller than their littermates.

Table 3. Incidence of spontaneous lung tumor formation in wild-type and *Lmnb1*+/- mice.

	WT	*Lmnb1* +/-
6 months	1/15 (6.67%)	7/12 (58.3%)
1.5 year	2/27 (7.4%)	21/23 (91.3%)

Data are shown as number of tumor-bearing mice/ total number of mice.

Importantly, older mice had a very high incidence of spontaneous lung tumor formation. Seven out of 12 mice developed spontaneous tumors after 6 months, whereas 21 out of 23 mice showed tumors by 1.5 years of age (Figure 49, Table 3).

3.7.2 Most of the lung tumors induced by lamin B1 haploinsufficiency were histologically similar to small cell lung cancer

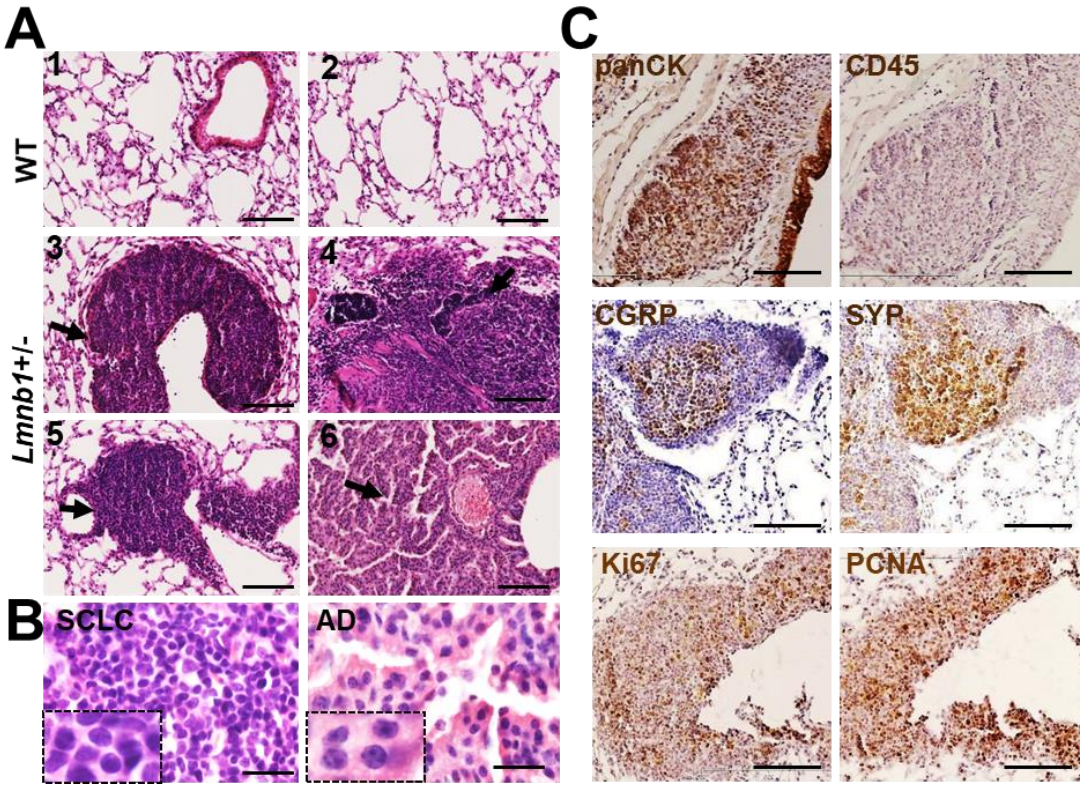

Figure 49. Lamin B1 haploinsufficiency induces aggressive lung tumor formation with most of them histologically similar to small cell lung cancer. (**A**) Histological analysis of representative lung sections of wild-type and Lmnb1+/- mice at 1,5 year of age; tumors are indicated by arrows. Scale bars, 100 μm. (**B**) High magnification images of tumors with SCLC characteristics (left panel) and tumors with AD characteristics (right panel). Scale bars, 20 μm. (**C**) Immunohistochemical staining of tumors in lungs of Lmnb1+/- mice with pan-cytokeratin (PanCK), CD45, CGRP, Syp, Ki67 and PCNA. Scale bars, 100 μm.

To further evaluate the cancer type of the spontaneous pulmonary tumor in the

Lmnb1+/- mice, we performed histological examination and IHC staining of WT and *Lmnb1*+/- lungs. We found that apart from a small fraction of tumors which exhibited morphological similarities to adenocarcinoma (Figure 49A panel 6, Figure 49B right panel), most of the tumors in *Lmnb1*+/- mice showed strikingly similar characteristics to small cell lung cancer (Figure 49A, panel 3-5, Figure 49B, left panel). The cells in these tumors were small with scant cytoplasm and densely packed chromatin, which obscured the nucleoli (Figure 49B, left panel). Furthermore, these tumors express, on the one hand, a high level of pan-cytokeratins (panCK), which marks epithelial tumors, and on the other hand, calcitonin gene-related peptide (CGRP) and synaptophysin (Syp), markers for small cell lung cancer of neuroendocrine origin (Meuwissen et al., 2003). Importantly, the lesions were negative for CD45, a marker for cells of haematopoietic origin (Figure 49 C), which ruled out the possibility of being lymphocytes. Additionally, immunostaining of Ki67 and PCNA indicates a high proliferative index within these lesions (Figure 49 C).

Taken together, these data reveal that the lack of a single functional Lmnb1 allele is sufficient to efficiently induce the formation of aggressive lung tumors, most of which display remarkable similarities to small cell lung cancer in human patients.

3.7.3 Tumors were also found in the kidney and liver of *Lmnb1*+/- mice

Analyses of other organs revealed tumors in the kidney and the liver. Similarly to the SCLC-like tumors in the lungs of the *Lmnb1*+/- mice (Figure 49), the cells in the tumor nodules in livers and kidneys were small with scant cytoplasm, expressed CGRP, Syp, panCK, but were negative for CD45 and were found close to blood vessels (Figure 50), suggesting that these might be extrapulmonary metastases rather than primary tumors in these organs.

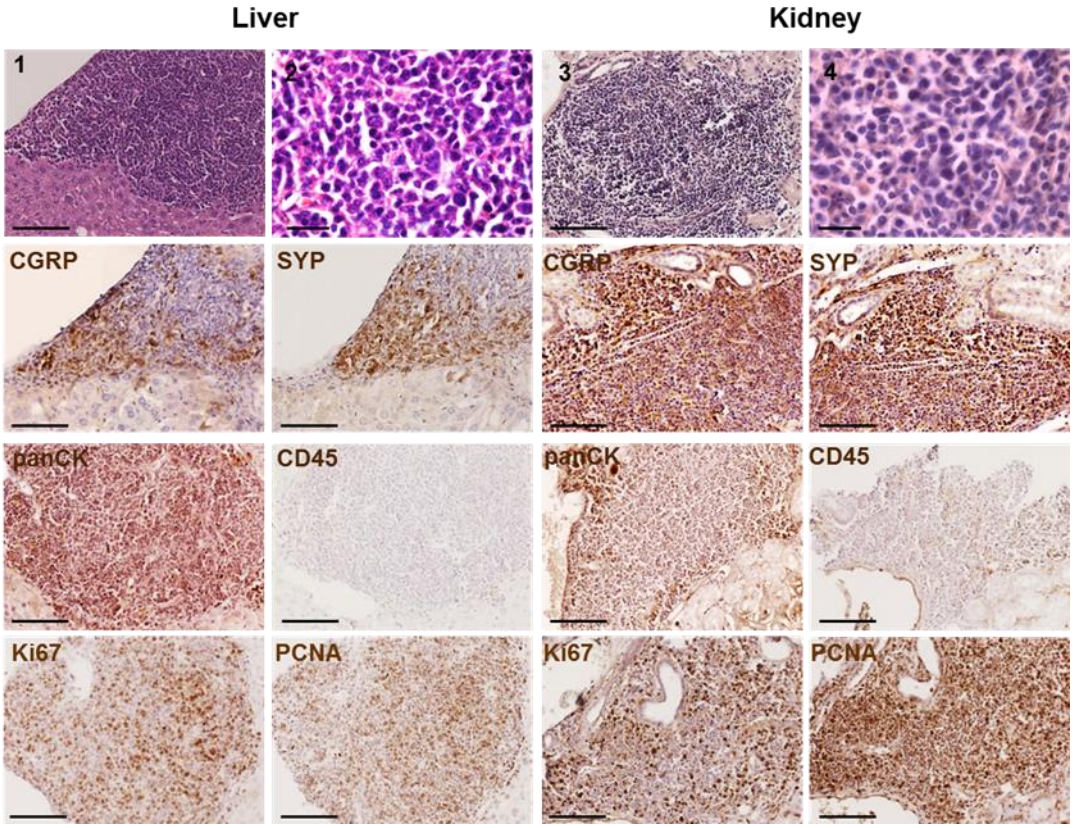

Figure 50. Immunohistochemical staining of representative metastatic tumors in lives and kidneys of Lmnb1+/- mice with anti-panCK, CGRP, Syp, CD45, Ki67 and PCNA antibodies. Scale bars: panel no. 2 and 4, 20 µm; the rest of panels, 100 µm

3.7.4 Pulmonary tumors in *Lmnb1*+/- mice show RET upregulation, RET/p38 activation as well as reduced enrichment of H3K27me3 and EZH1/2 at *Ret* promoter

In our cell culture studies, we found that loss of lamin B1 leads to RET upregulation and activation, followed by activation of the p38 signaling pathway. Thus, we next examined whether the tumors developed in *Lmnb1*+/- mice express RET, p-RET and p-p38. Indeed IHC analysis revealed that the tumors developed in *Lmnb1*+/- mice expressed very high RET, activated RET (p-RET) levels and activated p-p38 levels (Figure 51), supporting a link between lamin B1 deficiency, RET upregulation and RET/p38 activation in a genetic model of lamin B1 loss of function.

Next, we analyzed H3K27me3 levels and EZH1/2 recruitment to the RET locus in lungs of wild-type and Lmnb1+/- mice. Consistent with our cell culture studies, we observed a significant decrease in H3K27me3 levels and EZH1/2 occupancy at the *Ret* promoter (Figure 52).

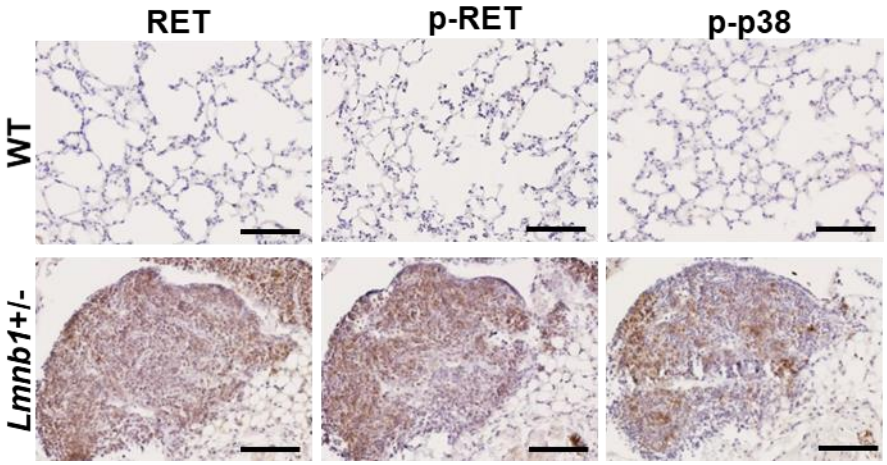

Figure 51. Lamin B1 haploinsufficiency induces RET upregulation and RET/p38 activation. Immunohistochemical staining of lungs of wild-type and Lmnb1+/- mice with RET, phospho-RET (p-RET Y1062) and phospho-p38 (p-p38 Thr180/Tyr182) antibody. Scale bars, 100 µm.

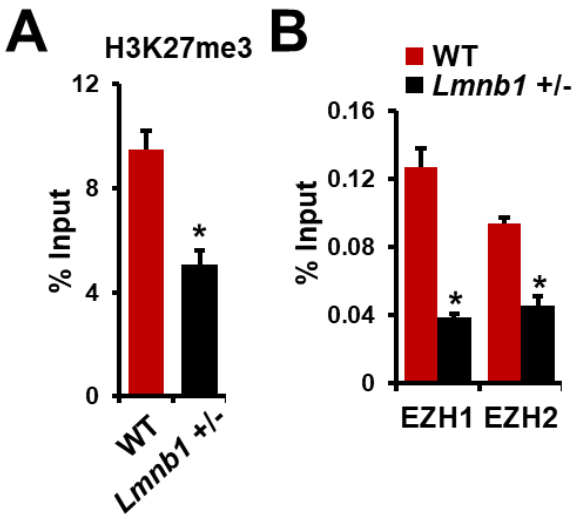

Figure 52. Lamin B1 haploinsufficiency decreases H3K27me3 levels and EZH1/2 occupancy at the *Ret* promoter (**A**) ChIP-qPCR analysis of H3K27me3 at the *Ret* promoter in wild-type and Lmnb1+/- lungs (n=4). (**B**) ChIP-qPCR analysis of EZH1, EZH2 binding to the *Ret* promoter in wild-type and Lmnb1+/- lungs (n=4).

3.8 Model of the role of lamin B1 as a tumor suppressor in lung cancer development and metastasis

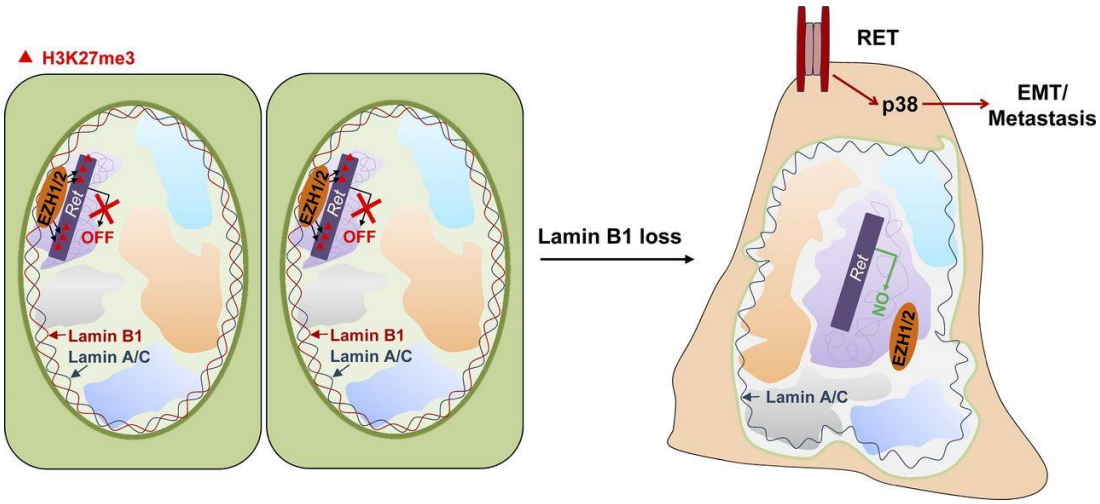

Figure 53. Model of the role of lamin B1 as a tumor suppressor in lung cancer development. In lung epithelial cells lamin B1 recruits the EZH1/2 histone methyltransferase to silence the expression of the RET proto-oncogene. Upon lamin B1 loss, recruitment of EZH1/2 to the *Ret* promoter is abolished leading to increases of RET expression, RET/p38 activation, EMT and metastasis.

In summary, our data demonstrate that loss of lamin B1 plays a key role in promoting lung cancer development and metastasis. We found that lamin B1 levels were reduced in lung cancer patients. Lamin B1 silencing in lung epithelial cells promoted epithelial–mesenchymal transition, cell migration, tumor growth, and metastasis. Mechanistically, we show that lamin B1 recruits the EZH1/2 to alter the H3K27me3 landscape and repress genes involved in cell migration and signaling. In particular, epigenetic derepression of the RET proto-oncogene by loss of EZH1/2 recruitment, and activation of the RET/p38 signaling axis, play a crucial role in mediating the malignant phenotype upon lamin B1 disruption. Importantly, loss of a single lamin B1 allele induced spontaneous lung tumor formation and RET activation. Thus, lamin B1 acts as a tumor suppressor in lung cancer, linking aberrant nuclear structure and

epigenetic patterning with malignancy (Figure 53).

4. Discussion

4.1 Lamin B1 as a potential marker of lung cancer

In the present study, we describe a crucial role of lamin B1 in lung cancer development and metastasis. Changes in the expression of lamins have been already linked to various tumor entities, however, the relationship appears to be complex and tumor type specific. Thus, while increased levels of lamins were reported in some cancers, such as hepatocellular carcinoma, colorectal and skin cancer (Marshall et al., 2010; Tilli et al., 2003; Willis et al., 2008), a reduction of lamins has been observed in others, including gastric and breast cancer as well as large B cell lymphoma (Agrelo et al., 2005; Capo-chichi et al., 2011; Wu et al., 2009). In respect to lung cancer specimens, the expression of lamins shows discrepancy among different studies. For instance, Broers et al. revealed a dramatic reduction of lamin A/C levels in both SCLC cell lines and specimens (Broers et al., 1993). This finding is in line with our observation showing a decrease of lamin A/C levels in SCLC specimens. However, elevated lamin A/C levels were observed in SCLC specimens and were positively correlated with enhanced malignancy of lung cancer (Kaufmann et al., 1991). In our study, we found reduced lamin B1 levels in different types of lung cancer specimens in comparison to normal lung tissues. In consistence with our finding, Broers et al. showed that B-type lamins expression was negative in non-small cell lung cancer cell lines, especially in adenocarcinomas (Broers et al., 1993). Although irregular expression of lamins is universally found in different types of human cancer cell lines and specimens, little is known about the mechanistic role of aberrant lamins expression in cancer initiation, progression, development and metastasis.

In addition, we observed that lower lamin B1 expression correlates with higher tumor grade in both adenocarcinoma and squamous cell carcinoma, suggesting that loss of lamin B1 associates with the progression and

malignancy of lung cancer. The role of lamin B1 in lung cancer initiation and progression were further corroborated by our finding that loss of a single lamin B1 functional allele is sufficient to dramatically elevate the occurrence of spontaneous pulmonary tumors in mice. Furthermore, the promoting role of lamin B1 in lung cancer development and progression is further supported by cell culture studies and intravenous/ subcutaneous injection of LLC1 and MLE12 cells.

4.2 The role of lamin B1 in cell proliferation and tumor initiation

The role of lamin B1 in cell proliferation is complex and cell type specific. Several studies have shown that lamin B1 depletion induces senescence and reduces proliferation in human embryonic fibroblasts (Shah et al., 2013; Shimi et al., 2011) and lead to an earlier onset of proliferative crisis in mouse embryonic fibroblasts (Vergnes et al., 2004). However, lamin B1 knockout embryonic stem cells do not show any obvious proliferation defects ((Kim et al., 2011) and our own observations). Moreover, lamin B1/lamin B2 double knockout keratinocytes proliferate normally in cell culture (Yang et al., 2011). In addition, the role of lamin B1 in modulating cell growth and proliferation appears to be O_2 concentration dependent. For instance, the lamin B1 depletion-induced proliferation defects in WI-38 human diploid fibroblasts can be rescued by growth under hypoxia (1.5% O2; (Shimi et al., 2011)), conditions which are characteristic of tumors and can even occur in normal tissues.

It is noteworthy that all the experiments in the above-mentioned studies were carried out in 2D adherent monolayer cultures, which often do not properly reflect the growth and transformation potential of cells in vivo. The latter is more faithfully recapitulated by 3D culture conditions that do not depend on anchorage to plastic surfaces, such as colony formation assays in soft agar. Therefore, in our study, we assessed the role of lamin B1 silencing not only on cell proliferation in adherent monolayers (anchorage-dependent conditions) but

also on anchorage-independent growth in soft agar. We observed that lamin B1 silencing led to decreased cell proliferation in monolayer cultures, which is consistent with some of the studies mentioned above. Importantly, however, the capacity of MLE12 cells to form colonies in soft agar as a measure of anchorage independent growth, one of the hallmarks of malignant transformation (Hanahan and Weinberg, 2011), was markedly increased by downregulation of lamin B1. Furthermore, the individual colony size was markedly increased by lamin B1 depletion. This is consistent with the pronounced differences in tumor growth and metastatic dissemination in vivo of lamin B1 knockdown MLE12 cells compared to control cells. In support of our finding, discrepancy between anchorage-dependent and -independent growth has also been observed in other studies. For example, Rotem et al (Rotem et al., 2015) showed that anchorage-dependent growth of cells did not correlate to anchorage-independent growth and that non-transformed cells grew faster than transformed cells in high-attachment conditions, in stark contrast to low-attachment conditions.

The potential mechanism by which lamin B1 depletion leads to lung cancer initiation still remains unknown. Studies found that lamin B1 depletion led to an increased accumulation of DNA damage and genomic instability (Butin-Israeli et al., 2015). Considering that DNA damage and genomic instability, together with the consequential mutations of genes, are widely regarded as a major cause of tumorigenesis (Hoeijmakers, 2009), loss of lamin B1 may lead to cancer initiation by inducing DNA damage and genomic instability.

Several gene mutations have been shown to drive pulmonary tumorigenesis. For instance, gain-of-function mutations of *EGFR*, *KRAS* and *RET* are frequently observed in non-small cell lung cancer (Carper and Claudio, 2015). Loss of the tumor suppressors *TP53* and *RB1* is also shown to be obligatory in SCLC by another study (George et al., 2015). Therefore, to investigate the potential mutations caused by lamin B1 depletion-mediated DNA damage and

genomic instability may help to reveal the molecular mechanism of tumorigenesis upon lamin B1 loss of function.

4.3 The role of lamin B1 in cancer cell migration and metastasis

Loss of nuclear lamins is implicated in regulating cell motility and migration by reducing the nuclear lamina stiffness (Harada et al., 2014). Successful migration and metastasis requires cell to deform in order to squeeze through tiny space between endothelial barriers to intrastate or extravasate. Therefore, as the largest single organelle in every cell, nucleus should soften in this procedure. After metastasis, a stiff nucleus helps cell withstand the stress from the microenvironment. Lamin A was shown to effectively stiffen nuclei, thereby reduced lamin A level facilitates cell migration by decreasing the nuclear stiffness (Harada et al., 2014; Song et al., 2016). In addition, lamin B1 regulates the expression of genes responsible for cell adhesion and extracellular matrix function in epicardial cell (Tran et al., 2016), implying a potential role of lamin B1 in regulating epicardial cell migration. In consistence with a previous observation in our group, we found a strong increase in migratory and invasive capacities in lamin B1 knockdown MLE12 and LLC1 cells in comparison with their control counterpart, respectively. Importantly, silencing of lamin B1 in both cell types dramatically increased tumor growth and metastasis showing by mice model intravenously/subcutaneously injected with control and lamin B1 depleted cells.

Theoretically, lamin depletion may contribute to cell migration and metastasis by increasing the plasticity of nuclear shape, thus facilitating changes in cell form that are required for penetrating restricted spaces, in particular during intravasation of cancer cells from primary tumors into the vasculature and extravasation into metastatic sites (Denais et al., 2016; Friedl et al., 2011). However, RNA-seq analysis on control and lamin B1 knockdown cells revealed significant enrichment of differentially expressed genes linked to migration and

metastasis related signaling in the genes upregulated upon lamin B1 depletion, suggesting a direct role of lamin B1 in the regulation of cancer cell migration and metastasis at the gene expression level. On the other hand, the fact that lamin B1 depletion mainly upregulates migration and metastasis related genes, instead of the genes associated with other biological processes, suggesting that lamin B1 might not randomly bind to the genome in lung epithelial cells, but specifically interact with certain genome regions thereby specifically repress the transcription of genes involved in EMT and cell migration.

Consistently, we observed a dramatic loss of cell-cell adhesion molecule E-cadherin and changes in cell morphology in MLE12 cells upon lamin B1 depletion. In contrast to the control cells which show cobblestone-like epithelial appearance, the lamin B1 KD MLE12 cells exhibit spindle-shaped morphology and increased expression of mesenchymal markers, suggesting that lamin B1-depleted cells undergo EMT. Since EMT has been widely considered as a major contributor to cancer cell migration and metastasis (Heerboth et al., 2015; Kalluri and Weinberg, 2009), therefore lamin B1 depletion-mediated EMT phenotype may play an important role in facilitating the migration and metastasis of lamin B1 knockdown cells. Taken together, our study for the first time correlates loss of lamin B1 with EMT phenotype in cancer migration and metastasis.

4.4 Loss of lamin B1 upregulates RET thereby triggering EMT and cancer cell migration and metastasis

Nuclear lamins, including lamin B1, are in close association with heterochromatin, which is tightly packed and inaccessible to transcription factors. Therefore, genomic regions that are in close contact with the nuclear lamins, termed lamina-associated domains (LADs), are usually transcriptionally silenced (van Steensel and Belmont, 2017). In consistence with the repressive role of lamin B1 in transcription regulation, we observed a higher number of

upregulated genes than downregulated genes upon lamin B1 depletion. By analyzing the data of RNA-seq, we observed upregulation of RET proto-oncogene and its co-receptor Gfra1, which are well known as positive regulators of cancer migration and metastasis (Mulligan, 2014). Moreover, we observed a high enrichment of lamin B1 at *Ret* promoter in MLE12 cells by ChIP analysis. Rationally this occupancy is profoundly disrupted by lamin B1 loss of function. In consistence with our own ChIP-seq data, we also found a localization of *Ret* gene in LADs by analyzing a published ChIP-seq data in human lung tissue (Shah et al., 2013), suggesting a direct role of lamin B1 in transcriptional repression of *Ret* gene.

Besides, other migration related genes are also upregulated upon lamin B1 depletion. For instance, in consistence with a published study showing an indispensable role of β3 integrin (Itgb3) in RET-induced cell invasion and migration (Cockburn et al., 2010), we also observed increased levels of Itgb3 in lamin B1 knockdown cells in comparison with control cells. Other than Itgb3, in alignment with another study showing that ITGA9 was upregulated by chimeric oncogene RET/PTC1 in thyroid tumors (Degl'Innocenti et al., 2010), we also observed the upregulation of Itga9 upon lamin B1 depletion. The increased levels of critical factors required for RET-mediated migration and invasion upon lamin B1 loss, including Gfra1, Itgb3 and Itga9, suggest a mechanism by which lamin B1 reinforces RET function in cell migration and invasion. Indeed, we found that silencing of RET dramatically reduced the highly elevated migratory and metastatic ability of lamin B1-depleted cells by both in vitro and in vivo studies. Taken together, these data suggest that upregulation of RET plays a critical role in mediating migration and metastasis phenotype upon lamin B1 loss of function.

Receptor tyrosine kinase RET is indispensable for a proper development of neural and genitourinary tissues (Mulligan, 2014). Deregulation of RET expression and activity, either by gain-of-function mutations or by altering

binding of ligands with RET co-receptors, is a critical contributor to several human cancers. Particularly in lung cancer, several studies show that gain-of-function RET rearrangement KIF5B–RET, which induces constitutively active cytosolic chimeric proteins, leads to a subset of NSCLCs and plays an important role in driving lung cancer progression and malignancy (Dabir et al., 2014; Ju et al., 2012; Kohno et al., 2012; Takeuchi et al., 2012).

Moreover, we observed high incidence of SCLC in lamin B1 haploinsufficient mice. Importantly, in agreement with another study showing a high RET expression in SCLC tumor specimens (Dabir et al., 2014), we also observed that these SCLC tumors developed in lamin B1 haploinsufficient mice showed a high expression level of RET. Considering the neuroendocrine origin of SCLC (Sutherland et al., 2011), this finding also supports other studies showing that deregulation of RET signaling is mostly observed in neuroendocrine cancers (Mulligan, 2014). Besides, oncogenic RET mutations and copy number amplification were found in lung cancer specimens (Dabir et al., 2014; Kohno et al., 2012; Takeuchi et al., 2012; Yang and Horten, 2014). In line with this, we also observed high RET expression in different types of lung cancer specimens. Most importantly, RET expression in lung cancer patients is negatively correlated with lamin B1 level, supporting a link between gain of RET and loss of lamin B1 in human lung cancer patients. Other than RET, the activated/phosphorylated RET (phosphorylation of tyrosine 1062) is also highly expressed in the pulmonary tumors in *Lmnb1*+/- mice, suggesting that RET activation might also play a key role in lung cancer initiation, progression and metastasis upon lamin B1 loss of function.

4.5 RET/p38 axis is responsible for lamin B1 depletion-mediated cancer cell migration and metastasis

As a receptor tyrosine kinase, activated/phosphorylated RET activates a variety of cell signaling pathways (Mulligan, 2014). In particular, phosphorylation of

tyrosine 1062 is crucial for activation of PI3K/AKT, p38 MAPK, JNK and ERK pathways. Activated p38 MAPK signaling pathway plays critical roles in mediating EMT and driving cancer cell migration and metastasis (Al-Mulla et al., 2011; Bakin et al., 2002; Lin et al., 2016). In line with this, we found a high level of activated p38 along with the upregulation and activation of RET in lamin B1-depleted lung epithelial cells as well as in lamin B1 haploinsufficient mice.

Our study sheds a light on the molecular mechanism by which loss of lamin B1 results in lung cancer migration and metastasis by upregulating RET and the subsequent metastatic events, including EMT and activation of p38 signaling pathway. We found that RET inhibitor vandetanib or p38 inhibitor SB202190 efficiently reduced the migration mediated by lamin B1 depletion, suggesting a therapeutic potential of both vandetanib and SB202190 to clinically inhibit metastasis of cancer cells with decreased lamin B1 expression. Indeed, the application of vandetanib in patients with RET-rearranged metastatic non–small-cell lung cancer is currently undergoing phase II clinical trials evaluation (ClinicalTrials.gov Identifier: NCT01823068) (Lee et al., 2017). Other than vandetanib, the benefit of other RET inhibitors (cabozantinib and lenvatinib), in terms of response and median progression free survival of NSCLC patients with activating RET rearrangements and mutations, has been demonstrated in several clinical trials (reviewed in Mendoza, 2018 (Mendoza, 2018)). Ongoing early phase clinical trials using the highly potent and selective RET kinase inhibitors, BLU-667 and LOXO-292, have generated great interest, given the high level of response and very mild toxicity profiles (Subbiah et al., 2018a; Subbiah et al., 2018b).

4.6 Loss of lamin B1 leads to specific gene repositioning and chromatin decondensation

Numerous studies have shown the link between gene repositioning and gene activity. In some cases gene repositioning leads to changes in gene activity,

however, in other cases it does not (reviewed in Shachar and Misteli, 2017 (Shachar and Misteli, 2017)). We found that loss of lamin B1 led to RET repositioning from the nuclear lamina toward the center, concomitant with RET upregulation. Interestingly, knockdown of Ascl1 in lamin B1 depleted MLE12 cells led to significantly downregulation of RET without affecting *Ret* gene positioning, suggesting that *Ret* gene repositioning is not sufficient to activate *Ret* gene expression. Furthermore, knockdown of EZH1 or EZH2 showed no effect on *Ret* gene repositioning, but elicited a significant increase in RET expression and migratory capacity of MLE12 cells, suggesting that not only lack of tethering to the nuclear periphery but also loss of EZH1/2 binding to chromatin is essential for *Ret* gene activation.

Moreover, chromosome painting revealed that Chromosome 6, which harbors the highest percentage of upregulated genes, is decondensed and located more centrally in lamin B1-depleted cells. Taken together, these data suggest an important role of lamin B1 in chromatin positioning and compaction in lung epithelial cells.

4.7 Lamin B1 depletion impedes the recruitment of EZH1/2, thus derepressing the transcription of *Ret*

Nuclear lamins have been shown to repress gene expression via influencing chromatin structure and modification. In particular, lamins contribute to maintain the repressive heterochromatin makers in the target gene area, thus inhibiting the transcription of their target genes. Lamina-associated domains (LADs) tightly associate with heterochromatin and are enriched with histone modifications H3K9me2 and H3K9me3 which are the markers for heterochromatin (van Steensel and Belmont, 2017). In some cell types, facultative heterochromatin mark H3K27me3 is also enriched at LADs regions (van Steensel and Belmont, 2017). Consistently, in our study, we also observed a direct interaction between lamin B1 and H3K27me3. Importantly, we observed

a global decrease of H3K27me3 upon lamin B1 loss-of-function, suggesting a role of lamin B1 in modulating H3K27me3, thereby influencing the transcription of its target genes, such as *RET*. Decreased H3K27me3 might lead to increase in chromatin accessibility, transcription factor binding and RNA polymerase recruitment at lamin B1 associated genes, thus resulting in transcriptional activation. Consistent with this, in lamin B1-depleted cells we observed an increased enrichment of transcription factor Ascl1 at the *Ret* promoter. Importantly, Ascl1 has been shown to directly activate RET expression and play a critical role in lung cancer development (Augustyn et al., 2014; Borromeo et al., 2016).

Furthermore, we found that lamin B1 depletion led to a decrease in the recruitment of EZH1/2 to chromatin and *Ret* promoter without affecting the protein level of EZH1/2. These data suggest that lamin B1 function as a scaffold to facilitate the proper landing of EZH1/2 to the chromatin and *Ret* promoter, which is indispensable for the role of EZH1/2 to catalyze H3K27me3. Indeed, we observed a direct lamin B1-EZH1/2 interaction in MLE12 cells. However, in the absence of lamin B1, EZH1/2 lost the ability to bind to chromatin due to the disruption of lamin B1- EZH1/2 interaction, thus failing to catalyze H3K27me3 at the *Ret* promoter. In fact, it has already been shown that nuclear lamins act as a dynamic molecular scaffold for chromatin and chromatin interacting/modifying proteins, thus playing an important role in chromatin organization, DNA replication as well as transcription (Bridger et al., 2007; Dechat et al., 2008; Dorner et al., 2007).

4.8 EZH1/2 mediate the function of lamin B1 in regulating cell migration

Similar to lamin B1, the role of EZH1/2 and H3K27me3 in cancer initiation, progression and metastasis are also context and cancer type- specific. In particular, the role of EZH1/2 and H3K27me3 in lung cancer appears to be a

complex picture. On the one hand, several studies support an oncogenic role of EZH2 in NSCLC and define EZH2 as a prognostic marker and a therapeutic target, prospecting EZH2 inhibition as anti-cancer treatment(Fillmore et al., 2015; Takawa et al., 2011). However, several other recent studies also showed a tumor-suppressive function of EZH1/2 in NSCLC (Li et al., 2014; Serresi et al., 2016). In alignment with these studies, our data show that inhibition of EZH1/2, either by inhibitor treatment or by shRNA-mediated depletion, dramatically increased the mRNA level of RET and induced migratory capacity of MLE12 cells, suggesting an anti-tumor role of EZH1 and EZH2 in lung. Importantly, the increased migratory ability of MLE12 cells upon EZH1/2 loss of function was significantly reduced by RET inhibitor treatment. It suggests that RET functions as a downstream target of EZH1 and EZH2. Moreover, several recent studies showed a promoting role of EZH1/2 and H3K27me3 inhibition in EMT (Cardenas et al., 2016; Li et al., 2015; Ramadoss et al., 2012), which supports our finding that EZH1/2 loss of function upon lamin B1 depletion facilitates lung cancer metastasis by upregulating RET and inducing EMT. Thus, our study, in alignment with other above-mentioned studies, suggests a better therapeutic strategy to lung cancer metastasis by targeting molecules downstream of the lamin B1-EZH1/2 axis.

In addition, lamin A/C has been reported to sustain PRC2-mediated chromatin structure and loss of lamin A/C led to impaired PRC2 repressive function (Cesarini et al., 2015). Considering that A- and B-type lamins form separate but interacting structures, thus lamin B1 might lead to changes in lamin A/C function thereby indirectly influencing EZH1/2 function in a lamin A/C dependent manner. However, our data revealed that loss of lamin B1 did not affect the expression of lamin A/C. Importantly, in contrast to lamin B1 loss of function, silencing of lamin A did not have any effect on *Ret* gene positioning and expression or cell migration, suggesting a specific role of lamin B1 in gene regulation and EMT in mouse lung epithelial cells.

In addition, we observed a more profound upregulation of RET upon EZH1 knockdown than EZH2 knockdown. Similarly, EZH1 depletion leads to a significantly higher increase in cell migratory ability than EZH2 depletion does. These data suggest a more prominent role of EZH1 than EZH2 in mediating the malignant phenotype of lung epithelial cells with reduced lamin B1 levels. In support of this finding, Kaplan-Meier survival curve showed that lung cancer patients expressing low levels of EZH1 had a significantly poorer prognosis than patients with higher EZH1 expression. Indeed, many studies have shown that EZH1 and EZH2 containing complexes have both common and distinct functions (Margueron et al., 2008; Shen et al., 2008). EZH1 maintains H3K27me3 in terminally differentiated cells, whereas EZH2 establishes and maintains H3K27me3 in proliferating cells (Margueron et al., 2008). In support of this, we observed a markedly higher enrichment of EZH1 in comparison with EZH2 at the *Ret* promoter. Furthermore, EZH1 and EZH2 also show different biochemical properties. EZH2 has higher catalytic activity towards H3K27me3 than EZH1 and binds to chromatin through JARID2 (Son et al., 2013), whereas EZH1 binds to nucleosomes and induces chromatin compaction independently of PRC1 recruitment (Margueron et al., 2008), suggesting a role of EZH1 loss in chromatin decompaction upon lamin B1 loss.

Taken together, our study demonstrates a novel role of loss of lamin B1 in promoting lung cancer development and metastasis by epigenetically upregulating proto-oncogene RET and RET-mediated epigenetically upregulation of EMT and activation of p38 signalling pathway. Therefore, targeting RET might be a novel therapeutic approach of a significant fraction of human lung cancers caused by perturbation of the lamin B1-EZH1/2.

5. Future perspective

In the present study, we for the first time demonstrate a novel role of lamin B1 loss of function in promoting lung cancer metastasis by upregulating RET/p38 axis. Loss of lamin B1 upregulate genes which are mainly correlated with possitive regulation of cell migration and metastasis in mouse lung epithelial cells. Therefore we hypothesize that lamin B1, instead of randomly binding to the genome in lung epithelial cells, might specifically associates with genes with specific biologic functions. To corroborate this hypothesis, ChIP followed by sequencing analysis with a lamin B1 specific antibody will help to visualize the genomic binding profile of lamin B1 in lung epithelial cells as well as in lung cancer patients, thus uncovering the mechanism by which loss of lamin B1 leads to upregulation of genes with certain biologic functions, for instance cell migration and metastasis.

In addition to cancer cell migration and metastais, we also found a promoting role of lamin B1 loss of function in lung cancer initiation and malignancy. However, the molecular mechanism remains to be defined. Previous study in our group observed an increase in DNA damage and genomic instability as well as a disrupted DNA damage repair process upon lamin B1 depletion. Given the fact that oncogenic mutations, which mainly result from DNA damage and genomic instability, are major diver of tumorigenesis, therefore, discovering the oncogenic mutations occuring upon lamin B1 loss of function is critical to clarify the mechanism by which loss of lamin B1 triggers lung cancer initiation. In this case, performing whole exome sequencing (WES) or whole genome sequencing (WGS) on the pulmonary tumors of *Lmnb1*+/- mice would help to reveal the potential oncogenic mutations upon lamin B1 depletion and how similar they are to human lung cancer. In addition, by doing WES or WGS on the metastatic tumors in the kidneys and livers of *Lmnb*+/- mice would help to corroborate the origin of these tumors. Moreover, we observed chromosome decompaction upon lamin B1 loss in lung epithelial cells that could lead to

cancer-causing chromosome rearrangement. Multicolor-FISH technology based karyotyping will help to identify the potential carcinogenic chromosome rearrangement upon lamin B1 loss.

In our study, most of the tumors in *Lmnb1*+/- mice showed strikingly similar characteristics to small cell lung cancer. Biallelic loss of *Rb1* and *Tp53* is observed in nearly 100% of human SCLC and has been identified as the predominant driver of SCLC. Thus, checking the status of *Rb1* and *Tp53* in the pulmonary tumors of *Lmnb1*+/- mice would help to identify whether *Lmnb1* haploinsufficiency leads to loss of *Rb1* and *Tp53*, thereby triggering SCLC formation.

Moreover, The *Lmnb1*+/- mice used in the present study carried Cre-mediated heterozygous germline deletion of *Lmnb1* gene. Therefore, single *Lmnb1* functional allele was deleted throughout the entire mouse. To further specifically study lamin B1 function in lung cancer development and metastasis, lung-specific knockout of *Lmnb1* by intratracheal intubation with Adeno-Cre viruses in *Lmnb1*$^{flox/flox}$ mice will be helpful.

An intriguing question that needs further investigation concerns the upstream mechanisms leading to lamin B1 downregulation in lung cancer patients, which may involve e.g. truncating or missense mutations, DNA deletions or epigenetic mechanisms such as promoter hypermethylation. For example, the CpG island promoter hypermethylation leads to lamin A/C silencing in lymphoma and neuroblastoma cells (Agrelo et al., 2005; Rauschert et al., 2017). Since LMNB1 has a TATA-less CpG island-associated promoter, promoter hypermethylation might be also responsible for LMNB1 downregulation. Indeed, previous study in our group revealed that promoter of LMNB1 gene is hypermethylated in lung cancer specimens. It shows the reason how lamin B1 expression is significantly downregulated in lung cancer specimens in comparison to the normal lung tissue. However, the cause of the DNA hypermethylation at the promoter of LMNB1 gene remains to be defined. DNA affinity chromatography-pulldown of

LMNB1 promoter sequence followed by mass spectrometry analysis will help to identify the multiprotein complex and enzyme system which are responsible for the hypermethylation of *LMNB1* promoter in lung cancer specimens.

Moreover, our data demonstrate that lamin B1 acts as a scaffold to provide a platform for the interaction between EZH1/2, chromatin and *Ret* promoter. Loss of lamin B1 leads to global dissociation of EZH1/2 from chromatin as well as *Ret* promoter. However, how EZH1 and EZH2 are recruited to lamin B1, chromatin as well as *Ret* promoter still remains to be defined. Co-immunoprecipitation of EZH1/2 followed by mass spectrometry or sequencing analysis might help to define novel subunits of the functional complex, such as functional proteins or non-coding RNAs, which could play a role as a navigator to guide EZH1/2 to chromatin and the *Ret* promoter.

6. Materials and Methods

6.1 Materials

6.1.1 Chemicals and compounds

Substance	Supplier	Reference number
1-Phenyl-2-thiourea (PTU)	Acros	207250250
2-Log DNA ladder (0.1-10.0 kb)	NEB	#N3200L
Acetic anhydride ($(CH_3CO)_2O$)	Sigma-Aldrich	A6404-200ML
Agarose, low melt	Roth	6351.2
Agarose NEEO Ultra	Roth	2267,3
Noble agar	Sigma-Aldrich	A5431
Albumin fraction V (BSA)	Roth	8076.2
Ammonium persulfate (APS) ($(NH_4)_2S_2O_8$)	Sigma-Aldrich	A3678-25G
Ampicillin sodium salt	Sigma-Aldrich	A99518-25G
BM purple AP substrate, precipitating	Roche	11 442 074 001
Bradford reagent, ready-to-use	Fermentas	R1271
Chloroform ($CHCl_3$)	Roth	Y015,1
Chlorophenolred-ß-D-galactopyranoside (CPRG)	Sigma-Aldrich	59767
ddH_2O		
DEAB (4-diethylaminobenzaldehyde)	Sigma-Aldrich	31830
Dimethyl sulfoxide (DMSO) ($(CH_3)_2SO$)	Sigma-Aldrich	D-8779
dNTP (Nucleoside triphosphate) Set 1	Roth	178,1
DTT (Dithiothreitol) ($C_4H_{10}O_2S_2$)	Roth	6908.3
Dry-milk, non fat milk	BIO-RAD	170-6404
EGTA (ethylene glycol tetraacetic acid) ($C_{14}H_{24}N_2O_{10}$)	Roth	3054.2
Ethanol denatured (CH_3CH_2OH)	Roth	K928,3
Ethanol pro analysis (CH_3CH_2OH)	Merck	1,00983,2511
Ethidium bromide solution ($C_{21}H_{20}BrN_3$)	Sigma-Aldrich	E1510-10ML
Ethylenediaminetetraacetic acid (EDTA) ($C_{10}H_{16}N_2O_8$)	Sigma-Aldrich	E5134-250G
FuGENE® HD Transfection Reagent	Roche	4709705/100
Formamide (CH_3NO)	Fluka	47670
Gelatin from bovine skin, Type B	Sigma-Aldrich	G9391-100g
Glutaraldehyde ($CH_2(CH_2CHO)_2$)	Sigma-Aldrich	G5882-10ML
Glycerol ($C_3H_8O_3$)	Roth	3783,1
Glycine (NH_2CH_2COOH)	Sigma-Aldrich	15527

Substance	Supplier	Reference number
Hexadimethrine bromide (polybrene)	Sigma-Aldrich	#H9268
Isopropanol (C_3H_8O)	Roth	6752,4
Kanamycinsulfate	Roth	T832,1
LB-agar (Lennox)	Roth	X965,2
LB-medium (Lennox)	Roth	X964,2
Levamisole ($\underline{C}_{11}\underline{H}_{12}\underline{N}_2\underline{S}$)	Fluka	31742
Lithium chloride (LiCl)	Roth	3739.1
Maleic acid ($C_4H_4O_4$)	Roth	K304.1
Methanol (CH_3OH)	Roth	4627,5
MG-132	Calbiochem	474790
Magnesium chloride ($MgCl_2$)	Sigma-Aldrich	M2393-500G
Magnesium sulfate ($MgSO_4$)	Fischer Scientific	M120,37
Magnesium sulfate-heptahydrate ($MgSO_4 \cdot 7H_2O$)	Merck	1.05886.0500
TEMED (Tetramethylethylenediamine) ($(CH_3)_2NCH_2CH_2N(CH_3)_2$)	Roth	2367,1
Nonidet P-40 (NP-40)	Fluka	74385
Paraformaldehyde (PFA) ($OH(CH_2O)_nH$ (n = 8 - 100))	Sigma-Aldrich	15,812-7
Phenol red ($C_{19}H_{14}O_5S$)	Sigma-Aldrich	P0290
Phosphatase inhibitor Cocktail set V	Calbiochem	524632
PIPES (Piperazine-N,N′-bis(2-ethanesulfonic acid)) ($C_8H_{18}N_2O_6S_2$)	Sigma-Aldrich	P1851
PMSF (Phenylmethylsulfonyl fluoride) ($C_7H_7FO_2S$)	Serva	32395
Poly(2-hydroxyethylmethacrylate) PoliHEMA	Sigma-Aldrich	P3932-10G
Potassium chloride (KCl)	Roth	6781.3
Potassium hexacyanidoferrate (II) trihydrate	Sigma-Aldrich	P9387
Potassium hexacyanoferrate (III)	Sigma-Aldrich	P8131-100G
Prestained protein molecular weight marker	Fermentas	#SM0441
Protease inhibitor cocktail set I	Calbiochem	535142
Puromycin	Sigma-Aldrich	#P8833
Rotiphorese® Gel 30 (37.5:1)	Roth	3029.1
Salmon sperm DNA	Upstate	16-157
Sodium dodecyl sulfate (SDS) ($NaC_{12}H_{25}SO_4$)	Sigma-Aldrich	L4390-100G
Sodium phosphate monobasic monohydrate ($NaH_2PO_4 \cdot H_2O$)	Sigma-Aldrich	53522-1KG
Sodium phosphate dibasic dodecahydrate	Sigma-Aldrich	04273

Substance	Supplier	Reference number
($Na_2HPO_4 \cdot 12H_2O$)		
TRIzol® reagent	Invitrogen	15596026
Triethanolamine ($C_6H_{15}NO_3$)	Sigma-Aldrich	T1377-500ML
Tricaine methane sulphonate (Tricaine) ($C_{10}H_{15}NO_5S$)	Pharmaq	MS222-100G-V1
TRIS (tris(hydroxymethyl)aminomethane) ($(HOCH_2)_3CNH_2$)	Roth	4855.2
Sodium citrate dihydrate	Sigma-Aldrich	W302600
Triton X-100 ($(C_{14}H_{22}O(C_2H_4O)_n)$)	Sigma-Aldrich	X100-500ML
Tween 20 EP, NF	Sigma-Aldrich	T2700-500ML
Yeast tRNA	Roche	10 109 517 001
X-gal	Roth	2315.2
β-mercaptoethanol (C_2H_6SO)	Sigma-Aldrich	60-24-2
Xylene	Roth	CN80.2
Vandetanib	Selleckchem	S1046
SB202190	Adipogen	AG-CR1-0028
UNC1999	Sigma-Aldrich	1431612-23-5
CellTiter 96® AQueous One Solution Cell Proliferation Assay (MTS)	Promega	G3580

6.1.2 Kits

Kit	Supplier
2x SYBRGreen	Applied Biosystems
Duolink® In Situ Orange Starter Kit Goat/Rabbit	Sigma-Aldrich
VECTASTAIN Universal Quick HRP Kit	Vector Laboratories
DAB Peroxidase (HRP) Substrate Kit	Vector Laboratories
RNeasy Microarray kit	Qiagen
MinElute PCR Purification Kit	Qiagen
GenElute™ gel extraction kit	Sigma-Aldrich
GenElute™ HP plasmid midiprep kit	Sigma-Aldrich
GenElute™ HP plasmid miniprep kit	Sigma-Aldrich
GenElute™ PCR clean-up kit	Sigma-Aldrich
High-Capacity cDNA Reverse Transcription Kit	Applied Biosystems
PowerUp™ SYBR™ Green Master Mix	Applied Biosystems
RedTaq® ReadyMix™ PCR Reaction Mix	Sigma-Aldrich
Thermo Scientific™ Pierce™ BCA™ Protein Assay	Thermo Fisher

Kit	Supplier
Subcellular Protein Fractionation Kit for Cultured Cells	Thermo Scientific Fisher Scientific
Nick Translation Kit	Roche

6.1.3 Solutions, reagents and media

Name	Composition or supplier
10% Ammonium persulfate	0.44M Ammonium persulfate ($H_8N_2O_8S_2$)
2x SDS PAGE sample buffer	150mM TRIS pH=6.8 (added in solution) 1.2% (v/v) SDS 30% (v/v) glycerol 6.7% (v/v) β-mercaptoethanol 1.8mg bromophenol blue
10x PBS	1.37M NaCl 27mM KCl 0.1M $Na_2HPO_4 \cdot 12H_2O$ 17.6mM KH_2PO_4 (pH titrated to 7.4)
PBST	0.05% (v/v) Tween 20 in 1xPBS
Blotting buffer	20% (v/v) methanol 192mM glycine 25mM TRIS
Buffer A (cytosolic/nuclear fractioning)	10mM HEPES pH=7.9 (added in solution) 10mM KCl 1.5mM $MgCl_2$
Buffer B (cytosolic/nuclear fractioning)	0.45M NaCl 12.5% (w/v) glycerol 15mM HEPES pH=7.9 (added in solution) 5mM KCl 1.5mM MgCl2 0.1mM EDTA
10x agarose gel sample buffer	250mg/100ml (w/v) bromophenol blue 250mg/100ml (w/v) xylene cyanol 50mM TRIS pH=7.6 (added

Name	Composition or supplier
	in solution) 60% (v/v) glycerol
10x SDS PAGE running buffer	35mM SDS 250mM TRIS 0.86M glycin
2x RNA-loading dye	100µl Formamide 40µl Formaldehyde 20µl 10xTBE 2µl Ethidium bromide
10x TBE	0.89M TRIS 0.89M H_3BO_3 20mM Na_2EDTA pH=8.0
Co-IP buffer	50mM TRIS-HCl pH=7.5 15mM EGTA 100mM NaCl 0.1% (v/v) Triton X-100
Stripping solution 1	200mM glycine 500mM NaCl (pH titrated to 2.8)
Stripping solution 2	200mM glycine 500mM NaCl (pH titrated to 2.2)
Stripping solution 3	200mM TRIS-HCl (pH titrated to 7.4)
Washing buffer	0.1% (v/v) Tween 20 in PBS
L1 lysis buffer (ChIP)	50 mM Tris pH=8 2mM EDTA pH=8 0.1% (v/v) NP40 10% (v/v) glycerol
L2 nuclear resuspension buffer (ChIP)	50mM Tris pH=8 5mM EDTA pH=8 1% (w/v) SDS
DB-dilution buffer (ChIP)	200mM NaCl 50mM Tris pH=8 5mM EDTA, 50mM 0.5% NP40
NaCl-washing buffer (ChIP)	500mM NaCl 20mM Tris pH= 2mM EDTA NP40 (v/v) 1% 0.1% (w/v) SDS

Name	Composition or supplier
LiCl-washing buffer (ChIP)	500mM LiCl 20mM Tris pH=8 2mM EDTA 1% (v/v) NP40 0.1% (w/v) SDS
EB-extraction buffer (ChIP)	10mM Tris pH=8 1mM EDTA 2% (w/v) SDS
TE-buffer	10mM Tris pH=8 1mM EDTA
Tail Lysis Buffer	100 mM Tris pH=8.5 5mM EDTA 0.2% SDS 200 mM NaCl 100 µg/ml Proteinase K
Cytoskeletal (CSK) buffer	10 mM PIPES, pH 6.8 100 mM NaCl 300 mM sucrose 1 mM EGTA 1 mM MgCl2
DMEM 4.5g GlutMax	GIBCO
DMEM 4.5g without GlutMax	GIBCO
RPMI 1640	GIBCO
DMEM/F12 (1:1)	GIBCO
Fetal bovine serum	GIBCO
100x Pen/Strep	GIBCO
100x Pyruvate	GIBCO
100x Non-essential amino acids (NEAA)	GIBCO
100x L-glutamine	GIBCO
β-mercaptoethanol	Sigma-Aldrich
Matrigel® Growth Factor Reduced (GFR) Basement Membrane Matrix	Corning (354230)
Hematoxylin Solution	Sigma-Aldrich (GHS116)
Eosin Y solution	Sigma-Aldrich (HT110216)
Crystal violet solution	Sigma-Aldrich (HT901)
Fisher Chemical™ Permount™ Mounting Medium	Fisher Scientific
ProLong ™ Gold Antifade Mountant	Thermo Fisher Scientific

6.1.4 Antibodies

Name	Company	Cat. No.
Lamin B1	Sigma-Aldrich	HPA050524
Lamin A/C	Santa Cruz	sc-6215
Pan-Cytokeratin	Dako	Z0622
CD45	Abcam	ab10558
CGRP	Sigma-Aldrich	c8198
Synaptophysin	Invitrogen	PA5-27286
Ki67	Abcam	ab15580
PCNA	Santa Cruz	sc-56
E-cadherin	Abcam	ab11512
Fibronectin	Abcam	ab2413
N-cadherin	Sigma-Aldrich	c3865
Vimentin	CST	5741
α-tubulin	Sigma-Aldrich	T5168
RET	Abcam	ab134100
RET	Santa Cruz	sc-167
p-p38 (Thr180/Tyr182)	CST	4511
p38	CST	9212
p-JNK (Thr183/Tyr185)	CST	9255
p-ERK1/2	Santa Cruz	sc-7383
p-RET (Tyr 1062)	Santa Cruz	sc-20252-R
EZH1	Abcam	ab13665
EZH2	Abcam	ab3748
H3K27me3	Millipore	07-449
H3K9me2	Abcam	ab1220
H3K9me3	Abcam	ab8898
Histone H3	Abcam	ab1791
Ascl1	BD Pharmingen	556604
Pol II	Abcam	ab817
Anti-Digoxigenin Fab fragments	Sigma-Aldrich	11207750910

6.1.5 Primers

Primer	Sequence (5’-3’)
Lmnb1 forward M. musculus	AGATCAGGGACCAGATGCAG
Lmnb1 reverse M. musculus	GAAGGGCTTGGAGAGAGCTT
Lmnb1 forward H. sapiens	GACCAGCTGCTCCTCAACTATG

Primer	Sequence (5'-3')
Lmnb1 reverse H. sapiens	ATTCTCGAAGCTTGATCTGGGC
Lmna forward M. musculus	GGAAGTCGATGAAGAGGGAAAG
Lmna reverse M. musculus	TTTAGGGTGAACTTCGGTGG
Tuba1a forward M. musculus	CCGCGAAGCAGCAACCAT
Tuba1a reverse M. musculus	CCAGGTCTACGAACACTGCC
Tuba1a forward H. sapiens	GAAGCAGCAACCATGCGTGA
Tuba1a reverse H. sapiens	TCTCCTCCCCCAATGGTCTT
RET forward M. musculus	ACACGGCTGCATGAGAATGA
RET reverse M. musculus	GGAAACCACCATTGCGGATG
RET forward H. sapiens	GAAGGCGACGTCCGGTG
RET reverse H. sapiens	TAGAGGCCCAATGCCACTTT
Gfra1 forward M. musculus	TTTCCAGCAAGTGGAACACA
Gfra1 reverse M. musculus	GCGGTTGCAGACTTCATTGG
Ascl1 forward M. musculus	CCCTCTTAGCCCAGAGGAAC
Ascl1 reverse M. musculus	TGCCATCCTGCTTCCAAAGTC
EZH1 forward M. musculus	TCCATGAGGAAAATGGATATAGCA
EZH1 reverse M. musculus	TCCCATATTTGCCTGGAGCC
EZH2 forward M. musculus	ACTGCTTCCTACATCCCTTCC
EZH2 reverse M. musculus	ACGCTCAGCAGTAAGAGCAG
Ret promoter forward M. musculus	GAAAGAGGGACAGAGAGCCT
Ret promoter reverse M. musculus	GACAACGGTAGCAGGTCTCT
RET promoter forward H. sapiens	TAGCCGCAGTCCCTCCAG
RET promoter reverse H. sapiens	CCCACGGCAAACAGAAAGG
Gfra1 promoter forward M. musculus	GACCCGCTTTTAGGGGTTCA
Gfra1 promoter reverse M. musculus	CTTCAGCACTCTGGGCTCTC
GFRA1 promoter forward H. sapiens	TGCGGTAATCTTCGAGAGCT
GFRA1 promoter reverse H. sapiens	GAACAGGAGCAGGCCGAG

6.1.6 Cell lines and plasmids

MLE12, LLC1, BEAS-2B (B2B), NCI-H69 (H69) and HEK293T cells were purchased from ATCC (CRL-2110, CRL-1642, CRL-9609, HTB-119, CRL-3216). Control shRNA and shRNA against mouse Lmnb1 (SHCLNG-NM_010721), human Lmnb1 (SHCLND-NM_005573), mouse Lmna (SHCLNG-NM_001002011.2), mouse RET (SHCLNG-NM_009050), mouse Ascl1 (SHCLNG-NM_008553.4), EZH1 (SHCLND-NM_007970) and EZH2 (SHCLND-NM_007971) were obtained from MISSION™ shRNA Library, Sigma-Aldrich.

6.1.7 Mouse lines

The Lmnb1 tm1a (EUCOMM)Wtsi mouse line was obtained from Genome Research Limited (Sanger, UK). C57BL/6J werer obtained from Charles River Laboratory.

6.2 Methods

6.2.1 Cell culture and generating stable cell lines

MLE12 cells were cultured in DMEM/F12 medium supplemented with 10% fetal bovine serum (FCS) and penicillin/streptomycin/glutamine (PSG). HEK293T and LLC1 cells were cultured in DMEM supplemented with 10% FCS and PSG. B2B and H69 cells were cultured in RPMI1640 supplemented with 10% FCS and PSG.

For the generation of stable cell lines, 0.5×10^6 HEK293T cells were plated on a 6-well plate and transfected with 2 µg of plasmids containing shRNA or control and RET overexpressing constructs, along with packaging plasmids and envelop plasmid, using FuGENE (Roche) transfection reagent. Media containing lentivirus was harvested 48 hrs after transfection, followed by centrifugation at 4,200 rpm for 20 min to pellet any packaging cells that were collected during harvesting. Viral supernatant together with polybrene (working concentration.: 8µg/ml) was added into the cells to be transduced. After 24 hrs,

viral medium was removed and complete culturing medium was added into the cells. After 24 hrs, transfected cells were selected with 10 µg/ml puromycin for 2 passages and selected cells were maintained with 2 µg/ml puromycin as stable cell lines. All cell lines used in the present study were free from mycoplasma contamination.

6.2.2 Immunohistochemistry and immunofluorescence staining

6.2.2.1 Immunohistochemical staining on paraffin sections

For immunohistochemical (IHC) staining on paraffin sections, slides were heated at 55 °C for 10 min and submerged into xylene (Sigma-Aldrich), followed by serial deparaffinization and rehydration steps (3 times xylene, 3 times 100% ethanol, 90% ethanol, 75% ethanol, 50% ethanol, distilled water, each 5 min). Antigen retrieval was done by microwave boiling in 10 mM citrate buffer for 10 min. The subsequent steps were done with the VECTASTAIN Universal Quick HRP Kit (PK-7800, Vector Laboratories) following the manufacturer's instructions. In detail, after antigen retrieval, slides were blocked with blocking serum for 1 hour, followed by incubation in primary antibody diluted in blocking serum at 4°C overnight. On the next day, slides were washed for 5 min with PBS. Slides were incubated with biotinylated panspecific universal secondary antibody for 10 minutes, followed by washing for 5 minutes with PBS. Next slides were incubated with streptavidin/peroxidase complex reagent for 5 minutes, followed by washing for 5 minutes with PBS. Staining was then developed with DAB Peroxidase (HRP) Substrate Kit (SK-4100, Vector Laboratories) and counterstained with hematoxylin solution for 30 seconds. Slides were then quickly dehydrated by incubation in a series of ethanol solutions with increasing concentrations (50%, 75%, 90%, 3×100%) for 5 min each. Next slides were washed in 2 changes of xylene for 5 minutes each and then mount with xylene based mounting medium.

6.2.2.2 Immunofluorescence staining on paraffin sections

For immunofluorescence staining on paraffin sections, slides were deparaffinized, rehydrated and followed by antigen retrieval in the same way as described for IHC staining on paraffin sections. Slides were then blocked with 10% FCS with 0.5% Triton X-100 (Sigma-Aldrich) in PBS for 1 hr and incubated with primary antibodies in blocking buffer at 4°C overnight. On the next day, slides were washed and secondary antibodies were added for 2 hr. Slides were then washed with PBS and mounted with anti-fade mounting medium.

6.2.2.3 Immunofluorescence staining on cultured cells

For immunofluorescence staining of cultured cells, cells were counted and seeded on coverslips in 24-well plates. Next, cells were washed with PBS and fixed with 3.7% formaldehyde for 10 min, followed by the same blocking and staining procedures as described for IF on paraffin sections. All of the fluorescence images were acquired using LSM 700 laser scanning microscope (Carl Zeiss Micro Imaging) with a 25× or 40× or 63× objective and analyzed with ImageJ (National Institutes of Health) or Zeiss ZEN Microscope Software (Carl Zeiss Micro Imaging).

6.2.2.4 Immunohistochemical staining on tissue microarray

For tissue microarray immunostaining and analysis, the tissue microarray slides were purchased from US Biomax Inc (LC2085c). The steps of deparaffinization, antigen retrieval, blocking and staining procedures were the same as described for IHC staining on paraffin sections. For lamin B1 and lamin A/C staining, only the nuclear staining signal of cancer cells excluding non-malignant stromal cells and immune cell was quantified. The quantification of the signal was performed by measurement of signal intensity and percentage of stained cells. The intensity of the staining signal was semiquantitatively graded on a scale from 0 to 3 (lowest to highest). H-score of the staining was calculated by multiplying the staining intensity by the percentage of stained cells. The staining score

ranges from 0 to 300.

6.2.2.5 Antibodies used for IHC and IF

Name	Company	Cat. No.	Dilution
Lamin B1	Santa Cruz	sc-6216	1:100
Lamin B1	Sigma-Aldrich	HPA050524	1:100
Lamin A/C	Santa Cruz	sc-6215	1:100
Pan-Cytokeratin	Dako	Z0622	1:300
CD45	Abcam	ab10558	1:200
CGRP	Sigma-Aldrich	c8198	1:100
Synaptophysin	Invitrogen	PA5-27286	1:100
Ki67	Abcam	ab15580	1:200
PCNA	Santa Cruz	sc-56	1:100
E-cadherin	Abcam	ab11512	1:150
Fibronectin	Abcam	ab2413	1:100
N-cadherin	Sigma-Aldrich	c3865	1:100
Vimentin	CST	5741	1:100
RET	Santa Cruz	sc-167	1:50
p-p38 (Thr180/Tyr182)	CST	4511	1:100
p-RET (Tyr 1062)	Santa Cruz	sc-20252-R	1:50
EZH1	Abcam	ab13665	1:100
EZH2	Abcam	ab3748	1:100

6.2.3 Histology

Lungs were perfused with PBS, dissected and fixed with 3.7% paraformaldehyde at room temperature for one day, followed by 3 washes with PBS. Tissues were dehydrated by incubation in a series of ethanol solutions with increasing concentrations. Ethanol was replaced by xylene and paraffin followed by embedding in paraffin. For hematoxylin and eosin (H&E) staining, slides were deparaffinized and rehydrated as described for IHC staining on paraffin sections. Slides were then stained with hematoxylin solution for 10 min, followed by washing in running tap water for 5 min. Slides were then stained with eosin solution for 5 min, followed by quick dehydration through incubation in a series of ethanol solutions with increasing concentrations. Slides were wash in 2 changes of xylene for 5 minutes each and then mount with xylene

based mounting medium. Images were captured by NanoZoomer 2.0-HT whole slide imager (Hamamatsu) or Axio Scan.Z1 (ZEISS) and analyzed by NDP.view2 Viewing software (Hamamatsu) or ZEN 2.3 SP1 (ZEISS), respectively. Representative images of histological analysis of mice with the same genotype are presented.

6.2.4 Animal experiments

All animal experiments were done in accordance to the institutional guidelines and are covered in an approved animal experimental protocol by the Committee for Animal Rights Protection of the State of Hessen (Regierungspraesidium Darmstadt, Germany, Experimental protocol Az.: V54 – 19 c 20/15 – B2/363 and V54-19c20/15-B2/1113).

The Lmnb1tm1a (EUCOMM)Wtsi mouse line was obtained from Genome Research Limited (Sanger, UK). Lmnb1tm1a were backcrossed to C57BL/6 for six generations before the use in these studies.

Female C57/BL6 and BALB/c nu/nu mice were purchased from Charles Rivers, Sulzfeld, Germany and kept under pathogen-free conditions.

For induction of experimental metastasis, 1×10^6 wild-type, control or lamin B1, RET and lamin B1/RET shRNA-expressing LLC1 cells were injected intravenously into 7-8 weeks old C57BL/6 mice, respectively. After 20 days (LLC1 cells) or 24 days (MLE12 cells), the mice were sacrificed and imaged, the lungs were isolated, imaged, fixed with 3.7% PFA and embedded into paraffin. 5 µm thick paraffin sections were stained with hematoxylin and eosin.

For subcutaneous transplantation, 1×10^6 control or lamin B1, RET and lamin B1/RET shRNA-expressing LLC1 cells were injected into the flanks of C57BL/6 mice (Charles River). After 20 days the mice were sacrificed, imaged and the subcutaneous tumors and lungs were isolated, imaged, fixed with 3.7% PFA and embedded into paraffin. 5 µm thick paraffin sections were used hematoxylin and eosin staining or IHC staining.

Metastatic area was defined as the percentage of lung area occupied by

metastatic tumor, measured by ImageJ. Tumor volumes and number of tumor nodules in the lung were quantitated from H&E stained lung sections using ImageJ.

6.2.5 Boyden chamber migration and invasion assay

6.2.5.1 Transwell migration assay

Falcon Cell Culture Inserts for 24 Well Plate with 8.0um Pore Transparent PET Membrane (Corning, Cat. No. 353097) were placed on 24-well plates containing 10% FCS medium. 1×10^5 MLE12 cells or 5×10^4 LLC1 cells or 1.2×10^5 B2B cells or 2×10^5 H69 cells were seeded on top of the insert in a 0 % FCS medium. 5 hrs later (for H69 cells, 24hrs later), the insert membranes were fixed with 3.7% formaldehyde for 10 min and washed 3 times with PBS. The upper surface of the membranes was cleaned by wiping with a piece of wet paper. Membranes were then stained with crystal violet for 10 minutes. Images of randomly selected areas were acquired with a 20x objective and the number of cells that had migrated to the lower surface of the membrane was quantified using ImageJ (http://imagej.nih.gov/ij/).

6.2.5.2 Matrigel invasion assay

The in vitro Matrigel invasion assay was essentially similar to the cell migration assay described above, except that the membrane filter was precoated with 50 µl diluted Matrigel (diluted with serum free culture medium, final working concentration 1 mg/ml) for 2 hrs before seeding the cells. 24 hrs later, the insert membranes were fixed.

6.2.6 Cell proliferation and soft agar colony formation assay

Cell proliferation was measured using CellTiter 96 AQueous One Solution Cell Proliferation Assay (MTS) according to the manufacturer's instructions. In detail, 1000 cells were seeded into each well of a 96-well plate, and the cells were incubated for the 1, 2, 3, 4 and 5 days respectively. After incubation, CellTiter

96® AQueous One Solution Reagent were directly added to the culture wells followed by incubation for 1 hour. Absorbance, which is proportional to the number of living cells in culture was then measured at 490 nm with a 96-well plate reader. For soft agar colony formation assay, control and Lmnb1 KD MLE12 cells were suspended in complete DMEM/F12 medium containing 0.3% low melting agarose, and plated onto solidified 0.6% agarose in complete DMEM/F12 medium in 12-well culture plates at a density of 5 000 cells per well. After 14 days the colonies were stained with 0.005% Crystal Violet.

6.2.7 RNA Isolation, RT-PCR and Real-Time PCR

For real-time PCR analysis, RNA was isolated using the TRIzol RNA Isolation Reagent (Invitrogen). cDNA was synthesized with the High Capacity cDNA Reverse Transcription Kit (Applied Biosystems) according to the manual. Real-time PCR was performed using the SYBR GREEN PCR master mix (Applied Biosystems). Cycle numbers were normalized to these of α-Tubulin (Tuba1a). Primer details are given in Chapter Primers.

For RNA-Seq, the RNA was isolated using RNeasy Microarray kit (Qiagen #73304).

6.2.8 RNA-Seq data analysis

Raw RNA-seq reads were trimmed with reaper (http://www.ebi.ac.uk/~stijn/reaper/reaper.html) using the following parameters -geom no-bc -3pa -clean-length 20 -qqq-check 53/10 -trim-length 150 –nozip. Trimmed reads were mapped to the reference genome mm10 (UCSC assembly) using the default settings of STAR software (Dobin et al., 2013) (--outFilterMismatchNoverLmax 0.1 --chimSegmentMin 18 --chimScoreMin 12). Differential expression (Log2FC≥1, FDR<0.05, BaseMean >=2 for upregulated genes, Log2FC≤-1, FDR<0.05, BaseMean >=2 for downreagulated genes) was quantified and normalized by the use of DESEq2. Gene ontology analysis was performed using DAVID Bioinformatics Resources 6.8, adjusted p-value (FDR)

for the GO terms was calculated in R using the Benjamini-Hochberg method (Benjamini and Hochberg, 1995). The percentage of up-regulated genes per chromosome was calculated by dividing the number of genes upregulated upon Lmnb1 KD in MLE12 cells at specific chromosome to the total number of upregulated genes. To determine the number of genes per chromosome a custom script in bash was developed. Briefly, the coordinate of mm10 transcripts of Refseq database were obtained by using (analyzeRepeats.pl rna mm10 -strand both -count genes) and annotated by annotatePeaks.pl (default settings). Single genes per chomosomes were substracted with the help of a R script (mat_u <- mat[!duplicated(mat$gene_name),] followed by mat_u <- subset(mat_u, chr==n; where n is each chromosome)).

6.2.9 Immunoprecipitation and immunoblotting

6.2.9.1 Samples preparation

For isolating nuclear extract, cells were lysed with buffer A (10 mM HEPES pH 7.9, 1.5 mM MgCl2, 10 mM KCl, protease inhibitors SET-I (Sigma-Aldrich)) on ice for 10 min. 10% NP40 was added into the lysates (volume ratio is 1:16) and vortexed for 10 sec. Lysates were centrifuged at 12,000g for 30 sec at 4 °C. The supernatant (cytoplasmic extract) were removed and the pellets was resuspended with cold buffer B (15 mM HEPES pH 7.9, 12.5% glycerol, 1.5 mM MgCl2, 5 mM KCl, 0.1 mM EDTA, 0.45 M NaCl, protease inhibitors SET-I (Sigma-Aldrich)) and incubated for 15 min at 4 °C. Lysates were centrifuged at 12,000g for 5 min at 4 °C. The supernatant is nuclear extract.

The chromatin bound fraction was isolated using Subcellular Protein Fractionation Kit for Cultured Cells (ThermoFisher Scientific) according to the manual. In detail, 2 × 10^6 cells were harvested into a 1.5 mL microcentrifuge tube and pellet by centrifugation at 500 × g for 5 minutes. Supernatant was then removed. Ice-cold Cytoplasmic Extraction Buffer (CEB) containing protease inhibitors was then added to the cell pellet followed by incubation at 4°C for 10

minutes by gentle mixing. Lysate was then centrifuged at 500 × g for 5 minutes. Supernatant (cytoplasmic extract) was removed and pellet was resuspended with ice-cold Membrane Extraction Buffer (MEB) containing protease inhibitors. After vortexing for 5 seconds on the highest setting, the lysate was incubated at 4°C for 10 minutes by gentle mixing. After centrifugation at 3000 × g for 5 minutes, supernatant (membrane extract) was removed and pellet was resuspended with ice-cold Nuclear Extraction Buffer (NEB) containing protease inhibitors, followed by vortexing on the highest setting for 15 seconds and incubation at 4°C for 30 minutes by gentle mixing. After centrifugation at 5000 × g for 5 minutes, supernatant (soluble nuclear extract) fraction was removed and pellet was resuspended with chromatin-bound extraction buffer (NEB containing protease inhibitors, CaCl2 and Micrococcal Nuclease), followed by Vortexing on the highest setting for 15 seconds and incubation at room temperature for 15 minutes. After incubation, lysate was vortexed on the highest setting for 15 seconds and centrifuged at 16,000 × g for 5 minutes. The supernatant is chromatin bound fraction.

Total cell lysate was obtained by lysing the cells in co-IP buffer (50 mM Tris pH7.5, 100 mM NaCl, 15 mM EGTA, 0.1% Triton-X100, protease inhibitors SET-I (Sigma-Aldrich)), followed by sonication (Bandelin Sonopuls) for 10 sec. Lysates were then centrifuged at 12,000g for 10 min at 4 °C. The supernatant is total protein extract.

6.2.9.2 Immunoprecipitation

For Immunoprecipitation (co-IP), total cell lysates were obtained as described in chapter 6.2.9.1. For each co-IP experiment, 1mg total cell lysate was diluted with co-IP buffer (50 mM Tris pH7.5, 100 mM NaCl, 15 mM EGTA, 0.1% Triton-X100, protease inhibitors SET-I (Sigma-Aldrich)) to 1ml. The diluted lysates were then incubated with 2µg indicated antibodies overnight at 4 °C followed by 3 hrs incubation with Protein-A/G-Sepharose beads (GE Healthcare). Immunoprecipitates were washed five times in 1ml co-IP buffer, dissolved in

30µl 2x SDS-PAGE sample buffer, and subjected to standard western blot analysis.

6.2.9.3 Western blot

Cell lysates were mixed with 5x SDS-PAGE loading buffer (250 mM Tris·HCl, pH 6.8, 10% SDS, 30% (v/v) Glycerol, 10 mM DTT, 0.05% (w/v) Bromophenol Blue) at the ratio 4:1 before boiling at 95°C for 10 min. Then the samples were loaded for electrophoresis. After electrophoresis, the gel was transferred carefully to a nitrocellulose membrane using a wet-transfer system at 90V for 1 hour. After transfer, nitrocellulose membranes were stained with Ponceau G solution to validate transfer quality and loading equality. Then, the nitrocellulose membranes were briefly washed with PBS containing 0.5% Tween-20 before being blocked with PBS containing 5% non-fat dried milk and 0.5% Tween-20. The membranes were incubated with primary antibodies with appropriate dilutions overnight at 4 °C. After overnight incubation, the membranes were washed for 3 times for 10 minutes with PBST and incubated with HRP-conjugated secondary antibodies for 1 hour at room temperature. After 3 times washes with PBST for 10min each, antigen-antibody complexes were detected and imaged using the ECL detection kit and digital western blot detection system.

6.2.9.4 Antibodies used for western blot

Name	**Company**	**Cat. No.**	**Dilution**
Lamin B1	Santa Cruz	sc-6216	1:1000
Lamin A/C	Santa Cruz	sc-6215	1:1000
E-cadherin	Abcam	ab11512	1:2000
Fibronectin	Abcam	ab2413	1:1000
N-cadherin	Sigma-Aldrich	c3865	1:500
α-tubulin	Sigma-Aldrich	T5168	1:8000
RET	Abcam	ab134100	1:2000
p-p38 (Thr180/Tyr182)	CST	4511	1:1000
p38	CST	9212	1:1000
p-JNK (Thr183/Tyr185)	CST	9255	1:2000
p-ERK1/2	Santa Cruz	sc-7383	1:1000

Name	Company	Cat. No.	Dilution
p-RET (Tyr 1062)	Santa Cruz	sc-20252-R	1:1000
EZH1	Abcam	ab13665	1:500
EZH2	Abcam	ab3748	1:1000
H3K27me3	Millipore	07-449	1:2000
Histone H3	Abcam	ab1791	1:8000

6.2.10 DNA Fluorescence In Situ Hybridization (FISH)

DNA FISH probes were labeled with digoxigenin by Nick Translation kit (Roche) according to manufacturer's protocol using BAC DNA clones: RET (RP23-98B12, ThermoFisher) and Gfra1 (RP23-180P13, ThermoFisher). Whole chromosome painting probes for mouse chromosome 6 and 10 were purchased from MetaSystems Probes. For DNA FISH, cells were grown on coverslips, fixed with 4% formaldehyde for 10min, permeabilized with 0.5% Triton X-100 for 10min. Cells were incubated with 20% glycerol/ PBS for 60min and then 0.1N HCl for 20min. Cells were equilibrated in 2×SSC (1×SSC: 0.15M NaCl and 0.015M sodium citrate, pH 7.0) for 5min and then in 50% formamide/2×SSC for 30min. Next, labeled DNA probes were added to the cells, followed by co-denaturation of cells and probes on a hot plate at 75 °C for 3 min and then incubation at 37°C for 24 hrs for the hybridization. Probes were detected by 10 µg/ml anti-digoxigenin-rhodamine, Fab fragments (Roche) and cells were counterstained with DAPI. Images were captured with laser scanning microscopy LSM 700 (Carl Zeiss Micro Imaging) with 63× objective and analyzed with ImageJ (National Institutes of Health) or Zeiss ZEN Microscope Software (Carl Zeiss Micro Imaging).

6.2.11 Proximity ligation assay (PLA)

PLA was performed using Duolink® In Situ Orange Starter Kit Goat/Rabbit (Cat. No.: DUO92106, Sigma-Aldrich) following the manufacturer's instructions. In detail, the cell culture, fixation, blocking and primary antibody incubation were the same as described for immunofluorescence staining on cultured cells. After

primary antibody incubation, cells on coverslips were washed in PBS and followed by PLA® Probes incubation for 60 min at 37°C. Then the cells on coverslips were washed with Buffer A for 2 × 5 min. Ligation solution was made by diluting ligase (1 U/µl) at 1:40 with ligation buffer and then applied to the cells and incubated for 30 min at 37°C. Cells were washed in 1x Wash Buffer A for 2 × 2 min. Amplification solution was made by diluting polymerase (10 U/µl) at 1:80 in amplification buffer and then applied to the cells and incubated or 100 min at +37°C. Next cells were washed with wash buffer B for 2 × 10 min and then mounted with Duolink In Situ Mounting Medium with DAPI. Images were captured with laser scanning microscopy LSM 700 (Carl Zeiss Micro Imaging) with a 63× objective and analyzed with ImageJ (National Institutes of Health).

6.2.12 Chromatin immunoprecipitation (ChIP) and ChIP sequencing

6.2.12.1 ChIP

5×10^6 cells were fixed with 1% formaldehyde for 10min at room temperature. Fixation was quenched with 125mM pH 7.5 Tris HCl or glycine followed by washes with cold PBS for 3×10min. Cells were further lysed in 600 µl of ice-cold L1 lysis buffer (Tris pH 8 50mM, EDTA pH8 2mM, NP40 0.1%, glycerol 10%) for 5 min and nuclei were spun down. Next, nuclei were resuspended in 600 µl L2 lysis buffer (SDS 1%, EDTA pH8 5mM, Tris pH8 50mM) and DNA was sheared by sonication. Extracts were pre-cleared with 80µl protein G beads for 1h followed by incubation with 10 µg primary antibody overnight at 4 °C and binding to 30 µl BSA-coated protein G beads. Immunoprecipitates were washed two times with NaCl-washing buffer (0.1% SDS, NP40 1%, 2mM EDTA, 500mM NaCl, 20mM Tris pH8), followed by two washes with LiCl-washing buffer (0.1% SDS, 1% NP40, 2mM EDTA, 500mM LiCl, 20mM Tris pH8) and eluted with EB-extraction buffer (TE pH8, 2% SDS). Cross-linking was reverted by incubation overnight at 65°C. DNA was purified using Qiagen mini elute PCR purification kit (Cat#28004). Immunoprecipitated DNA was either used for qPCR analysis

or sequenced on NextSeq500 instrument (Illumina). Sequences of primers used for ChIP-qPCR are given in Chapter Primers.

6.2.12.2 ChIP-Seq data analysis

ChIP-sequencing reads were mapped to the mouse reference genome mm10 (UCSC assembly) using the default settings of Bowtie2 (Langmead and Salzberg, 2012) the PCR duplicates were removed with MarkDuplicates.jar from picard-tools-1.119. Peaks in H3K27me3-ChIP-seq were called using findPeaks from homer (-region -size 1000 -minDist 10000 -style histone) using the Input as control sample. The common peaks between replicates (n=2) were obtained by the use of bedtools intersect (-wa). Distribution of the H3K27me3-ChIP mapped reads from control and lamin B1 KD MLE12 cells at all peaks in MLE12 was performed using ngs.plot (Shen et al., 2014) with mm10. The BAM files were normalized to reads per genome coverage (RPGC), by the use of BamCoverage from deepTools2 (PMID: 24799436) (-b 20 -smooth 40 -e 150 --normalizeTo1x 2652783500).

6.2.13 In situ nuclear matrix extraction

Cells on the coverslips were washed and incubated with cytoskeletal (CSK) buffer (10 mM PIPES, pH 6.8, 100 mM NaCl, 300 mM sucrose, 1 mM EGTA, 1 mM MgCl2) supplemented with protease inhibitors and 0.5% Triton X-100 at room temperature for 3 min. Chromatin was digested with DNase I (50 ng/µl) in DNase I Buffer (10 mM Tris-HCl, pH 7.5, 2.5 mM MgCl2, 0.5 mM CaCl2) at room temperature for 30 min. The coverslips were washed with PBS, followed by immunostaining.

6.2.14 Statistical analysis

Results from quantitative analyses are presented as mean ± standard error of the mean (SEM). Statistical analysis was performed using Student’s t-test with two-tailed distribution. Sample sizes were determined based on previous experience with analogous experiments. The experiments were not

randomized and not blinded. For in vivo experiments, animals that unexpectedly died were excluded from the analysis. Statistical significance was defined as $p < 0.05$ (*, #: $p < 0.05$; **, ##: $p < 0.01$, ***$p < 0.001$).

7. References

1997. A clinical evaluation of the International Lymphoma Study Group classification of non-Hodgkin's lymphoma. The Non-Hodgkin's Lymphoma Classification Project. *Blood* 89:3909-3918.

Agger, K., P.A. Cloos, L. Rudkjaer, K. Williams, G. Andersen, J. Christensen, and K. Helin. 2009. The H3K27me3 demethylase JMJD3 contributes to the activation of the INK4A-ARF locus in response to oncogene- and stress-induced senescence. *Genes Dev* 23:1171-1176.

Aghdassi, A., M. Sendler, A. Guenther, J. Mayerle, C.O. Behn, C.D. Heidecke, H. Friess, M. Buchler, M. Evert, M.M. Lerch, and F.U. Weiss. 2012. Recruitment of histone deacetylases HDAC1 and HDAC2 by the transcriptional repressor ZEB1 downregulates E-cadherin expression in pancreatic cancer. *Gut* 61:439-448.

Agrelo, R., F. Setien, J. Espada, M.J. Artiga, M. Rodriguez, A. Perez-Rosado, A. Sanchez-Aguilera, M.F. Fraga, M.A. Piris, and M. Esteller. 2005. Inactivation of the lamin A/C gene by CpG island promoter hypermethylation in hematologic malignancies, and its association with poor survival in nodal diffuse large B-cell lymphoma. *J Clin Oncol* 23:3940-3947.

Agudo, D., F. Gomez-Esquer, F. Martinez-Arribas, M.J. Nunez-Villar, M. Pollan, and J. Schneider. 2004. Nup88 mRNA overexpression is associated with high aggressiveness of breast cancer. *Int J Cancer* 109:717-720.

Airoldi, I., C. Cocco, F. Morandi, I. Prigione, and V. Pistoia. 2008. CXCR5 may be involved in the attraction of human metastatic neuroblastoma cells to the bone marrow. *Cancer Immunol Immunother* 57:541-548.

Al-Mulla, F., M.S. Bitar, M. Al-Maghrebi, A.I. Behbehani, W. Al-Ali, O. Rath, B. Doyle, K.Y. Tan, A. Pitt, and W. Kolch. 2011. Raf kinase inhibitor protein RKIP enhances signaling by glycogen synthase kinase-3beta. *Cancer Res* 71:1334-1343.

Alexander, N.R., N.L. Tran, H. Rekapally, C.E. Summers, C. Glackin, and R.L. Heimark. 2006. N-cadherin gene expression in prostate carcinoma is modulated by integrin-dependent nuclear translocation of Twist1. *Cancer Res* 66:3365-3369.

Amersi, F.F., A.M. Terando, Y. Goto, R.A. Scolyer, J.F. Thompson, A.N. Tran, M.B. Faries, D.L. Morton, and D.S. Hoon. 2008. Activation of CCR9/CCL25 in cutaneous melanoma mediates preferential metastasis

to the small intestine. *Clin Cancer Res* 14:638-645.

Anderton, J.A., S. Bose, M. Vockerodt, K. Vrzalikova, W. Wei, M. Kuo, K. Helin, J. Christensen, M. Rowe, P.G. Murray, and C.B. Woodman. 2011. The H3K27me3 demethylase, KDM6B, is induced by Epstein-Barr virus and over-expressed in Hodgkin's Lymphoma. *Oncogene* 30:2037-2043.

Arriola, E., I. Canadas, M. Arumi, F. Rojo, A. Rovira, and J. Albanell. 2008. Genetic changes in small cell lung carcinoma. *Clin Transl Oncol* 10:189-197.

Au, S.L., C.C. Wong, J.M. Lee, C.M. Wong, and I.O. Ng. 2013. EZH2-Mediated H3K27me3 Is Involved in Epigenetic Repression of Deleted in Liver Cancer 1 in Human Cancers. *PLoS One* 8:e68226.

Augustyn, A., M. Borromeo, T. Wang, J. Fujimoto, C. Shao, P.D. Dospoy, V. Lee, C. Tan, J.P. Sullivan, J.E. Larsen, L. Girard, C. Behrens, Wistuba, II, Y. Xie, M.H. Cobb, A.F. Gazdar, J.E. Johnson, and J.D. Minna. 2014. ASCL1 is a lineage oncogene providing therapeutic targets for high-grade neuroendocrine lung cancers. *Proc Natl Acad Sci U S A* 111:14788-14793.

Bachelder, R.E., S.O. Yoon, C. Franci, A.G. de Herreros, and A.M. Mercurio. 2005. Glycogen synthase kinase-3 is an endogenous inhibitor of Snail transcription: implications for the epithelial-mesenchymal transition. *J Cell Biol* 168:29-33.

Baginska, J., E. Viry, G. Berchem, A. Poli, M.Z. Noman, K. van Moer, S. Medves, J. Zimmer, A. Oudin, S.P. Niclou, R.C. Bleackley, I.S. Goping, S. Chouaib, and B. Janji. 2013. Granzyme B degradation by autophagy decreases tumor cell susceptibility to natural killer-mediated lysis under hypoxia. *Proc Natl Acad Sci U S A* 110:17450-17455.

Bakin, A.V., C. Rinehart, A.K. Tomlinson, and C.L. Arteaga. 2002. p38 mitogen-activated protein kinase is required for TGFbeta-mediated fibroblastic transdifferentiation and cell migration. *J Cell Sci* 115:3193-3206.

Banat, G.A., A. Tretyn, S.S. Pullamsetti, J. Wilhelm, A. Weigert, C. Olesch, K. Ebel, T. Stiewe, F. Grimminger, W. Seeger, L. Fink, and R. Savai. 2015. Immune and Inflammatory Cell Composition of Human Lung Cancer Stroma. *PLoS One* 10:e0139073.

Bannister, A.J., P. Zegerman, J.F. Partridge, E.A. Miska, J.O. Thomas, R.C. Allshire, and T. Kouzarides. 2001. Selective recognition of methylated lysine 9 on histone H3 by the HP1 chromo domain. *Nature* 410:120-124.

Barboro, P., E. Repaci, C. D'Arrigo, and C. Balbi. 2012. The role of nuclear matrix proteins binding to matrix attachment regions (Mars) in prostate

cancer cell differentiation. *PLoS One* 7:e40617.

Barradas, M., E. Anderton, J.C. Acosta, S. Li, A. Banito, M. Rodriguez-Niedenfuhr, G. Maertens, M. Banck, M.M. Zhou, M.J. Walsh, G. Peters, and J. Gil. 2009. Histone demethylase JMJD3 contributes to epigenetic control of INK4a/ARF by oncogenic RAS. *Genes Dev* 23:1177-1182.

Barski, A., S. Cuddapah, K. Cui, T.Y. Roh, D.E. Schones, Z. Wang, G. Wei, I. Chepelev, and K. Zhao. 2007. High-resolution profiling of histone methylations in the human genome. *Cell* 129:823-837.

Bates, D.O. 2010. Vascular endothelial growth factors and vascular permeability. *Cardiovasc Res* 87:262-271.

Batlle, E., E. Sancho, C. Franci, D. Dominguez, M. Monfar, J. Baulida, and A. Garcia De Herreros. 2000. The transcription factor snail is a repressor of E-cadherin gene expression in epithelial tumour cells. *Nat Cell Biol* 2:84-89.

Bechert, K., M. Lagos-Quintana, J. Harborth, K. Weber, and M. Osborn. 2003. Effects of expressing lamin A mutant protein causing Emery-Dreifuss muscular dystrophy and familial partial lipodystrophy in HeLa cells. *Exp Cell Res* 286:75-86.

Belt, E.J., R.J. Fijneman, E.G. van den Berg, H. Bril, P.M. Delis-van Diemen, M. Tijssen, H.F. van Essen, E.S. de Lange-de Klerk, J.A. Belien, H.B. Stockmann, S. Meijer, and G.A. Meijer. 2011. Loss of lamin A/C expression in stage II and III colon cancer is associated with disease recurrence. *Eur J Cancer* 47:1837-1845.

Berger, S.L. 2007. The complex language of chromatin regulation during transcription. *Nature* 447:407-412.

Bernardi, R., and P.P. Pandolfi. 2003. Role of PML and the PML-nuclear body in the control of programmed cell death. *Oncogene* 22:9048-9057.

Boisvert, F.M., M.J. Hendzel, and D.P. Bazett-Jones. 2000. Promyelocytic leukemia (PML) nuclear bodies are protein structures that do not accumulate RNA. *J Cell Biol* 148:283-292.

Bolos, V., H. Peinado, M.A. Perez-Moreno, M.F. Fraga, M. Esteller, and A. Cano. 2003. The transcription factor Slug represses E-cadherin expression and induces epithelial to mesenchymal transitions: a comparison with Snail and E47 repressors. *J Cell Sci* 116:499-511.

Borromeo, M.D., T.K. Savage, R.K. Kollipara, M. He, A. Augustyn, J.K. Osborne, L. Girard, J.D. Minna, A.F. Gazdar, M.H. Cobb, and J.E. Johnson. 2016. ASCL1 and NEUROD1 Reveal Heterogeneity in Pulmonary Neuroendocrine Tumors and Regulate Distinct Genetic Programs. *Cell*

Rep 16:1259-1272.

Boyle, S., S. Gilchrist, J.M. Bridger, N.L. Mahy, J.A. Ellis, and W.A. Bickmore. 2001. The spatial organization of human chromosomes within the nuclei of normal and emerin-mutant cells. *Hum Mol Genet* 10:211-219.

Bridger, J.M., N. Foeger, I.R. Kill, and H. Herrmann. 2007. The nuclear lamina. Both a structural framework and a platform for genome organization. *FEBS J* 274:1354-1361.

Broers, J.L., B.M. Machiels, H.J. Kuijpers, F. Smedts, R. van den Kieboom, Y. Raymond, and F.C. Ramaekers. 1997. A- and B-type lamins are differentially expressed in normal human tissues. *Histochem Cell Biol* 107:505-517.

Broers, J.L., B.M. Machiels, G.J. van Eys, H.J. Kuijpers, E.M. Manders, R. van Driel, and F.C. Ramaekers. 1999. Dynamics of the nuclear lamina as monitored by GFP-tagged A-type lamins. *J Cell Sci* 112 (Pt 20):3463-3475.

Broers, J.L., E.A. Peeters, H.J. Kuijpers, J. Endert, C.V. Bouten, C.W. Oomens, F.P. Baaijens, and F.C. Ramaekers. 2004. Decreased mechanical stiffness in LMNA-/- cells is caused by defective nucleo-cytoskeletal integrity: implications for the development of laminopathies. *Hum Mol Genet* 13:2567-2580.

Broers, J.L., Y. Raymond, M.K. Rot, H. Kuijpers, S.S. Wagenaar, and F.C. Ramaekers. 1993. Nuclear A-type lamins are differentially expressed in human lung cancer subtypes. *Am J Pathol* 143:211-220.

Bruce, J., D.C. Carter, and J. Fraser. 1970. Patterns of recurrent disease in breast cancer. *Lancet* 1:433-435.

Butin-Israeli, V., S.A. Adam, A.E. Goldman, and R.D. Goldman. 2012. Nuclear lamin functions and disease. *Trends Genet* 28:464-471.

Butin-Israeli, V., S.A. Adam, N. Jain, G.L. Otte, D. Neems, L. Wiesmuller, S.L. Berger, and R.D. Goldman. 2015. Role of lamin b1 in chromatin instability. *Mol Cell Biol* 35:884-898.

Byles, V., L. Zhu, J.D. Lovaas, L.K. Chmilewski, J. Wang, D.V. Faller, and Y. Dai. 2012. SIRT1 induces EMT by cooperating with EMT transcription factors and enhances prostate cancer cell migration and metastasis. *Oncogene* 31:4619-4629.

Cambien, B., B.F. Karimdjee, P. Richard-Fiardo, H. Bziouech, R. Barthel, M.A. Millet, V. Martini, D. Birnbaum, J.Y. Scoazec, J. Abello, T. Al Saati, M.G. Johnson, T.J. Sullivan, J.C. Medina, T.L. Collins, A. Schmid-Alliana, and H. Schmid-Antomarchi. 2009. Organ-specific inhibition of metastatic

colon carcinoma by CXCR3 antagonism. *Br J Cancer* 100:1755-1764.

Cano, A., M.A. Perez-Moreno, I. Rodrigo, A. Locascio, M.J. Blanco, M.G. del Barrio, F. Portillo, and M.A. Nieto. 2000. The transcription factor snail controls epithelial-mesenchymal transitions by repressing E-cadherin expression. *Nat Cell Biol* 2:76-83.

Cao, R., L. Wang, H. Wang, L. Xia, H. Erdjument-Bromage, P. Tempst, R.S. Jones, and Y. Zhang. 2002. Role of histone H3 lysine 27 methylation in Polycomb-group silencing. *Science* 298:1039-1043.

Cao, R., and Y. Zhang. 2004. SUZ12 is required for both the histone methyltransferase activity and the silencing function of the EED-EZH2 complex. *Mol Cell* 15:57-67.

Capo-chichi, C.D., K.Q. Cai, J. Smedberg, P. Ganjei-Azar, A.K. Godwin, and X.X. Xu. 2011. Loss of A-type lamin expression compromises nuclear envelope integrity in breast cancer. *Chin J Cancer* 30:415-425.

Cardenas, H., J. Zhao, E. Vieth, K.P. Nephew, and D. Matei. 2016. EZH2 inhibition promotes epithelial-to-mesenchymal transition in ovarian cancer cells. *Oncotarget* 7:84453-84467.

Carmeliet, P. 2005. VEGF as a key mediator of angiogenesis in cancer. *Oncology* 69 Suppl 3:4-10.

Carper, M.B., and P.P. Claudio. 2015. Clinical potential of gene mutations in lung cancer. *Clin Transl Med* 4:33.

Castellone, M.D., A. Celetti, V. Guarino, A.M. Cirafici, F. Basolo, R. Giannini, E. Medico, M. Kruhoffer, T.F. Orntoft, F. Curcio, A. Fusco, R.M. Melillo, and M. Santoro. 2004. Autocrine stimulation by osteopontin plays a pivotal role in the expression of the mitogenic and invasive phenotype of RET/PTC-transformed thyroid cells. *Oncogene* 23:2188-2196.

Cesarini, E., C. Mozzetta, F. Marullo, F. Gregoretti, A. Gargiulo, M. Columbaro, A. Cortesi, L. Antonelli, S. Di Pelino, S. Squarzoni, D. Palacios, A. Zippo, B. Bodega, G. Oliva, and C. Lanzuolo. 2015. Lamin A/C sustains PcG protein architecture, maintaining transcriptional repression at target genes. *J Cell Biol* 211:533-551.

Chan, J.Y., W. Chin, C.T. Liew, K.S. Chang, and P.J. Johnson. 1998. Altered expression of the growth and transformation suppressor PML gene in human hepatocellular carcinomas and in hepatitis tissues. *Eur J Cancer* 34:1015-1022.

Chapman-Rothe, N., E. Curry, C. Zeller, D. Liber, E. Stronach, H. Gabra, S. Ghaem-Maghami, and R. Brown. 2013. Chromatin H3K27me3/H3K4me3 histone marks define gene sets in high-grade

serous ovarian cancer that distinguish malignant, tumour-sustaining and chemo-resistant ovarian tumour cells. *Oncogene* 32:4586-4592.

Cho, M.H., J.H. Park, H.J. Choi, M.K. Park, H.Y. Won, Y.J. Park, C.H. Lee, S.H. Oh, Y.S. Song, H.S. Kim, Y.H. Oh, J.Y. Lee, and G. Kong. 2015. DOT1L cooperates with the c-Myc-p300 complex to epigenetically derepress CDH1 transcription factors in breast cancer progression. *Nat Commun* 6:7821.

Chow, K.H., R.E. Factor, and K.S. Ullman. 2012. The nuclear envelope environment and its cancer connections. *Nat Rev Cancer* 12:196-209.

Cockburn, J.G., D.S. Richardson, T.S. Gujral, and L.M. Mulligan. 2010. RET-mediated cell adhesion and migration require multiple integrin subunits. *J Clin Endocrinol Metab* 95:E342-346.

Coradeghini, R., P. Barboro, A. Rubagotti, F. Boccardo, S. Parodi, G. Carmignani, C. D'Arrigo, E. Patrone, and C. Balbi. 2006. Differential expression of nuclear lamins in normal and cancerous prostate tissues. *Oncol Rep* 15:609-613.

Coutinho, H.D., V.S. Falcao-Silva, G.F. Goncalves, and R.B. da Nobrega. 2009. Molecular ageing in progeroid syndromes: Hutchinson-Gilford progeria syndrome as a model. *Immun Ageing* 6:4.

Cremer, M., K. Kupper, B. Wagler, L. Wizelman, J. von Hase, Y. Weiland, L. Kreja, J. Diebold, M.R. Speicher, and T. Cremer. 2003. Inheritance of gene density-related higher order chromatin arrangements in normal and tumor cell nuclei. *J Cell Biol* 162:809-820.

Croft, J.A., J.M. Bridger, S. Boyle, P. Perry, P. Teague, and W.A. Bickmore. 1999. Differences in the localization and morphology of chromosomes in the human nucleus. *J Cell Biol* 145:1119-1131.

Czermin, B., R. Melfi, D. McCabe, V. Seitz, A. Imhof, and V. Pirrotta. 2002. Drosophila enhancer of Zeste/ESC complexes have a histone H3 methyltransferase activity that marks chromosomal Polycomb sites. *Cell* 111:185-196.

Dabir, S., S. Babakoohi, A. Kluge, J.J. Morrow, A. Kresak, M. Yang, D. MacPherson, G. Wildey, and A. Dowlati. 2014. RET mutation and expression in small-cell lung cancer. *J Thorac Oncol* 9:1316-1323.

Dahl, K.N., A.J. Ribeiro, and J. Lammerding. 2008. Nuclear shape, mechanics, and mechanotransduction. *Circ Res* 102:1307-1318.

Dave, N., S. Guaita-Esteruelas, S. Gutarra, A. Frias, M. Beltran, S. Peiro, and A.G. de Herreros. 2011. Functional cooperation between Snail1 and twist in the regulation of ZEB1 expression during epithelial to

mesenchymal transition. *J Biol Chem* 286:12024-12032.

David, J.M., and A.K. Rajasekaran. 2012. Dishonorable discharge: the oncogenic roles of cleaved E-cadherin fragments. *Cancer Res* 72:2917-2923.

Dechat, T., S.A. Adam, P. Taimen, T. Shimi, and R.D. Goldman. 2010. Nuclear lamins. *Cold Spring Harb Perspect Biol* 2:a000547.

Dechat, T., K. Pfleghaar, K. Sengupta, T. Shimi, D.K. Shumaker, L. Solimando, and R.D. Goldman. 2008. Nuclear lamins: major factors in the structural organization and function of the nucleus and chromatin. *Genes Dev* 22:832-853.

Degl'Innocenti, D., C. Alberti, G. Castellano, A. Greco, C. Miranda, M.A. Pierotti, E. Seregni, M.G. Borrello, S. Canevari, and A. Tomassetti. 2010. Integrated ligand-receptor bioinformatic and in vitro functional analysis identifies active TGFA/EGFR signaling loop in papillary thyroid carcinomas. *PLoS One* 5:e12701.

del Barco Barrantes, I., and A.R. Nebreda. 2012. Roles of p38 MAPKs in invasion and metastasis. *Biochem Soc Trans* 40:79-84.

Denais, C.M., R.M. Gilbert, P. Isermann, A.L. McGregor, M. te Lindert, B. Weigelin, P.M. Davidson, P. Friedl, K. Wolf, and J. Lammerding. 2016. Nuclear envelope rupture and repair during cancer cell migration. *Science* 352:353-358.

Derynck, R., and Y.E. Zhang. 2003. Smad-dependent and Smad-independent pathways in TGF-beta family signalling. *Nature* 425:577-584.

Dittmer, T.A., and T. Misteli. 2011. The lamin protein family. *Genome Biol* 12:222.

Dong, C., Y. Wu, Y. Wang, C. Wang, T. Kang, P.G. Rychahou, Y.I. Chi, B.M. Evers, and B.P. Zhou. 2013. Interaction with Suv39H1 is critical for Snail-mediated E-cadherin repression in breast cancer. *Oncogene* 32:1351-1362.

Dong, C., Y. Wu, J. Yao, Y. Wang, Y. Yu, P.G. Rychahou, B.M. Evers, and B.P. Zhou. 2012. G9a interacts with Snail and is critical for Snail-mediated E-cadherin repression in human breast cancer. *J Clin Invest* 122:1469-1486.

Dorner, D., J. Gotzmann, and R. Foisner. 2007. Nucleoplasmic lamins and their interaction partners, LAP2alpha, Rb, and BAF, in transcriptional regulation. *FEBS J* 274:1362-1373.

Doucet, C.M., and M.W. Hetzer. 2010. Nuclear pore biogenesis into an intact nuclear envelope. *Chromosoma* 119:469-477.

Emerling, B.M., L.C. Platanias, E. Black, A.R. Nebreda, R.J. Davis, and N.S.

Chandel. 2005. Mitochondrial reactive oxygen species activation of p38 mitogen-activated protein kinase is required for hypoxia signaling. *Mol Cell Biol* 25:4853-4862.

Favreau, C., E. Dubosclard, C. Ostlund, C. Vigouroux, J. Capeau, M. Wehnert, D. Higuet, H.J. Worman, J.C. Courvalin, and B. Buendia. 2003. Expression of lamin A mutated in the carboxyl-terminal tail generates an aberrant nuclear phenotype similar to that observed in cells from patients with Dunnigan-type partial lipodystrophy and Emery-Dreifuss muscular dystrophy. *Exp Cell Res* 282:14-23.

Feng, X.H., and R. Derynck. 2005. Specificity and versatility in tgf-beta signaling through Smads. *Annu Rev Cell Dev Biol* 21:659-693.

Ferlay, J., I. Soerjomataram, R. Dikshit, S. Eser, C. Mathers, M. Rebelo, D.M. Parkin, D. Forman, and F. Bray. 2015. Cancer incidence and mortality worldwide: sources, methods and major patterns in GLOBOCAN 2012. *Int J Cancer* 136:E359-386.

Fey, E.G., G. Krochmalnic, and S. Penman. 1986. The nonchromatin substructures of the nucleus: the ribonucleoprotein (RNP)-containing and RNP-depleted matrices analyzed by sequential fractionation and resinless section electron microscopy. *J Cell Biol* 102:1654-1665.

Fillmore, C.M., C. Xu, P.T. Desai, J.M. Berry, S.P. Rowbotham, Y.J. Lin, H. Zhang, V.E. Marquez, P.S. Hammerman, K.K. Wong, and C.F. Kim. 2015. EZH2 inhibition sensitizes BRG1 and EGFR mutant lung tumours to TopoII inhibitors. *Nature* 520:239-242.

Finlan, L.E., D. Sproul, I. Thomson, S. Boyle, E. Kerr, P. Perry, B. Ylstra, J.R. Chubb, and W.A. Bickmore. 2008. Recruitment to the nuclear periphery can alter expression of genes in human cells. *PLoS Genet* 4:e1000039.

Fischer, A.H., D.N. Chadee, J.A. Wright, T.S. Gansler, and J.R. Davie. 1998. Ras-associated nuclear structural change appears functionally significant and independent of the mitotic signaling pathway. *J Cell Biochem* 70:130-140.

Fogal, V., M. Gostissa, P. Sandy, P. Zacchi, T. Sternsdorf, K. Jensen, P.P. Pandolfi, H. Will, C. Schneider, and G. Del Sal. 2000. Regulation of p53 activity in nuclear bodies by a specific PML isoform. *EMBO J* 19:6185-6195.

Fonseca-Pereira, D., S. Arroz-Madeira, M. Rodrigues-Campos, I.A. Barbosa, R.G. Domingues, T. Bento, A.R. Almeida, H. Ribeiro, A.J. Potocnik, H. Enomoto, and H. Veiga-Fernandes. 2014. The neurotrophic factor receptor RET drives haematopoietic stem cell survival and function.

Nature 514:98-101.

Friedl, P., K. Wolf, and J. Lammerding. 2011. Nuclear mechanics during cell migration. *Curr Opin Cell Biol* 23:55-64.

Frost, J.K. 1986. The cell in health and disease. An evaluation of cellular morphologic expression of biologic behavior. 2nd, revised edition. *Monogr Clin Cytol* 2:1-304.

Fu, J., L. Qin, T. He, J. Qin, J. Hong, J. Wong, L. Liao, and J. Xu. 2011. The TWIST/Mi2/NuRD protein complex and its essential role in cancer metastasis. *Cell Res* 21:275-289.

Galiova, G., E. Bartova, I. Raska, J. Krejci, and S. Kozubek. 2008. Chromatin changes induced by lamin A/C deficiency and the histone deacetylase inhibitor trichostatin A. *Eur J Cell Biol* 87:291-303.

Gao, D., D.J. Nolan, A.S. Mellick, K. Bambino, K. McDonnell, and V. Mittal. 2008. Endothelial progenitor cells control the angiogenic switch in mouse lung metastasis. *Science* 319:195-198.

Gao, Y., Y. Zhao, J. Zhang, Y. Lu, X. Liu, P. Geng, B. Huang, Y. Zhang, and J. Lu. 2016. The dual function of PRMT1 in modulating epithelial-mesenchymal transition and cellular senescence in breast cancer cells through regulation of ZEB1. *Sci Rep* 6:19874.

Gattelli, A., I. Nalvarte, A. Boulay, T.C. Roloff, M. Schreiber, N. Carragher, K.K. Macleod, M. Schlederer, S. Lienhard, L. Kenner, M.I. Torres-Arzayus, and N.E. Hynes. 2013. Ret inhibition decreases growth and metastatic potential of estrogen receptor positive breast cancer cells. *EMBO Mol Med* 5:1335-1350.

George, J., J.S. Lim, S.J. Jang, Y. Cun, L. Ozretic, G. Kong, F. Leenders, X. Lu, L. Fernandez-Cuesta, G. Bosco, C. Muller, I. Dahmen, N.S. Jahchan, K.S. Park, D. Yang, A.N. Karnezis, D. Vaka, A. Torres, M.S. Wang, J.O. Korbel, R. Menon, S.M. Chun, D. Kim, M. Wilkerson, N. Hayes, D. Engelmann, B. Putzer, M. Bos, S. Michels, I. Vlasic, D. Seidel, B. Pinther, P. Schaub, C. Becker, J. Altmuller, J. Yokota, T. Kohno, R. Iwakawa, K. Tsuta, M. Noguchi, T. Muley, H. Hoffmann, P.A. Schnabel, I. Petersen, Y. Chen, A. Soltermann, V. Tischler, C.M. Choi, Y.H. Kim, P.P. Massion, Y. Zou, D. Jovanovic, M. Kontic, G.M. Wright, P.A. Russell, B. Solomon, I. Koch, M. Lindner, L.A. Muscarella, A. la Torre, J.K. Field, M. Jakopovic, J. Knezevic, E. Castanos-Velez, L. Roz, U. Pastorino, O.T. Brustugun, M. Lund-Iversen, E. Thunnissen, J. Kohler, M. Schuler, J. Botling, M. Sandelin, M. Sanchez-Cespedes, H.B. Salvesen, V. Achter, U. Lang, M. Bogus, P.M. Schneider, T. Zander, S. Ansen, M. Hallek, J. Wolf, M.

Vingron, Y. Yatabe, W.D. Travis, P. Nurnberg, C. Reinhardt, S. Perner, L. Heukamp, R. Buttner, S.A. Haas, E. Brambilla, M. Peifer, J. Sage, and R.K. Thomas. 2015. Comprehensive genomic profiles of small cell lung cancer. *Nature* 524:47-53.

Ghosh, S., B. Liu, Y. Wang, Q. Hao, and Z. Zhou. 2015. Lamin A Is an Endogenous SIRT6 Activator and Promotes SIRT6-Mediated DNA Repair. *Cell Rep* 13:1396-1406.

Gilkes, D.M., G.L. Semenza, and D. Wirtz. 2014. Hypoxia and the extracellular matrix: drivers of tumour metastasis. *Nat Rev Cancer* 14:430-439.

Gloerich, M., M.J. Vliem, E. Prummel, L.A. Meijer, M.G. Rensen, H. Rehmann, and J.L. Bos. 2011. The nucleoporin RanBP2 tethers the cAMP effector Epac1 and inhibits its catalytic activity. *J Cell Biol* 193:1009-1020.

Goldman, R.D., Y. Gruenbaum, R.D. Moir, D.K. Shumaker, and T.P. Spann. 2002. Nuclear lamins: building blocks of nuclear architecture. *Genes Dev* 16:533-547.

Graham, T.R., H.E. Zhau, V.A. Odero-Marah, A.O. Osunkoya, K.S. Kimbro, M. Tighiouart, T. Liu, J.W. Simons, and R.M. O'Regan. 2008. Insulin-like growth factor-I-dependent up-regulation of ZEB1 drives epithelial-to-mesenchymal transition in human prostate cancer cells. *Cancer Res* 68:2479-2488.

Grotegut, S., D. von Schweinitz, G. Christofori, and F. Lehembre. 2006. Hepatocyte growth factor induces cell scattering through MAPK/Egr-1-mediated upregulation of Snail. *EMBO J* 25:3534-3545.

Guarino, V., P. Faviana, G. Salvatore, M.D. Castellone, A.M. Cirafici, V. De Falco, A. Celetti, R. Giannini, F. Basolo, R.M. Melillo, and M. Santoro. 2005. Osteopontin is overexpressed in human papillary thyroid carcinomas and enhances thyroid carcinoma cell invasiveness. *J Clin Endocrinol Metab* 90:5270-5278.

Guelen, L., L. Pagie, E. Brasset, W. Meuleman, M.B. Faza, W. Talhout, B.H. Eussen, A. de Klein, L. Wessels, W. de Laat, and B. van Steensel. 2008. Domain organization of human chromosomes revealed by mapping of nuclear lamina interactions. *Nature* 453:948-951.

Guo, H., Y. Lu, J. Wang, X. Liu, E.T. Keller, Q. Liu, Q. Zhou, and J. Zhang. 2014. Targeting the Notch signaling pathway in cancer therapeutics. *Thorac Cancer* 5:473-486.

Gurrieri, C., P. Capodieci, R. Bernardi, P.P. Scaglioni, K. Nafa, L.J. Rush, D.A. Verbel, C. Cordon-Cardo, and P.P. Pandolfi. 2004. Loss of the tumor suppressor PML in human cancers of multiple histologic origins. *J Natl*

Cancer Inst 96:269-279.

Gyorffy, B., P. Surowiak, J. Budczies, and A. Lanczky. 2013. Online survival analysis software to assess the prognostic value of biomarkers using transcriptomic data in non-small-cell lung cancer. *PLoS One* 8:e82241.

Hagedorn, H.G., B.E. Bachmeier, and A.G. Nerlich. 2001. Synthesis and degradation of basement membranes and extracellular matrix and their regulation by TGF-beta in invasive carcinomas (Review). *Int J Oncol* 18:669-681.

Hakelien, A.M., E. Delbarre, K.G. Gaustad, B. Buendia, and P. Collas. 2008. Expression of the myodystrophic R453W mutation of lamin A in C2C12 myoblasts causes promoter-specific and global epigenetic defects. *Exp Cell Res* 314:1869-1880.

Hanahan, D., and R.A. Weinberg. 2011. Hallmarks of cancer: the next generation. *Cell* 144:646-674.

Harada, T., J. Swift, J. Irianto, J.W. Shin, K.R. Spinler, A. Athirasala, R. Diegmiller, P.C. Dingal, I.L. Ivanovska, and D.E. Discher. 2014. Nuclear lamin stiffness is a barrier to 3D migration, but softness can limit survival. *J Cell Biol* 204:669-682.

He, S., K.L. Dunn, P.S. Espino, B. Drobic, L. Li, J. Yu, J.M. Sun, H.Y. Chen, S. Pritchard, and J.R. Davie. 2008. Chromatin organization and nuclear microenvironments in cancer cells. *J Cell Biochem* 104:2004-2015.

Hebbes, T.R., A.W. Thorne, and C. Crane-Robinson. 1988. A direct link between core histone acetylation and transcriptionally active chromatin. *EMBO J* 7:1395-1402.

Heerboth, S., G. Housman, M. Leary, M. Longacre, S. Byler, K. Lapinska, A. Willbanks, and S. Sarkar. 2015. EMT and tumor metastasis. *Clin Transl Med* 4:6.

Heessen, S., and M. Fornerod. 2007. The inner nuclear envelope as a transcription factor resting place. *EMBO Rep* 8:914-919.

Helfand, B.T., Y. Wang, K. Pfleghaar, T. Shimi, P. Taimen, and D.K. Shumaker. 2012. Chromosomal regions associated with prostate cancer risk localize to lamin B-deficient microdomains and exhibit reduced gene transcription. *J Pathol* 226:735-745.

Herranz, N., D. Pasini, V.M. Diaz, C. Franci, A. Gutierrez, N. Dave, M. Escriva, I. Hernandez-Munoz, L. Di Croce, K. Helin, A. Garcia de Herreros, and S. Peiro. 2008. Polycomb complex 2 is required for E-cadherin repression by the Snail1 transcription factor. *Mol Cell Biol* 28:4772-4781.

Higgins, D.F., K. Kimura, W.M. Bernhardt, N. Shrimanker, Y. Akai, B.

Hohenstein, Y. Saito, R.S. Johnson, M. Kretzler, C.D. Cohen, K.U. Eckardt, M. Iwano, and V.H. Haase. 2007. Hypoxia promotes fibrogenesis in vivo via HIF-1 stimulation of epithelial-to-mesenchymal transition. *J Clin Invest* 117:3810-3820.

Hiratsuka, S., D.G. Duda, Y. Huang, S. Goel, T. Sugiyama, T. Nagasawa, D. Fukumura, and R.K. Jain. 2011. C-X-C receptor type 4 promotes metastasis by activating p38 mitogen-activated protein kinase in myeloid differentiation antigen (Gr-1)-positive cells. *Proc Natl Acad Sci U S A* 108:302-307.

Hock, H. 2012. A complex Polycomb issue: the two faces of EZH2 in cancer. *Genes Dev* 26:751-755.

Hoeijmakers, J.H. 2009. DNA damage, aging, and cancer. *N Engl J Med* 361:1475-1485.

Hong, J., J. Zhou, J. Fu, T. He, J. Qin, L. Wang, L. Liao, and J. Xu. 2011. Phosphorylation of serine 68 of Twist1 by MAPKs stabilizes Twist1 protein and promotes breast cancer cell invasiveness. *Cancer Res* 71:3980-3990.

Hoot, K.E., J. Lighthall, G. Han, S.L. Lu, A. Li, W. Ju, M. Kulesz-Martin, E. Bottinger, and X.J. Wang. 2008. Keratinocyte-specific Smad2 ablation results in increased epithelial-mesenchymal transition during skin cancer formation and progression. *J Clin Invest* 118:2722-2732.

Hou, Z., H. Peng, K. Ayyanathan, K.P. Yan, E.M. Langer, G.D. Longmore, and F.J. Rauscher, 3rd. 2008. The LIM protein AJUBA recruits protein arginine methyltransferase 5 to mediate SNAIL-dependent transcriptional repression. *Mol Cell Biol* 28:3198-3207.

Houben, F., F.C. Ramaekers, L.H. Snoeckx, and J.L. Broers. 2007. Role of nuclear lamina-cytoskeleton interactions in the maintenance of cellular strength. *Biochim Biophys Acta* 1773:675-686.

Hoye, A.M., and J.T. Erler. 2016. Structural ECM components in the premetastatic and metastatic niche. *Am J Physiol Cell Physiol* 310:C955-967.

Hozak, P., A.M. Sasseville, Y. Raymond, and P.R. Cook. 1995. Lamin proteins form an internal nucleoskeleton as well as a peripheral lamina in human cells. *J Cell Sci* 108 (Pt 2):635-644.

Huang, R.Y., P. Guilford, and J.P. Thiery. 2012. Early events in cell adhesion and polarity during epithelial-mesenchymal transition. *J Cell Sci* 125:4417-4422.

Huang, S., T.J. Deerinck, M.H. Ellisman, and D.L. Spector. 1997. The dynamic

organization of the perinucleolar compartment in the cell nucleus. *J Cell Biol* 137:965-974.

Hunter, K.W., N.P. Crawford, and J. Alsarraj. 2008. Mechanisms of metastasis. *Breast Cancer Res* 10 Suppl 1:S2.

Ibiza, S., B. Garcia-Cassani, H. Ribeiro, T. Carvalho, L. Almeida, R. Marques, A.M. Misic, C. Bartow-McKenney, D.M. Larson, W.J. Pavan, G. Eberl, E.A. Grice, and H. Veiga-Fernandes. 2016. Glial-cell-derived neuroregulators control type 3 innate lymphoid cells and gut defence. *Nature* 535:440-443.

Ivorra, C., M. Kubicek, J.M. Gonzalez, S.M. Sanz-Gonzalez, A. Alvarez-Barrientos, J.E. O'Connor, B. Burke, and V. Andres. 2006. A mechanism of AP-1 suppression through interaction of c-Fos with lamin A/C. *Genes Dev* 20:307-320.

Jensen, S.M., A.F. Gazdar, F. Cuttitta, E.K. Russell, and R.I. Linnoila. 1990. A comparison of synaptophysin, chromogranin, and L-dopa decarboxylase as markers for neuroendocrine differentiation in lung cancer cell lines. *Cancer Res* 50:6068-6074.

Johansson, N., R. Ala-aho, V. Uitto, R. Grenman, N.E. Fusenig, C. Lopez-Otin, and V.M. Kahari. 2000. Expression of collagenase-3 (MMP-13) and collagenase-1 (MMP-1) by transformed keratinocytes is dependent on the activity of p38 mitogen-activated protein kinase. *J Cell Sci* 113 Pt 2:227-235.

Johnson-Holiday, C., R. Singh, E. Johnson, S. Singh, C.R. Stockard, W.E. Grizzle, and J.W. Lillard, Jr. 2011. CCL25 mediates migration, invasion and matrix metalloproteinase expression by breast cancer cells in a CCR9-dependent fashion. *Int J Oncol* 38:1279-1285.

Jordan, N.V., A. Prat, A.N. Abell, J.S. Zawistowski, N. Sciaky, O.A. Karginova, B. Zhou, B.T. Golitz, C.M. Perou, and G.L. Johnson. 2013. SWI/SNF chromatin-remodeling factor Smarcd3/Baf60c controls epithelial-mesenchymal transition by inducing Wnt5a signaling. *Mol Cell Biol* 33:3011-3025.

Joyce, J.A., and J.W. Pollard. 2009. Microenvironmental regulation of metastasis. *Nat Rev Cancer* 9:239-252.

Ju, Y.S., W.C. Lee, J.Y. Shin, S. Lee, T. Bleazard, J.K. Won, Y.T. Kim, J.I. Kim, J.H. Kang, and J.S. Seo. 2012. A transforming KIF5B and RET gene fusion in lung adenocarcinoma revealed from whole-genome and transcriptome sequencing. *Genome Res* 22:436-445.

Kalinowski, A., Z. Qin, K. Coffey, R. Kodali, M.J. Buehler, M. Losche, and K.N.

Dahl. 2013. Calcium causes a conformational change in lamin A tail domain that promotes farnesyl-mediated membrane association. *Biophys J* 104:2246-2253.

Kalluri, R., and R.A. Weinberg. 2009. The basics of epithelial-mesenchymal transition. *J Clin Invest* 119:1420-1428.

Kamath, R.V., A.D. Thor, C. Wang, S.M. Edgerton, A. Slusarczyk, D.J. Leary, J. Wang, E.L. Wiley, B. Jovanovic, Q. Wu, R. Nayar, P. Kovarik, F. Shi, and S. Huang. 2005. Perinucleolar compartment prevalence has an independent prognostic value for breast cancer. *Cancer Res* 65:246-253.

Kang, Y., C.R. Chen, and J. Massague. 2003. A self-enabling TGFbeta response coupled to stress signaling: Smad engages stress response factor ATF3 for Id1 repression in epithelial cells. *Mol Cell* 11:915-926.

Kaplan, R.N., R.D. Riba, S. Zacharoulis, A.H. Bramley, L. Vincent, C. Costa, D.D. MacDonald, D.K. Jin, K. Shido, S.A. Kerns, Z. Zhu, D. Hicklin, Y. Wu, J.L. Port, N. Altorki, E.R. Port, D. Ruggero, S.V. Shmelkov, K.K. Jensen, S. Rafii, and D. Lyden. 2005. VEGFR1-positive haematopoietic bone marrow progenitors initiate the pre-metastatic niche. *Nature* 438:820-827.

Kapoor-Vazirani, P., J.D. Kagey, D.R. Powell, and P.M. Vertino. 2008. Role of hMOF-dependent histone H4 lysine 16 acetylation in the maintenance of TMS1/ASC gene activity. *Cancer Res* 68:6810-6821.

Karachaliou, N., S. Pilotto, C. Lazzari, E. Bria, F. de Marinis, and R. Rosell. 2016. Cellular and molecular biology of small cell lung cancer: an overview. *Transl Lung Cancer Res* 5:2-15.

Kaufmann, S.H., M. Mabry, R. Jasti, and J.H. Shaper. 1991. Differential expression of nuclear envelope lamins A and C in human lung cancer cell lines. *Cancer Res* 51:581-586.

Kehat, I., F. Accornero, B.J. Aronow, and J.D. Molkentin. 2011. Modulation of chromatin position and gene expression by HDAC4 interaction with nucleoporins. *J Cell Biol* 193:21-29.

Kennedy, B.K., D.A. Barbie, M. Classon, N. Dyson, and E. Harlow. 2000. Nuclear organization of DNA replication in primary mammalian cells. *Genes Dev* 14:2855-2868.

Khan, S.A., D. Reddy, and S. Gupta. 2015. Global histone post-translational modifications and cancer: Biomarkers for diagnosis, prognosis and treatment? *World J Biol Chem* 6:333-345.

Khayyata, S., S. Yun, T. Pasha, B. Jian, C. McGrath, G. Yu, P. Gupta, and Z. Baloch. 2009. Value of P63 and CK5/6 in distinguishing squamous cell

carcinoma from adenocarcinoma in lung fine-needle aspiration specimens. *Diagn Cytopathol* 37:178-183.

Kilanczyk, E., A. Graczyk, H. Ostrowska, I. Kasacka, W. Lesniak, and A. Filipek. 2012. S100A6 is transcriptionally regulated by beta-catenin and interacts with a novel target, lamin A/C, in colorectal cancer cells. *Cell Calcium* 51:470-477.

Kim, H.J., B.C. Litzenburger, X. Cui, D.A. Delgado, B.C. Grabiner, X. Lin, M.T. Lewis, M.M. Gottardis, T.W. Wong, R.M. Attar, J.M. Carboni, and A.V. Lee. 2007. Constitutively active type I insulin-like growth factor receptor causes transformation and xenograft growth of immortalized mammary epithelial cells and is accompanied by an epithelial-to-mesenchymal transition mediated by NF-kappaB and snail. *Mol Cell Biol* 27:3165-3175.

Kim, K.H., and C.W. Roberts. 2016. Targeting EZH2 in cancer. *Nat Med* 22:128-134.

Kim, M.J., H.C. Shin, K.C. Shin, and J.Y. Ro. 2013. Best immunohistochemical panel in distinguishing adenocarcinoma from squamous cell carcinoma of lung: tissue microarray assay in resected lung cancer specimens. *Ann Diagn Pathol* 17:85-90.

Kim, Y., M.C. Kugler, Y. Wei, K.K. Kim, X. Li, A.N. Brumwell, and H.A. Chapman. 2009. Integrin alpha3beta1-dependent beta-catenin phosphorylation links epithelial Smad signaling to cell contacts. *J Cell Biol* 184:309-322.

Kim, Y., A.A. Sharov, K. McDole, M. Cheng, H. Hao, C.M. Fan, N. Gaiano, M.S. Ko, and Y. Zheng. 2011. Mouse B-type lamins are required for proper organogenesis but not by embryonic stem cells. *Science* 334:1706-1710.

Koenig, A., C. Mueller, C. Hasel, G. Adler, and A. Menke. 2006. Collagen type I induces disruption of E-cadherin-mediated cell-cell contacts and promotes proliferation of pancreatic carcinoma cells. *Cancer Res* 66:4662-4671.

Kohno, T., H. Ichikawa, Y. Totoki, K. Yasuda, M. Hiramoto, T. Nammo, H. Sakamoto, K. Tsuta, K. Furuta, Y. Shimada, R. Iwakawa, H. Ogiwara, T. Oike, M. Enari, A.J. Schetter, H. Okayama, A. Haugen, V. Skaug, S. Chiku, I. Yamanaka, Y. Arai, S. Watanabe, I. Sekine, S. Ogawa, C.C. Harris, H. Tsuda, T. Yoshida, J. Yokota, and T. Shibata. 2012. KIF5B-RET fusions in lung adenocarcinoma. *Nat Med* 18:375-377.

Koken, M.H., G. Linares-Cruz, F. Quignon, A. Viron, M.K. Chelbi-Alix, J. Sobczak-Thepot, L. Juhlin, L. Degos, F. Calvo, and H. de The. 1995. The PML growth-suppressor has an altered expression in human oncogenesis. *Oncogene* 10:1315-1324.

Kokura, K., L. Sun, M.T. Bedford, and J. Fang. 2010. Methyl-H3K9-binding protein MPP8 mediates E-cadherin gene silencing and promotes tumour cell motility and invasion. *EMBO J* 29:3673-3687.

Konety, B.R., T.S. Nguyen, R. Dhir, R.S. Day, M.J. Becich, W.M. Stadler, and R.H. Getzenberg. 2000. Detection of bladder cancer using a novel nuclear matrix protein, BLCA-4. *Clin Cancer Res* 6:2618-2625.

Kong, L., G. Schafer, H. Bu, Y. Zhang, Y. Zhang, and H. Klocker. 2012. Lamin A/C protein is overexpressed in tissue-invading prostate cancer and promotes prostate cancer cell growth, migration and invasion through the PI3K/AKT/PTEN pathway. *Carcinogenesis* 33:751-759.

Kontogianni, K., A.G. Nicholson, D. Butcher, and M.N. Sheppard. 2005. CD56: a useful tool for the diagnosis of small cell lung carcinomas on biopsies with extensive crush artefact. *J Clin Pathol* 58:978-980.

Koppens, M., and M. van Lohuizen. 2016. Context-dependent actions of Polycomb repressors in cancer. *Oncogene* 35:1341-1352.

Kornberg, R.D. 1974. Chromatin structure: a repeating unit of histones and DNA. *Science* 184:868-871.

Kornberg, R.D., and J.O. Thomas. 1974. Chromatin structure; oligomers of the histones. *Science* 184:865-868.

Kosari, F., C.M. Ida, M.C. Aubry, L. Yang, I.V. Kovtun, J.L. Klein, Y. Li, S. Erdogan, S.C. Tomaszek, S.J. Murphy, L.C. Bolette, C.P. Kolbert, P. Yang, D.A. Wigle, and G. Vasmatzis. 2014. ASCL1 and RET expression defines a clinically relevant subgroup of lung adenocarcinoma characterized by neuroendocrine differentiation. *Oncogene* 33:3776-3783.

Kouzarides, T. 2007. Chromatin modifications and their function. *Cell* 128:693-705.

Kumaran, R.I., and D.L. Spector. 2008. A genetic locus targeted to the nuclear periphery in living cells maintains its transcriptional competence. *J Cell Biol* 180:51-65.

Kummar, S., M. Fogarasi, A. Canova, A. Mota, and T. Ciesielski. 2002. Cytokeratin 7 and 20 staining for the diagnosis of lung and colorectal adenocarcinoma. *Br J Cancer* 86:1884-1887.

Lai, A.Y., and P.A. Wade. 2011. Cancer biology and NuRD: a multifaceted chromatin remodelling complex. *Nat Rev Cancer* 11:588-596.

Lammerding, J., P.C. Schulze, T. Takahashi, S. Kozlov, T. Sullivan, R.D. Kamm, C.L. Stewart, and R.T. Lee. 2004. Lamin A/C deficiency causes defective nuclear mechanics and mechanotransduction. *J Clin Invest* 113:370-378.

Lamouille, S., E. Connolly, J.W. Smyth, R.J. Akhurst, and R. Derynck. 2012. TGF-beta-induced activation of mTOR complex 2 drives epithelial-mesenchymal transition and cell invasion. *J Cell Sci* 125:1259-1273.

Lamouille, S., J. Xu, and R. Derynck. 2014. Molecular mechanisms of epithelial-mesenchymal transition. *Nat Rev Mol Cell Biol* 15:178-196.

Langst, G., and L. Manelyte. 2015. Chromatin Remodelers: From Function to Dysfunction. *Genes (Basel)* 6:299-324.

Laybourn, P.J., and J.T. Kadonaga. 1991. Role of nucleosomal cores and histone H1 in regulation of transcription by RNA polymerase II. *Science* 254:238-245.

Lee, S.H., J.K. Lee, M.J. Ahn, D.W. Kim, J.M. Sun, B. Keam, T.M. Kim, D.S. Heo, J.S. Ahn, Y.L. Choi, H.S. Min, Y.K. Jeon, and K. Park. 2017. Vandetanib in pretreated patients with advanced non-small cell lung cancer-harboring RET rearrangement: a phase II clinical trial. *Ann Oncol* 28:292-297.

Li, L., Y. Du, X. Kong, Z. Li, Z. Jia, J. Cui, J. Gao, G. Wang, and K. Xie. 2013. Lamin B1 is a novel therapeutic target of betulinic acid in pancreatic cancer. *Clin Cancer Res* 19:4651-4661.

Li, Q., L. Hou, G. Ding, Y. Li, J. Wang, B. Qian, J. Sun, and Q. Wang. 2015. KDM6B induces epithelial-mesenchymal transition and enhances clear cell renal cell carcinoma metastasis through the activation of SLUG. *Int J Clin Exp Pathol* 8:6334-6344.

Li, Y.M., Y. Pan, Y. Wei, X. Cheng, B.P. Zhou, M. Tan, X. Zhou, W. Xia, G.N. Hortobagyi, D. Yu, and M.C. Hung. 2004. Upregulation of CXCR4 is essential for HER2-mediated tumor metastasis. *Cancer Cell* 6:459-469.

Li, Z., L. Xu, N. Tang, Y. Xu, X. Ye, S. Shen, X. Niu, S. Lu, and Z. Chen. 2014. The polycomb group protein EZH2 inhibits lung cancer cell growth by repressing the transcription factor Nrf2. *FEBS Lett* 588:3000-3007.

Liang, Z., T. Wu, H. Lou, X. Yu, R.S. Taichman, S.K. Lau, S. Nie, J. Umbreit, and H. Shim. 2004. Inhibition of breast cancer metastasis by selective synthetic polypeptide against CXCR4. *Cancer Res* 64:4302-4308.

Lin, C.Y., P.H. Tsai, C.C. Kandaswami, P.P. Lee, C.J. Huang, J.J. Hwang, and M.T. Lee. 2011. Matrix metalloproteinase-9 cooperates with transcription factor Snail to induce epithelial-mesenchymal transition. *Cancer Sci* 102:815-827.

Lin, F., and H.J. Worman. 1993. Structural organization of the human gene encoding nuclear lamin A and nuclear lamin C. *J Biol Chem* 268:16321-16326.

Lin, T., A. Ponn, X. Hu, B.K. Law, and J. Lu. 2010a. Requirement of the histone demethylase LSD1 in Snai1-mediated transcriptional repression during epithelial-mesenchymal transition. *Oncogene* 29:4896-4904.

Lin, Y., J. Mallen-St Clair, G. Wang, J. Luo, F. Palma-Diaz, C. Lai, D.A. Elashoff, S. Sharma, S.M. Dubinett, and M. St John. 2016. p38 MAPK mediates epithelial-mesenchymal transition by regulating p38IP and Snail in head and neck squamous cell carcinoma. *Oral Oncol* 60:81-89.

Lin, Y., Y. Wu, J. Li, C. Dong, X. Ye, Y.I. Chi, B.M. Evers, and B.P. Zhou. 2010b. The SNAG domain of Snail1 functions as a molecular hook for recruiting lysine-specific demethylase 1. *EMBO J* 29:1803-1816.

Liu, B., J. Wang, K.M. Chan, W.M. Tjia, W. Deng, X. Guan, J.D. Huang, K.M. Li, P.Y. Chau, D.J. Chen, D. Pei, A.M. Pendas, J. Cadinanos, C. Lopez-Otin, H.F. Tse, C. Hutchison, J. Chen, Y. Cao, K.S. Cheah, K. Tryggvason, and Z. Zhou. 2005. Genomic instability in laminopathy-based premature aging. *Nat Med* 11:780-785.

Liu, C.D., L. Tilch, D. Kwan, and D.W. McFadden. 2002. Vascular endothelial growth factor is increased in ascites from metastatic pancreatic cancer. *J Surg Res* 102:31-34.

Liu, J., K.K. Lee, M. Segura-Totten, E. Neufeld, K.L. Wilson, and Y. Gruenbaum. 2003. MAN1 and emerin have overlapping function(s) essential for chromosome segregation and cell division in Caenorhabditis elegans. *Proc Natl Acad Sci U S A* 100:4598-4603.

Liu, N.A., J. Sun, K. Kono, Y. Horikoshi, T. Ikura, X. Tong, T. Haraguchi, and S. Tashiro. 2015a. Regulation of homologous recombinational repair by lamin B1 in radiation-induced DNA damage. *FASEB J* 29:2514-2525.

Liu, S., D. Ye, W. Guo, W. Yu, Y. He, J. Hu, Y. Wang, L. Zhang, Y. Liao, H. Song, S. Zhong, D. Xu, H. Yin, B. Sun, X. Wang, J. Liu, Y. Wu, B.P. Zhou, Z. Zhang, and J. Deng. 2015b. G9a is essential for EMT-mediated metastasis and maintenance of cancer stem cell-like characters in head and neck squamous cell carcinoma. *Oncotarget* 6:6887-6901.

Liu, Y., X. Yan, Y. Xu, F. Luo, J. Ye, H. Yan, X. Yang, X. Huang, J. Zhang, and G. Ji. 2014. HIFs enhance the migratory and neoplastic capacities of hepatocellular carcinoma cells by promoting EMT. *Tumour Biol* 35:8103-8114.

Lo, H.W., S.C. Hsu, W. Xia, X. Cao, J.Y. Shih, Y. Wei, J.L. Abbruzzese, G.N. Hortobagyi, and M.C. Hung. 2007. Epidermal growth factor receptor cooperates with signal transducer and activator of transcription 3 to induce epithelial-mesenchymal transition in cancer cells via up-

regulation of TWIST gene expression. *Cancer Res* 67:9066-9076.

Lopez-Giral, S., N.E. Quintana, M. Cabrerizo, M. Alfonso-Perez, M. Sala-Valdes, V.G. De Soria, J.M. Fernandez-Ranada, E. Fernandez-Ruiz, and C. Munoz. 2004. Chemokine receptors that mediate B cell homing to secondary lymphoid tissues are highly expressed in B cell chronic lymphocytic leukemia and non-Hodgkin lymphomas with widespread nodular dissemination. *J Leukoc Biol* 76:462-471.

Lu, Q.Y., Y. Yang, Y.S. Jin, Z.F. Zhang, D. Heber, F.P. Li, S.M. Dubinett, M.A. Sondej, J.A. Loo, and J.Y. Rao. 2009. Effects of green tea extract on lung cancer A549 cells: proteomic identification of proteins associated with cell migration. *Proteomics* 9:757-767.

Lu, Z., S. Ghosh, Z. Wang, and T. Hunter. 2003. Downregulation of caveolin-1 function by EGF leads to the loss of E-cadherin, increased transcriptional activity of beta-catenin, and enhanced tumor cell invasion. *Cancer Cell* 4:499-515.

Lukasova, E., S. Kozubek, M. Falk, M. Kozubek, J. Zaloudik, V. Vagunda, and Z. Pavlovsky. 2004. Topography of genetic loci in the nuclei of cells of colorectal carcinoma and adjacent tissue of colonic epithelium. *Chromosoma* 112:221-230.

Malhas, A.N., C.F. Lee, and D.J. Vaux. 2009. Lamin B1 controls oxidative stress responses via Oct-1. *J Cell Biol* 184:45-55.

Malouf, G.G., J.H. Taube, Y. Lu, T. Roysarkar, S. Panjarian, M.R. Estecio, J. Jelinek, J. Yamazaki, N.J. Raynal, H. Long, T. Tahara, A. Tinnirello, P. Ramachandran, X.Y. Zhang, S. Liang, S.A. Mani, and J.P. Issa. 2013. Architecture of epigenetic reprogramming following Twist1-mediated epithelial-mesenchymal transition. *Genome Biol* 14:R144.

Mancini, M.A., D. He, Ouspenski, II, and B.R. Brinkley. 1996. Dynamic continuity of nuclear and mitotic matrix proteins in the cell cycle. *J Cell Biochem* 62:158-164.

Maresca, G., M. Natoli, M. Nardella, I. Arisi, D. Trisciuoglio, M. Desideri, R. Brandi, S. D'Aguanno, M.R. Nicotra, M. D'Onofrio, A. Urbani, P.G. Natali, D. Del Bufalo, A. Felsani, and I. D'Agnano. 2012. LMNA knock-down affects differentiation and progression of human neuroblastoma cells. *PLoS One* 7:e45513.

Maretzky, T., K. Reiss, A. Ludwig, J. Buchholz, F. Scholz, E. Proksch, B. de Strooper, D. Hartmann, and P. Saftig. 2005. ADAM10 mediates E-cadherin shedding and regulates epithelial cell-cell adhesion, migration, and beta-catenin translocation. *Proc Natl Acad Sci U S A* 102:9182-9187.

Margueron, R., G. Li, K. Sarma, A. Blais, J. Zavadil, C.L. Woodcock, B.D. Dynlacht, and D. Reinberg. 2008. Ezh1 and Ezh2 maintain repressive chromatin through different mechanisms. *Mol Cell* 32:503-518.

Marquez-Vilendrer, S.B., S.K. Rai, S.J. Gramling, L. Lu, and D.N. Reisman. 2016. Loss of the SWI/SNF ATPase subunits BRM and BRG1 drives lung cancer development. *Oncoscience* 3:322-336.

Marshall, K.W., S. Mohr, F.E. Khettabi, N. Nossova, S. Chao, W. Bao, J. Ma, X.J. Li, and C.C. Liew. 2010. A blood-based biomarker panel for stratifying current risk for colorectal cancer. *Int J Cancer* 126:1177-1186.

Martinez, N., A. Alonso, M.D. Moragues, J. Ponton, and J. Schneider. 1999. The nuclear pore complex protein Nup88 is overexpressed in tumor cells. *Cancer Res* 59:5408-5411.

Maschler, S., G. Wirl, H. Spring, D.V. Bredow, I. Sordat, H. Beug, and E. Reichmann. 2005. Tumor cell invasiveness correlates with changes in integrin expression and localization. *Oncogene* 24:2032-2041.

Massague, J. 2012. TGFbeta signalling in context. *Nat Rev Mol Cell Biol* 13:616-630.

Mattern, K.A., B.M. Humbel, A.O. Muijsers, L. de Jong, and R. van Driel. 1996. hnRNP proteins and B23 are the major proteins of the internal nuclear matrix of HeLa S3 cells. *J Cell Biochem* 62:275-289.

Maxwell, P.H., G.U. Dachs, J.M. Gleadle, L.G. Nicholls, A.L. Harris, I.J. Stratford, O. Hankinson, C.W. Pugh, and P.J. Ratcliffe. 1997. Hypoxia-inducible factor-1 modulates gene expression in solid tumors and influences both angiogenesis and tumor growth. *Proc Natl Acad Sci U S A* 94:8104-8109.

Mazumdar, A., R.A. Wang, S.K. Mishra, L. Adam, R. Bagheri-Yarmand, M. Mandal, R.K. Vadlamudi, and R. Kumar. 2001. Transcriptional repression of oestrogen receptor by metastasis-associated protein 1 corepressor. *Nat Cell Biol* 3:30-37.

McDonald, O.G., H. Wu, W. Timp, A. Doi, and A.P. Feinberg. 2011. Genome-scale epigenetic reprogramming during epithelial-to-mesenchymal transition. *Nat Struct Mol Biol* 18:867-874.

McNiven, M.A. 2013. Breaking away: matrix remodeling from the leading edge. *Trends Cell Biol* 23:16-21.

Medici, D., E.D. Hay, and B.R. Olsen. 2008. Snail and Slug promote epithelial-mesenchymal transition through beta-catenin-T-cell factor-4-dependent expression of transforming growth factor-beta3. *Mol Biol Cell* 19:4875-4887.

Mehlen, P., and A. Puisieux. 2006. Metastasis: a question of life or death. *Nat*

Rev Cancer 6:449-458.

Meier, J., K.H. Campbell, C.C. Ford, R. Stick, and C.J. Hutchison. 1991. The role of lamin LIII in nuclear assembly and DNA replication, in cell-free extracts of Xenopus eggs. *J Cell Sci* 98 (Pt 3):271-279.

Mendoza, L. 2018. Clinical development of RET inhibitors in RET-rearranged non-small cell lung cancer: Update. *Oncol Rev* 12:352.

Messai, Y., M.Z. Noman, M. Hasmim, B. Janji, A. Tittarelli, M. Boutet, V. Baud, E. Viry, K. Billot, A. Nanbakhsh, T. Ben Safta, C. Richon, S. Ferlicot, E. Donnadieu, S. Couve, B. Gardie, F. Orlanducci, L. Albiges, J. Thiery, D. Olive, B. Escudier, and S. Chouaib. 2014. ITPR1 protects renal cancer cells against natural killer cells by inducing autophagy. *Cancer Res* 74:6820-6832.

Meuwissen, R., S.C. Linn, R.I. Linnoila, J. Zevenhoven, W.J. Mooi, and A. Berns. 2003. Induction of small cell lung cancer by somatic inactivation of both Trp53 and Rb1 in a conditional mouse model. *Cancer Cell* 4:181-189.

Min, J., Y. Zhang, and R.M. Xu. 2003. Structural basis for specific binding of Polycomb chromodomain to histone H3 methylated at Lys 27. *Genes Dev* 17:1823-1828.

Mise, N., R. Savai, H. Yu, J. Schwarz, N. Kaminski, and O. Eickelberg. 2012. Zyxin is a transforming growth factor-beta (TGF-beta)/Smad3 target gene that regulates lung cancer cell motility via integrin alpha5beta1. *J Biol Chem* 287:31393-31405.

Moir, R.D., M. Montag-Lowy, and R.D. Goldman. 1994. Dynamic properties of nuclear lamins: lamin B is associated with sites of DNA replication. *J Cell Biol* 125:1201-1212.

Moir, R.D., T.P. Spann, H. Herrmann, and R.D. Goldman. 2000a. Disruption of nuclear lamin organization blocks the elongation phase of DNA replication. *J Cell Biol* 149:1179-1192.

Moir, R.D., M. Yoon, S. Khuon, and R.D. Goldman. 2000b. Nuclear lamins A and B1: different pathways of assembly during nuclear envelope formation in living cells. *J Cell Biol* 151:1155-1168.

Molina, R., X. Filella, and J.M. Auge. 2004. ProGRP: a new biomarker for small cell lung cancer. *Clin Biochem* 37:505-511.

Molli, P.R., R.R. Singh, S.W. Lee, and R. Kumar. 2008. MTA1-mediated transcriptional repression of BRCA1 tumor suppressor gene. *Oncogene* 27:1971-1980.

Morita, T., T. Mayanagi, and K. Sobue. 2007. Dual roles of myocardin-related transcription factors in epithelial mesenchymal transition via slug

induction and actin remodeling. *J Cell Biol* 179:1027-1042.

Moserle, L., and O. Casanovas. 2013. Anti-angiogenesis and metastasis: a tumour and stromal cell alliance. *J Intern Med* 273:128-137.

Moss, S.F., V. Krivosheyev, A. de Souza, K. Chin, H.P. Gaetz, N. Chaudhary, H.J. Worman, and P.R. Holt. 1999. Decreased and aberrant nuclear lamin expression in gastrointestinal tract neoplasms. *Gut* 45:723-729.

Moustakas, A., and C.H. Heldin. 2005. Non-Smad TGF-beta signals. *J Cell Sci* 118:3573-3584.

Muller, A., B. Homey, H. Soto, N. Ge, D. Catron, M.E. Buchanan, T. McClanahan, E. Murphy, W. Yuan, S.N. Wagner, J.L. Barrera, A. Mohar, E. Verastegui, and A. Zlotnik. 2001. Involvement of chemokine receptors in breast cancer metastasis. *Nature* 410:50-56.

Muller, A., E. Sonkoly, C. Eulert, P.A. Gerber, R. Kubitza, K. Schirlau, P. Franken-Kunkel, C. Poremba, C. Snyderman, L.O. Klotz, T. Ruzicka, H. Bier, A. Zlotnik, T.L. Whiteside, B. Homey, and T.K. Hoffmann. 2006. Chemokine receptors in head and neck cancer: association with metastatic spread and regulation during chemotherapy. *Int J Cancer* 118:2147-2157.

Mulligan, L.M. 2014. RET revisited: expanding the oncogenic portfolio. *Nat Rev Cancer* 14:173-186.

Nair, S.S., and R. Kumar. 2012. Chromatin remodeling in cancer: a gateway to regulate gene transcription. *Mol Oncol* 6:611-619.

Najy, A.J., K.C. Day, and M.L. Day. 2008. The ectodomain shedding of E-cadherin by ADAM15 supports ErbB receptor activation. *J Biol Chem* 283:18393-18401.

Newport, J.W., K.L. Wilson, and W.G. Dunphy. 1990. A lamin-independent pathway for nuclear envelope assembly. *J Cell Biol* 111:2247-2259.

Nguyen, C.T., D.J. Weisenberger, M. Velicescu, F.A. Gonzales, J.C. Lin, G. Liang, and P.A. Jones. 2002. Histone H3-lysine 9 methylation is associated with aberrant gene silencing in cancer cells and is rapidly reversed by 5-aza-2'-deoxycytidine. *Cancer Res* 62:6456-6461.

Niehrs, C. 2012. The complex world of WNT receptor signalling. *Nat Rev Mol Cell Biol* 13:767-779.

Nikolova, V., C. Leimena, A.C. McMahon, J.C. Tan, S. Chandar, D. Jogia, S.H. Kesteven, J. Michalicek, R. Otway, F. Verheyen, S. Rainer, C.L. Stewart, D. Martin, M.P. Feneley, and D. Fatkin. 2004. Defects in nuclear structure and function promote dilated cardiomyopathy in lamin A/C-deficient mice. *J Clin Invest* 113:357-369.

Nisman, B., H. Biran, N. Ramu, N. Heching, V. Barak, and T. Peretz. 2009. The diagnostic and prognostic value of ProGRP in lung cancer. *Anticancer Res* 29:4827-4832.

Noe, V., B. Fingleton, K. Jacobs, H.C. Crawford, S. Vermeulen, W. Steelant, E. Bruyneel, L.M. Matrisian, and M. Mareel. 2001. Release of an invasion promoter E-cadherin fragment by matrilysin and stromelysin-1. *J Cell Sci* 114:111-118.

Norton, J.T., C.B. Pollock, C. Wang, J.C. Schink, J.J. Kim, and S. Huang. 2008. Perinucleolar compartment prevalence is a phenotypic pancancer marker of malignancy. *Cancer* 113:861-869.

Ntziachristos, P., A. Tsirigos, P. Van Vlierberghe, J. Nedjic, T. Trimarchi, M.S. Flaherty, D. Ferres-Marco, V. da Ros, Z. Tang, J. Siegle, P. Asp, M. Hadler, I. Rigo, K. De Keersmaecker, J. Patel, T. Huynh, F. Utro, S. Poglio, J.B. Samon, E. Paietta, J. Racevskis, J.M. Rowe, R. Rabadan, R.L. Levine, S. Brown, F. Pflumio, M. Dominguez, A. Ferrando, and I. Aifantis. 2012. Genetic inactivation of the polycomb repressive complex 2 in T cell acute lymphoblastic leukemia. *Nat Med* 18:298-301.

Oberdoerffer, P., and D.A. Sinclair. 2007. The role of nuclear architecture in genomic instability and ageing. *Nat Rev Mol Cell Biol* 8:692-702.

Oguchi, M., J. Sagara, K. Matsumoto, T. Saida, and S. Taniguchi. 2002. Expression of lamins depends on epidermal differentiation and transformation. *Br J Dermatol* 147:853-858.

Pajerowski, J.D., K.N. Dahl, F.L. Zhong, P.J. Sammak, and D.E. Discher. 2007. Physical plasticity of the nucleus in stem cell differentiation. *Proc Natl Acad Sci U S A* 104:15619-15624.

Palazon, A., A.W. Goldrath, V. Nizet, and R.S. Johnson. 2014. HIF transcription factors, inflammation, and immunity. *Immunity* 41:518-528.

Panorchan, P., B.W. Schafer, D. Wirtz, and Y. Tseng. 2004a. Nuclear envelope breakdown requires overcoming the mechanical integrity of the nuclear lamina. *J Biol Chem* 279:43462-43467.

Panorchan, P., D. Wirtz, and Y. Tseng. 2004b. Structure-function relationship of biological gels revealed by multiple-particle tracking and differential interference contrast microscopy: the case of human lamin networks. *Phys Rev E Stat Nonlin Soft Matter Phys* 70:041906.

Park, K.S., M.C. Liang, D.M. Raiser, R. Zamponi, R.R. Roach, S.J. Curtis, Z. Walton, B.E. Schaffer, C.M. Roake, A.F. Zmoos, C. Kriegel, K.K. Wong, J. Sage, and C.F. Kim. 2011a. Characterization of the cell of origin for small cell lung cancer. *Cell Cycle* 10:2806-2815.

Park, S.Y., K.J. Jeong, N. Panupinthu, S. Yu, J. Lee, J.W. Han, J.M. Kim, J.S. Lee, J. Kang, C.G. Park, G.B. Mills, and H.Y. Lee. 2011b. Lysophosphatidic acid augments human hepatocellular carcinoma cell invasion through LPA1 receptor and MMP-9 expression. *Oncogene* 30:1351-1359.

Partin, A.W., J.V. Briggman, E.N. Subong, R. Szaro, A. Oreper, S. Wiesbrock, J. Meyer, D.S. Coffey, and J.I. Epstein. 1997. Preliminary immunohistochemical characterization of a monoclonal antibody (PRO:4-216) prepared from human prostate cancer nuclear matrix proteins. *Urology* 50:800-808.

Pasini, D., A.P. Bracken, M.R. Jensen, E. Lazzerini Denchi, and K. Helin. 2004. Suz12 is essential for mouse development and for EZH2 histone methyltransferase activity. *EMBO J* 23:4061-4071.

Pasini, D., and L. Di Croce. 2016. Emerging roles for Polycomb proteins in cancer. *Curr Opin Genet Dev* 36:50-58.

Pearson, M., R. Carbone, C. Sebastiani, M. Cioce, M. Fagioli, S. Saito, Y. Higashimoto, E. Appella, S. Minucci, P.P. Pandolfi, and P.G. Pelicci. 2000. PML regulates p53 acetylation and premature senescence induced by oncogenic Ras. *Nature* 406:207-210.

Peinado, H., E. Ballestar, M. Esteller, and A. Cano. 2004. Snail mediates E-cadherin repression by the recruitment of the Sin3A/histone deacetylase 1 (HDAC1)/HDAC2 complex. *Mol Cell Biol* 24:306-319.

Peric-Hupkes, D., W. Meuleman, L. Pagie, S.W. Bruggeman, I. Solovei, W. Brugman, S. Graf, P. Flicek, R.M. Kerkhoven, M. van Lohuizen, M. Reinders, L. Wessels, and B. van Steensel. 2010. Molecular maps of the reorganization of genome-nuclear lamina interactions during differentiation. *Mol Cell* 38:603-613.

Peter, M., G.T. Kitten, C.F. Lehner, K. Vorburger, S.M. Bailer, G. Maridor, and E.A. Nigg. 1989. Cloning and sequencing of cDNA clones encoding chicken lamins A and B1 and comparison of the primary structures of vertebrate A- and B-type lamins. *J Mol Biol* 208:393-404.

Pettaway, C.A., S. Pathak, G. Greene, E. Ramirez, M.R. Wilson, J.J. Killion, and I.J. Fidler. 1996. Selection of highly metastatic variants of different human prostatic carcinomas using orthotopic implantation in nude mice. *Clin Cancer Res* 2:1627-1636.

Phillips, R.J., M.D. Burdick, M. Lutz, J.A. Belperio, M.P. Keane, and R.M. Strieter. 2003. The stromal derived factor-1/CXCL12-CXC chemokine receptor 4 biological axis in non-small cell lung cancer metastases. *Am*

J Respir Crit Care Med 167:1676-1686.

Poleshko, A., P.P. Shah, M. Gupta, A. Babu, M.P. Morley, L.J. Manderfield, J.L. Ifkovits, D. Calderon, H. Aghajanian, J.E. Sierra-Pagan, Z. Sun, Q. Wang, L. Li, N.C. Dubois, E.E. Morrisey, M.A. Lazar, C.L. Smith, J.A. Epstein, and R. Jain. 2017. Genome-Nuclear Lamina Interactions Regulate Cardiac Stem Cell Lineage Restriction. *Cell* 171:573-587 e514.

Pollock, C., and S. Huang. 2010. The perinucleolar compartment. *Cold Spring Harb Perspect Biol* 2:a000679.

Pradelli, E., B. Karimdjee-Soilihi, J.F. Michiels, J.E. Ricci, M.A. Millet, F. Vandenbos, T.J. Sullivan, T.L. Collins, M.G. Johnson, J.C. Medina, E.S. Kleinerman, A. Schmid-Alliana, and H. Schmid-Antomarchi. 2009. Antagonism of chemokine receptor CXCR3 inhibits osteosarcoma metastasis to lungs. *Int J Cancer* 125:2586-2594.

Prenzel, T., Y. Begus-Nahrmann, F. Kramer, M. Hennion, C. Hsu, T. Gorsler, C. Hintermair, D. Eick, E. Kremmer, M. Simons, T. Beissbarth, and S.A. Johnsen. 2011. Estrogen-dependent gene transcription in human breast cancer cells relies upon proteasome-dependent monoubiquitination of histone H2B. *Cancer Res* 71:5739-5753.

Radisky, D.C., D.D. Levy, L.E. Littlepage, H. Liu, C.M. Nelson, J.E. Fata, D. Leake, E.L. Godden, D.G. Albertson, M.A. Nieto, Z. Werb, and M.J. Bissell. 2005. Rac1b and reactive oxygen species mediate MMP-3-induced EMT and genomic instability. *Nature* 436:123-127.

Ramadoss, S., X. Chen, and C.Y. Wang. 2012. Histone demethylase KDM6B promotes epithelial-mesenchymal transition. *J Biol Chem* 287:44508-44517.

Rankin, E.B., and A.J. Giaccia. 2016. Hypoxic control of metastasis. *Science* 352:175-180.

Rauschert, I., F. Aldunate, J. Preussner, M. Arocena-Sutz, V. Peraza, M. Looso, J.C. Benech, and R. Agrelo. 2017. Promoter hypermethylation as a mechanism for Lamin A/C silencing in a subset of neuroblastoma cells. *PLoS One* 12:e0175953.

Reddy, K.L., J.M. Zullo, E. Bertolino, and H. Singh. 2008. Transcriptional repression mediated by repositioning of genes to the nuclear lamina. *Nature* 452:243-247.

Reymond, N., B.B. d'Agua, and A.J. Ridley. 2013. Crossing the endothelial barrier during metastasis. *Nat Rev Cancer* 13:858-870.

Ridley, A.J. 2011. Life at the leading edge. *Cell* 145:1012-1022.

Rober, R.A., H. Sauter, K. Weber, and M. Osborn. 1990. Cells of the cellular

immune and hemopoietic system of the mouse lack lamins A/C: distinction versus other somatic cells. *J Cell Sci* 95 (Pt 4):587-598.

Rotem, A., A. Janzer, B. Izar, Z. Ji, J.G. Doench, L.A. Garraway, and K. Struhl. 2015. Alternative to the soft-agar assay that permits high-throughput drug and genetic screens for cellular transformation. *Proc Natl Acad Sci U S A* 112:5708-5713.

Rubporn, A., C. Srisomsap, P. Subhasitanont, D. Chokchaichamnankit, K. Chiablaem, J. Svasti, and P. Sangvanich. 2009. Comparative proteomic analysis of lung cancer cell line and lung fibroblast cell line. *Cancer Genomics Proteomics* 6:229-237.

Rusinol, A.E., and M.S. Sinensky. 2006. Farnesylated lamins, progeroid syndromes and farnesyl transferase inhibitors. *J Cell Sci* 119:3265-3272.

Sakthivel, K.M., and P. Sehgal. 2016. A Novel Role of Lamins from Genetic Disease to Cancer Biomarkers. *Oncol Rev* 10:309.

Samant, R.S., M.J. Seraj, M.M. Saunders, T.S. Sakamaki, L.A. Shevde, J.F. Harms, T.O. Leonard, S.F. Goldberg, L. Budgeon, W.J. Meehan, C.R. Winter, N.D. Christensen, M.F. Verderame, H.J. Donahue, and D.R. Welch. 2000. Analysis of mechanisms underlying BRMS1 suppression of metastasis. *Clin Exp Metastasis* 18:683-693.

Sanchez-Tillo, E., A. Lazaro, R. Torrent, M. Cuatrecasas, E.C. Vaquero, A. Castells, P. Engel, and A. Postigo. 2010. ZEB1 represses E-cadherin and induces an EMT by recruiting the SWI/SNF chromatin-remodeling protein BRG1. *Oncogene* 29:3490-3500.

Sarvaiya, P.J., D. Guo, I. Ulasov, P. Gabikian, and M.S. Lesniak. 2013. Chemokines in tumor progression and metastasis. *Oncotarget* 4:2171-2185.

Savagner, P., K.M. Yamada, and J.P. Thiery. 1997. The zinc-finger protein slug causes desmosome dissociation, an initial and necessary step for growth factor-induced epithelial-mesenchymal transition. *J Cell Biol* 137:1403-1419.

Scaffidi, P., and T. Misteli. 2006. Lamin A-dependent nuclear defects in human aging. *Science* 312:1059-1063.

Serresi, M., G. Gargiulo, N. Proost, B. Siteur, M. Cesaroni, M. Koppens, H. Xie, K.D. Sutherland, D. Hulsman, E. Citterio, S. Orkin, A. Berns, and M. van Lohuizen. 2016. Polycomb Repressive Complex 2 Is a Barrier to KRAS-Driven Inflammation and Epithelial-Mesenchymal Transition in Non-Small-Cell Lung Cancer. *Cancer Cell* 29:17-31.

Sethi, N., X. Dai, C.G. Winter, and Y. Kang. 2011. Tumor-derived JAGGED1

promotes osteolytic bone metastasis of breast cancer by engaging notch signaling in bone cells. *Cancer Cell* 19:192-205.

Shachar, S., and T. Misteli. 2017. Causes and consequences of nuclear gene positioning. *J Cell Sci* 130:1501-1508.

Shah, P.P., G. Donahue, G.L. Otte, B.C. Capell, D.M. Nelson, K. Cao, V. Aggarwala, H.A. Cruickshanks, T.S. Rai, T. McBryan, B.D. Gregory, P.D. Adams, and S.L. Berger. 2013. Lamin B1 depletion in senescent cells triggers large-scale changes in gene expression and the chromatin landscape. *Genes Dev* 27:1787-1799.

Shen, X., Y. Liu, Y.J. Hsu, Y. Fujiwara, J. Kim, X. Mao, G.C. Yuan, and S.H. Orkin. 2008. EZH1 mediates methylation on histone H3 lysine 27 and complements EZH2 in maintaining stem cell identity and executing pluripotency. *Mol Cell* 32:491-502.

Sheppard, D. 2005. Integrin-mediated activation of latent transforming growth factor beta. *Cancer Metastasis Rev* 24:395-402.

Shi, J., Y. Wang, L. Zeng, Y. Wu, J. Deng, Q. Zhang, Y. Lin, J. Li, T. Kang, M. Tao, E. Rusinova, G. Zhang, C. Wang, H. Zhu, J. Yao, Y.X. Zeng, B.M. Evers, M.M. Zhou, and B.P. Zhou. 2014. Disrupting the interaction of BRD4 with diacetylated Twist suppresses tumorigenesis in basal-like breast cancer. *Cancer Cell* 25:210-225.

Shi, Y., F. Lan, C. Matson, P. Mulligan, J.R. Whetstine, P.A. Cole, R.A. Casero, and Y. Shi. 2004. Histone demethylation mediated by the nuclear amine oxidase homolog LSD1. *Cell* 119:941-953.

Shi, Y., J. Sawada, G. Sui, B. Affar el, J.R. Whetstine, F. Lan, H. Ogawa, M.P. Luke, Y. Nakatani, and Y. Shi. 2003. Coordinated histone modifications mediated by a CtBP co-repressor complex. *Nature* 422:735-738.

Shimi, T., V. Butin-Israeli, S.A. Adam, R.B. Hamanaka, A.E. Goldman, C.A. Lucas, D.K. Shumaker, S.T. Kosak, N.S. Chandel, and R.D. Goldman. 2011. The role of nuclear lamin B1 in cell proliferation and senescence. *Genes Dev* 25:2579-2593.

Shimi, T., K. Pfleghaar, S. Kojima, C.G. Pack, I. Solovei, A.E. Goldman, S.A. Adam, D.K. Shumaker, M. Kinjo, T. Cremer, and R.D. Goldman. 2008. The A- and B-type nuclear lamin networks: microdomains involved in chromatin organization and transcription. *Genes Dev* 22:3409-3421.

Shindo, Y., K. Iwamoto, K. Mouri, K. Hibino, M. Tomita, H. Kosako, Y. Sako, and K. Takahashi. 2016. Conversion of graded phosphorylation into switch-like nuclear translocation via autoregulatory mechanisms in ERK signalling. *Nat Commun* 7:10485.

Shirakihara, T., M. Saitoh, and K. Miyazono. 2007. Differential regulation of epithelial and mesenchymal markers by deltaEF1 proteins in epithelial mesenchymal transition induced by TGF-beta. *Mol Biol Cell* 18:3533-3544.

Shogren-Knaak, M., H. Ishii, J.M. Sun, M.J. Pazin, J.R. Davie, and C.L. Peterson. 2006. Histone H4-K16 acetylation controls chromatin structure and protein interactions. *Science* 311:844-847.

Shumaker, D.K., T. Dechat, A. Kohlmaier, S.A. Adam, M.R. Bozovsky, M.R. Erdos, M. Eriksson, A.E. Goldman, S. Khuon, F.S. Collins, T. Jenuwein, and R.D. Goldman. 2006. Mutant nuclear lamin A leads to progressive alterations of epigenetic control in premature aging. *Proc Natl Acad Sci U S A* 103:8703-8708.

Shumaker, D.K., L. Solimando, K. Sengupta, T. Shimi, S.A. Adam, A. Grunwald, S.V. Strelkov, U. Aebi, M.C. Cardoso, and R.D. Goldman. 2008. The highly conserved nuclear lamin Ig-fold binds to PCNA: its role in DNA replication. *J Cell Biol* 181:269-280.

Siegel, R., D. Naishadham, and A. Jemal. 2013. Cancer statistics, 2013. *CA Cancer J Clin* 63:11-30.

Simon, C., J. Chagraoui, J. Krosl, P. Gendron, B. Wilhelm, S. Lemieux, G. Boucher, P. Chagnon, S. Drouin, R. Lambert, C. Rondeau, A. Bilodeau, S. Lavallee, M. Sauvageau, J. Hebert, and G. Sauvageau. 2012. A key role for EZH2 and associated genes in mouse and human adult T-cell acute leukemia. *Genes Dev* 26:651-656.

Simonetti, O., G. Goteri, G. Lucarini, A. Filosa, T. Pieramici, C. Rubini, G. Biagini, and A. Offidani. 2006. Potential role of CCL27 and CCR10 expression in melanoma progression and immune escape. *Eur J Cancer* 42:1181-1187.

Singh, R., C.R. Stockard, W.E. Grizzle, J.W. Lillard, Jr., and S. Singh. 2011. Expression and histopathological correlation of CCR9 and CCL25 in ovarian cancer. *Int J Oncol* 39:373-381.

Skvortsov, S., G. Schafer, T. Stasyk, C. Fuchsberger, G.K. Bonn, G. Bartsch, H. Klocker, and L.A. Huber. 2011. Proteomics profiling of microdissected low- and high-grade prostate tumors identifies Lamin A as a discriminatory biomarker. *J Proteome Res* 10:259-268.

Smallwood, A., P.O. Esteve, S. Pradhan, and M. Carey. 2007. Functional cooperation between HP1 and DNMT1 mediates gene silencing. *Genes Dev* 21:1169-1178.

Son, J., S.S. Shen, R. Margueron, and D. Reinberg. 2013. Nucleosome-binding activities within JARID2 and EZH1 regulate the function of PRC2 on

chromatin. *Genes Dev* 27:2663-2677.

Song, K.H., J. Lee, H. Park, H.M. Kim, J. Park, K.W. Kwon, and J. Doh. 2016. Roles of endothelial A-type lamins in migration of T cells on and under endothelial layers. *Sci Rep* 6:23412.

Spann, T.P., A.E. Goldman, C. Wang, S. Huang, and R.D. Goldman. 2002. Alteration of nuclear lamin organization inhibits RNA polymerase II-dependent transcription. *J Cell Biol* 156:603-608.

Spann, T.P., R.D. Moir, A.E. Goldman, R. Stick, and R.D. Goldman. 1997. Disruption of nuclear lamin organization alters the distribution of replication factors and inhibits DNA synthesis. *J Cell Biol* 136:1201-1212.

Speetjens, F.M., G.J. Liefers, C.J. Korbee, W.E. Mesker, C.J. van de Velde, R.L. van Vlierberghe, H. Morreau, R.A. Tollenaar, and P.J. Kuppen. 2009. Nuclear localization of CXCR4 determines prognosis for colorectal cancer patients. *Cancer Microenviron* 2:1-7.

Strambio-De-Castillia, C., M. Niepel, and M.P. Rout. 2010. The nuclear pore complex: bridging nuclear transport and gene regulation. *Nat Rev Mol Cell Biol* 11:490-501.

Su, L., J. Zhang, H. Xu, Y. Wang, Y. Chu, R. Liu, and S. Xiong. 2005. Differential expression of CXCR4 is associated with the metastatic potential of human non-small cell lung cancer cells. *Clin Cancer Res* 11:8273-8280.

Su, Y.C., Y.C. Hsu, and C.Y. Chai. 2006. Role of TTF-1, CK20, and CK7 immunohistochemistry for diagnosis of primary and secondary lung adenocarcinoma. *Kaohsiung J Med Sci* 22:14-19.

Subbiah, V., J.F. Gainor, R. Rahal, J.D. Brubaker, J.L. Kim, M. Maynard, W. Hu, Q. Cao, M.P. Sheets, D. Wilson, K.J. Wilson, L. DiPietro, P. Fleming, M. Palmer, M.I. Hu, L. Wirth, M.S. Brose, S.I. Ou, M. Taylor, E. Garralda, S. Miller, B. Wolf, C. Lengauer, T. Guzi, and E.K. Evans. 2018a. Precision Targeted Therapy with BLU-667 for RET-Driven Cancers. *Cancer Discov* 8:836-849.

Subbiah, V., V. Velcheti, B.B. Tuch, K. Ebata, N.L. Busaidy, M.E. Cabanillas, L.J. Wirth, S. Stock, S. Smith, V. Lauriault, S. Corsi-Travali, D. Henry, M. Burkard, R. Hamor, K. Bouhana, S. Winski, R.D. Wallace, D. Hartley, S. Rhodes, M. Reddy, B.J. Brandhuber, S. Andrews, S.M. Rothenberg, and A. Drilon. 2018b. Selective RET kinase inhibition for patients with RET-altered cancers. *Ann Oncol* 29:1869-1876.

Suganuma, T., and J.L. Workman. 2008. Crosstalk among Histone Modifications. *Cell* 135:604-607.

Sukhai, M.A., X. Wu, Y. Xuan, T. Zhang, P.P. Reis, K. Dube, E.M. Rego, M.

Bhaumik, D.J. Bailey, R.A. Wells, S. Kamel-Reid, and P.P. Pandolfi. 2004. Myeloid leukemia with promyelocytic features in transgenic mice expressing hCG-NuMA-RARalpha. *Oncogene* 23:665-678.

Sullivan, T., D. Escalante-Alcalde, H. Bhatt, M. Anver, N. Bhat, K. Nagashima, C.L. Stewart, and B. Burke. 1999. Loss of A-type lamin expression compromises nuclear envelope integrity leading to muscular dystrophy. *J Cell Biol* 147:913-920.

Sun, L., and J. Fang. 2016. Epigenetic regulation of epithelial-mesenchymal transition. *Cell Mol Life Sci* 73:4493-4515.

Sun, L., K. Kokura, V. Izumi, J.M. Koomen, E. Seto, J. Chen, and J. Fang. 2015. MPP8 and SIRT1 crosstalk in E-cadherin gene silencing and epithelial-mesenchymal transition. *EMBO Rep* 16:689-699.

Sun, S., M.Z. Xu, R.T. Poon, P.J. Day, and J.M. Luk. 2010. Circulating Lamin B1 (LMNB1) biomarker detects early stages of liver cancer in patients. *J Proteome Res* 9:70-78.

Sutherland, K.D., N. Proost, I. Brouns, D. Adriaensen, J.Y. Song, and A. Berns. 2011. Cell of origin of small cell lung cancer: inactivation of Trp53 and Rb1 in distinct cell types of adult mouse lung. *Cancer Cell* 19:754-764.

Takanami, I. 2003. Overexpression of CCR7 mRNA in nonsmall cell lung cancer: correlation with lymph node metastasis. *Int J Cancer* 105:186-189.

Takawa, M., K. Masuda, M. Kunizaki, Y. Daigo, K. Takagi, Y. Iwai, H.S. Cho, G. Toyokawa, Y. Yamane, K. Maejima, H.I. Field, T. Kobayashi, T. Akasu, M. Sugiyama, E. Tsuchiya, Y. Atomi, B.A. Ponder, Y. Nakamura, and R. Hamamoto. 2011. Validation of the histone methyltransferase EZH2 as a therapeutic target for various types of human cancer and as a prognostic marker. *Cancer Sci* 102:1298-1305.

Takeuchi, K., M. Soda, Y. Togashi, R. Suzuki, S. Sakata, S. Hatano, R. Asaka, W. Hamanaka, H. Ninomiya, H. Uehara, Y. Lim Choi, Y. Satoh, S. Okumura, K. Nakagawa, H. Mano, and Y. Ishikawa. 2012. RET, ROS1 and ALK fusions in lung cancer. *Nat Med* 18:378-381.

Tan, J., X. Yang, L. Zhuang, X. Jiang, W. Chen, P.L. Lee, R.K. Karuturi, P.B. Tan, E.T. Liu, and Q. Yu. 2007. Pharmacologic disruption of Polycomb-repressive complex 2-mediated gene repression selectively induces apoptosis in cancer cells. *Genes Dev* 21:1050-1063.

Tang, C.W., A. Maya-Mendoza, C. Martin, K. Zeng, S. Chen, D. Feret, S.A. Wilson, and D.A. Jackson. 2008. The integrity of a lamin-B1-dependent nucleoskeleton is a fundamental determinant of RNA synthesis in human cells. *J Cell Sci* 121:1014-1024.

Thiery, J.P. 2002. Epithelial-mesenchymal transitions in tumour progression. *Nat Rev Cancer* 2:442-454.

Thiery, J.P., and J.P. Sleeman. 2006. Complex networks orchestrate epithelial-mesenchymal transitions. *Nat Rev Mol Cell Biol* 7:131-142.

Tian, X., Z. Liu, B. Niu, J. Zhang, T.K. Tan, S.R. Lee, Y. Zhao, D.C. Harris, and G. Zheng. 2011. E-cadherin/beta-catenin complex and the epithelial barrier. *J Biomed Biotechnol* 2011:567305.

Tilli, C.M., F.C. Ramaekers, J.L. Broers, C.J. Hutchison, and H.A. Neumann. 2003. Lamin expression in normal human skin, actinic keratosis, squamous cell carcinoma and basal cell carcinoma. *Br J Dermatol* 148:102-109.

Tran, J.R., X. Zheng, and Y. Zheng. 2016. Lamin-B1 contributes to the proper timing of epicardial cell migration and function during embryonic heart development. *Mol Biol Cell* 27:3956-3963.

Travis, W.D., E. Brambilla, and G.J. Riely. 2013. New pathologic classification of lung cancer: relevance for clinical practice and clinical trials. *J Clin Oncol* 31:992-1001.

Tremblay, P.L., F.A. Auger, and J. Huot. 2006. Regulation of transendothelial migration of colon cancer cells by E-selectin-mediated activation of p38 and ERK MAP kinases. *Oncogene* 25:6563-6573.

Turner, B.M., P.T. Cagle, I.M. Sainz, J. Fukuoka, S.S. Shen, and J. Jagirdar. 2012. Napsin A, a new marker for lung adenocarcinoma, is complementary and more sensitive and specific than thyroid transcription factor 1 in the differential diagnosis of primary pulmonary carcinoma: evaluation of 1674 cases by tissue microarray. *Arch Pathol Lab Med* 136:163-171.

Van Berlo, J.H., J.W. Voncken, N. Kubben, J.L. Broers, R. Duisters, R.E. van Leeuwen, H.J. Crijns, F.C. Ramaekers, C.J. Hutchison, and Y.M. Pinto. 2005. A-type lamins are essential for TGF-beta1 induced PP2A to dephosphorylate transcription factors. *Hum Mol Genet* 14:2839-2849.

van Steensel, B., and A.S. Belmont. 2017. Lamina-Associated Domains: Links with Chromosome Architecture, Heterochromatin, and Gene Repression. *Cell* 169:780-791.

Vaughan, A., M. Alvarez-Reyes, J.M. Bridger, J.L. Broers, F.C. Ramaekers, M. Wehnert, G.E. Morris, W.G.F. Whitfield, and C.J. Hutchison. 2001. Both emerin and lamin C depend on lamin A for localization at the nuclear envelope. *J Cell Sci* 114:2577-2590.

Veit, C., F. Genze, A. Menke, S. Hoeffert, T.M. Gress, P. Gierschik, and K. Giehl.

2004. Activation of phosphatidylinositol 3-kinase and extracellular signal-regulated kinase is required for glial cell line-derived neurotrophic factor-induced migration and invasion of pancreatic carcinoma cells. *Cancer Res* 64:5291-5300.

Venables, R.S., S. McLean, D. Luny, E. Moteleb, S. Morley, R.A. Quinlan, E.B. Lane, and C.J. Hutchison. 2001. Expression of individual lamins in basal cell carcinomas of the skin. *Br J Cancer* 84:512-519.

Verdin, E., and M. Ott. 2015. 50 years of protein acetylation: from gene regulation to epigenetics, metabolism and beyond. *Nat Rev Mol Cell Biol* 16:258-264.

Vergnes, L., M. Peterfy, M.O. Bergo, S.G. Young, and K. Reue. 2004. Lamin B1 is required for mouse development and nuclear integrity. *Proc Natl Acad Sci U S A* 101:10428-10433.

Vigouroux, C., M. Auclair, E. Dubosclard, M. Pouchelet, J. Capeau, J.C. Courvalin, and B. Buendia. 2001. Nuclear envelope disorganization in fibroblasts from lipodystrophic patients with heterozygous R482Q/W mutations in the lamin A/C gene. *J Cell Sci* 114:4459-4468.

Vincent, T., E.P. Neve, J.R. Johnson, A. Kukalev, F. Rojo, J. Albanell, K. Pietras, I. Virtanen, L. Philipson, P.L. Leopold, R.G. Crystal, A.G. de Herreros, A. Moustakas, R.F. Pettersson, and J. Fuxe. 2009. A SNAIL1-SMAD3/4 transcriptional repressor complex promotes TGF-beta mediated epithelial-mesenchymal transition. *Nat Cell Biol* 11:943-950.

Vissers, J.H., M. van Lohuizen, and E. Citterio. 2012. The emerging role of Polycomb repressors in the response to DNA damage. *J Cell Sci* 125:3939-3948.

Vorburger, K., G.T. Kitten, and E.A. Nigg. 1989. Modification of nuclear lamin proteins by a mevalonic acid derivative occurs in reticulocyte lysates and requires the cysteine residue of the C-terminal CXXM motif. *EMBO J* 8:4007-4013.

Wang, H., R. Cao, L. Xia, H. Erdjument-Bromage, C. Borchers, P. Tempst, and Y. Zhang. 2001. Purification and functional characterization of a histone H3-lysine 4-specific methyltransferase. *Mol Cell* 8:1207-1217.

Wang, H., L. Wang, H. Erdjument-Bromage, M. Vidal, P. Tempst, R.S. Jones, and Y. Zhang. 2004. Role of histone H2A ubiquitination in Polycomb silencing. *Nature* 431:873-878.

Wang, Z.G., D. Ruggero, S. Ronchetti, S. Zhong, M. Gaboli, R. Rivi, and P.P. Pandolfi. 1998. PML is essential for multiple apoptotic pathways. *Nat Genet* 20:266-272.

Wazir, U., M.H. Ahmed, J.M. Bridger, A. Harvey, W.G. Jiang, A.K. Sharma, and K. Mokbel. 2013. The clinicopathological significance of lamin A/C, lamin B1 and lamin B receptor mRNA expression in human breast cancer. *Cell Mol Biol Lett* 18:595-611.

Webster, M., K.L. Witkin, and O. Cohen-Fix. 2009. Sizing up the nucleus: nuclear shape, size and nuclear-envelope assembly. *J Cell Sci* 122:1477-1486.

Wei, Y., W. Xia, Z. Zhang, J. Liu, H. Wang, N.V. Adsay, C. Albarracin, D. Yu, J.L. Abbruzzese, G.B. Mills, R.C. Bast, Jr., G.N. Hortobagyi, and M.C. Hung. 2008. Loss of trimethylation at lysine 27 of histone H3 is a predictor of poor outcome in breast, ovarian, and pancreatic cancers. *Mol Carcinog* 47:701-706.

Wendt, M.K., A.N. Cooper, and M.B. Dwinell. 2008. Epigenetic silencing of CXCL12 increases the metastatic potential of mammary carcinoma cells. *Oncogene* 27:1461-1471.

Wendt, M.K., P.A. Johanesen, N. Kang-Decker, D.G. Binion, V. Shah, and M.B. Dwinell. 2006. Silencing of epithelial CXCL12 expression by DNA hypermethylation promotes colonic carcinoma metastasis. *Oncogene* 25:4986-4997.

Wente, S.R., and M.P. Rout. 2010. The nuclear pore complex and nuclear transport. *Cold Spring Harb Perspect Biol* 2:a000562.

Willis, N.D., T.R. Cox, S.F. Rahman-Casans, K. Smits, S.A. Przyborski, P. van den Brandt, M. van Engeland, M. Weijenberg, R.G. Wilson, A. de Bruine, and C.J. Hutchison. 2008. Lamin A/C is a risk biomarker in colorectal cancer. *PLoS One* 3:e2988.

Wilson, B.G., X. Wang, X. Shen, E.S. McKenna, M.E. Lemieux, Y.J. Cho, E.C. Koellhoffer, S.L. Pomeroy, S.H. Orkin, and C.W. Roberts. 2010. Epigenetic antagonism between polycomb and SWI/SNF complexes during oncogenic transformation. *Cancer Cell* 18:316-328.

Wistuba, II, A.F. Gazdar, and J.D. Minna. 2001. Molecular genetics of small cell lung carcinoma. *Semin Oncol* 28:3-13.

Wong, C.C., D.M. Gilkes, H. Zhang, J. Chen, H. Wei, P. Chaturvedi, S.I. Fraley, C.M. Wong, U.S. Khoo, I.O. Ng, D. Wirtz, and G.L. Semenza. 2011a. Hypoxia-inducible factor 1 is a master regulator of breast cancer metastatic niche formation. *Proc Natl Acad Sci U S A* 108:16369-16374.

Wong, C.M., C.C. Wong, Y.L. Ng, S.L. Au, F.C. Ko, and I.O. Ng. 2011b. Transcriptional repressive H3K9 and H3K27 methylations contribute to DNMT1-mediated DNA methylation recovery. *PLoS One* 6:e16702.

Wong, K.F., and J.M. Luk. 2012. Discovery of lamin B1 and vimentin as circulating biomarkers for early hepatocellular carcinoma. *Methods Mol Biol* 909:295-310.

Wu, Z., L. Wu, D. Weng, D. Xu, J. Geng, and F. Zhao. 2009. Reduced expression of lamin A/C correlates with poor histological differentiation and prognosis in primary gastric carcinoma. *J Exp Clin Cancer Res* 28:8.

Xia, R., F.Y. Jin, K. Lu, L. Wan, M. Xie, T.P. Xu, W. De, and Z.X. Wang. 2015. SUZ12 promotes gastric cancer cell proliferation and metastasis by regulating KLF2 and E-cadherin. *Tumour Biol* 36:5341-5351.

Xu, L., Y. Kang, S. Col, and J. Massague. 2002. Smad2 nucleocytoplasmic shuttling by nucleoporins CAN/Nup214 and Nup153 feeds TGFbeta signaling complexes in the cytoplasm and nucleus. *Mol Cell* 10:271-282.

Yanagisawa, J., J. Ando, J. Nakayama, Y. Kohwi, and T. Kohwi-Shigematsu. 1996. A matrix attachment region (MAR)-binding activity due to a p114 kilodalton protein is found only in human breast carcinomas and not in normal and benign breast disease tissues. *Cancer Res* 56:457-462.

Yang, H.S., and B. Horten. 2014. Gain of copy number and amplification of the RET gene in lung cancer. *Exp Mol Pathol* 97:465-469.

Yang, L., H.C. Dan, M. Sun, Q. Liu, X.M. Sun, R.I. Feldman, A.D. Hamilton, M. Polokoff, S.V. Nicosia, M. Herlyn, S.M. Sebti, and J.Q. Cheng. 2004. Akt/protein kinase B signaling inhibitor-2, a selective small molecule inhibitor of Akt signaling with antitumor activity in cancer cells overexpressing Akt. *Cancer Res* 64:4394-4399.

Yang, L., C. Lin, and Z.R. Liu. 2006. P68 RNA helicase mediates PDGF-induced epithelial mesenchymal transition by displacing Axin from beta-catenin. *Cell* 127:139-155.

Yang, M.H., D.S. Hsu, H.W. Wang, H.J. Wang, H.Y. Lan, W.H. Yang, C.H. Huang, S.Y. Kao, C.H. Tzeng, S.K. Tai, S.Y. Chang, O.K. Lee, and K.J. Wu. 2010. Bmi1 is essential in Twist1-induced epithelial-mesenchymal transition. *Nat Cell Biol* 12:982-992.

Yang, M.H., M.Z. Wu, S.H. Chiou, P.M. Chen, S.Y. Chang, C.J. Liu, S.C. Teng, and K.J. Wu. 2008. Direct regulation of TWIST by HIF-1alpha promotes metastasis. *Nat Cell Biol* 10:295-305.

Yang, S.H., S.Y. Chang, L. Yin, Y. Tu, Y. Hu, Y. Yoshinaga, P.J. de Jong, L.G. Fong, and S.G. Young. 2011. An absence of both lamin B1 and lamin B2 in keratinocytes has no effect on cell proliferation or the development of skin and hair. *Hum Mol Genet* 20:3537-3544.

Yao, R., H. Jiang, Y. Ma, L. Wang, L. Wang, J. Du, P. Hou, Y. Gao, L. Zhao, G.

Wang, Y. Zhang, D.X. Liu, B. Huang, and J. Lu. 2014. PRMT7 induces epithelial-to-mesenchymal transition and promotes metastasis in breast cancer. *Cancer Res* 74:5656-5667.

Ye, J., J.J. Findeis-Hosey, Q. Yang, L.A. McMahon, J.L. Yao, F. Li, and H. Xu. 2011. Combination of napsin A and TTF-1 immunohistochemistry helps in differentiating primary lung adenocarcinoma from metastatic carcinoma in the lung. *Appl Immunohistochem Mol Morphol* 19:313-317.

Yilmaz, M., and G. Christofori. 2009. EMT, the cytoskeleton, and cancer cell invasion. *Cancer Metastasis Rev* 28:15-33.

Yu, H., D.L. Simons, I. Segall, V. Carcamo-Cavazos, E.J. Schwartz, N. Yan, N.S. Zuckerman, F.M. Dirbas, D.L. Johnson, S.P. Holmes, and P.P. Lee. 2012. PRC2/EED-EZH2 complex is up-regulated in breast cancer lymph node metastasis compared to primary tumor and correlates with tumor proliferation in situ. *PLoS One* 7:e51239.

Zentner, G.E., and S. Henikoff. 2013. Regulation of nucleosome dynamics by histone modifications. *Nat Struct Mol Biol* 20:259-266.

Zhang, P., W. Chin, L.T. Chow, A.S. Chan, A.P. Yim, S.F. Leung, T.S. Mok, K.S. Chang, P.J. Johnson, and J.Y. Chan. 2000. Lack of expression for the suppressor PML in human small cell lung carcinoma. *Int J Cancer* 85:599-605.

Zhang, Z.Y., Z.R. Zhao, L. Jiang, J.C. Li, Y.M. Gao, D.S. Cui, C.J. Wang, J. Schneider, M.W. Wang, and X.F. Sun. 2007. Nup88 expression in normal mucosa, adenoma, primary adenocarcinoma and lymph node metastasis in the colorectum. *Tumour Biol* 28:93-99.

Zhao, F., C. Falk, W. Osen, M. Kato, D. Schadendorf, and V. Umansky. 2009. Activation of p38 mitogen-activated protein kinase drives dendritic cells to become tolerogenic in ret transgenic mice spontaneously developing melanoma. *Clin Cancer Res* 15:4382-4390.

Zheng, X., Y. Kim, and Y. Zheng. 2015. Identification of lamin B-regulated chromatin regions based on chromatin landscapes. *Mol Biol Cell* 26:2685-2697.

Zhong, S., P. Salomoni, and P.P. Pandolfi. 2000. The transcriptional role of PML and the nuclear body. *Nat Cell Biol* 2:E85-90.

Zink, D., A.H. Fischer, and J.A. Nickerson. 2004. Nuclear structure in cancer cells. *Nat Rev Cancer* 4:677-687.

8. Acknowledgements

I would like to heartily thank everyone who has ever given me a hand during the past years of doctoral research life in Germany.

Firstly, I would like to express my deepest gratitude to my supervisor Prof. Dr. Gergana Dobreva for giving me this valuable opportunity to come to Germany and work as a PhD candidate on this interesting scientific project. I am truly grateful for her endless patience and understanding during these years. Especially when I first came to Germany, my English was not good, at that moment I could hardly understand her or other colleagues. However, she always patiently explained everything, which I did not understand, to me in slower speaking rates and different ways until I fully comprehended. Besides, I also greatly appreciate her professional supervision and guidance in my study. Without her help, I would never have been able to finish my PhD study and dissertation.

Secondly, I would like to thank Prof. Dammann for his kind suggestions and support. I also thank Dr. Rajkumar Savai and Dr. Guillermo Barreto for their important help and advices on the project. I would like to acknowledge Dr. Luca Caputo as well for his kind support and guidance on this study.

Thirdly, I would like to thank all my labmates and all the other members of the institute and collaborating groups who helped me and contributed to this project: Dr. Julio Cordero for bioinformatical assistance and sequencing analysis; Yanina Knepper for the mice injections and so on.

Last but not least, I would also like to thank all my family members, especially my parents. They have been always supporting me and encouraging me with their best wishes. Most importantly, I would like to thank my wife for her understanding and supports. Her accompaniment and encouragement have always been there fueling me up.

Thank you all.

9. EIDESSTATTLICHE ERKLÄRUNG

„Ich erkläre: Ich habe die vorgelegte Dissertation selbständig und ohne unerlaubte fremde Hilfe und nur mit den Hilfen angefertigt, die ich in der Dissertation angegeben habe. Alle Textstellen, die wörtlich oder sinngemäß aus veröffentlichten Schriften entnommen sind, und alle Angaben, die auf mündlichen Auskünften beruhen, sind als solche kenntlich gemacht. Bei den von mir durchgeführten und in der Dissertation erwähnten Untersuchungen habe ich die Grundsätze guter wissenschaftlicher Praxis, wie sie in der „Satzung der Justus-Liebig-Universität Gießen zur Sicherung guter wissenschaftlicher Praxis“ niedergelegt sind, eingehalten.“

Bad Nauheim, Yanhan Jia